# Adaptation of the CRISPR/Cas9 System as a tool for *in vivo* Screening

Alexandra Katigbak

A thesis submitted to McGill University in partial fulfillment
of the requirement of the degree of
Master of Science

Department of Biochemistry
McGill University
Montreal, QC, Canada

December 2016

# Table of Contents

List of Figures ..... xii
List of Tables ..... xiii
List of Abbreviations ..... xiv
Abstract ..... xvii
Résumé ..... xviii
Author Contributions ..... xix
Original Contributions to Knowledge ..... xx
Acknowledgements ..... xxi
Chapter 1: General Introduction ..... 1
1.1 Targeted Genome Editing ..... 2
*1.1.1 A Historical Perspective* ..... 2
*1.1.2 Zinc Finger Nucleases* ..... 5
*1.1.3 Transcriptional Activator-Like Effector Nucleases* ..... 7
1.2 From Prokaryote Immune System to Eukaryote Genome Editing Revolutionary ..... 10
*1.2.1 Quit Bugging Me: CRISPR as defense against foreign viral and plasmid DNA* ..... 10
*1.2.2 Adaptation of CRISPR/Cas9 for Targeted Vertebrate Genome Editing* ..... 11
*1.2.3 CRISPR as screening tool* ..... 13
1.3 The E*μ*-Myc Mouse Model ..... 14
1.4 Overview and Basis for Thesis ..... 14
Chapter 2: A Multiplexed CRISPR/Cas9 Functional Screen Identifies Rare Tumor Suppressors ..... 16
2.1 Preface to the Manuscript ..... 17
2.2 Abstract ..... 17
2.3 Introduction ..... 17
2.4 Materials and Methods ..... 21
*2.4.1 Retroviral Infections, Stem Cell Isolation, and Adoptive Transfer* ..... 21
*2.4.2 Recovery of sgRNAs and T7 Endonuclease I Assay (T7EI)* ..... 22
*2.4.3 Sequencing of Modified Loci* ..... 22
*2.4.4 Small Hairpin (sh) RNA Design* ..... 22
*2.4.5 PHIP and PHIP$^{R1212\Delta}$ Plasmids* ..... 23
*2.4.6 Antibody Generation and Western Blotting* ..... 23
2.5 Results ..... 24
*2.5.1 Coupling CRISPR/Cas9 and the Eμ-Myc model to identify rare BL oncogenic drivers* ..... 24
*2.5.2 In vivo screening identifies candidate sgRNAs capable of promoting lymphomagenesis* ..... 29
*2.5.3 In vivo validation of candidate tumor suppressors* ..... 31
*2.5.4 SP3 and PHIP display tumor suppressive activity in vivo* ..... 37
2.6 Discussion ..... 40

2.7 Acknowledgements ..... 42
Chapter 3: Inducible Genome Editing with Conditional CRISPR/Cas9 Mice ..... 43
3.1 Preface to the Manuscript ..... 44
3.2 Abstract ..... 44
3.3 Introduction ..... 44
3.4 Materials And Methods ..... 46
*3.4.1 Generating Col1A1 Knock-in Cas9 Mice* ..... 46
*3.4.2 Genotyping* ..... 47
*3.4.3 Construction of pUSPPC sgRNA-expression Vectors* ..... 47
*3.4.4 T7 Endonuclease I (T7EI) Cleavage Assay* ..... 48
*3.4.5 HSPC Adoptive Transfers* ..... 48
*3.4.6 Immunoblotting* ..... 49
*3.4.7 Southern Blot Analysis of the Col1A1 Locus* ..... 49
*3.4.8 Immunophenotyping and Immunohistochemical Analysis* ..... 50
3.5 RESULTS ..... 52
*3.5.1 Generation of a Doxycyline (DOX)-Inducible Cas9 Mouse* ..... 52
*3.5.2 Characterization of Inducible Cas9 Expression in Mice* ..... 52
*3.5.3 Ex Vivo Genome Editing in Primary Hematopoietic Stem and Progenitor Cells (HSPCs)* ..... 58
3.5.4 *Ex vivo manipulation of HSPCs and adoptive transfer experiment in the Eμ-Myc GEMM* ..... 58
3.6 DISCUSSION ..... 61
3.7 ACKNOWLEDGEMENTS ..... 62
Chapter 4: General Discussion ..... 63
4.1 CRISPR/Cas9 in functional in vivo screening ..... 64
4.2 Improvements on the Eμ-Myc Screen ..... 65
4.3 Utility of a Genetically Engineered Inducible Cas9 Mouse ..... 65
References ..... 68
Appendices ..... I

# List of Figures

Figure 1.1 Schematic outlining two DNA repair pathways after induction of a double-stranded break. ..... 4
Figure 1.2. A schematic demonstrating specificity of offset ZFNs..... 6
Figure 1.3. Schematic demonstrating the DNA-targeting specificity of TALENs..... 9
Figure 1.4. Adaptation of prokaryotic CRISPR system for eukaryotic genome editing 12
Figure 2.1 Representation of genes containing rare nonsense or frameshift mutations in BL and design of functional in vivo screen. ..... 19
Figure 2.2. Testing functionality of pQGiG2 constructs ..... 26
Figure 2.3 Testing functional pool complexity and onset curves for non-significant pools ..... 28
Figure 2.4 Analysis of sgRNA pools exhibiting accelerated tumorigenesis. ..... 30
Figure 2.5. Validation of Sp3 as a tumor suppressor. ..... 32
Figure 2.6. Validation of Phip as a tumor suppressor. ..... 33
Figure 2.7. Validation experiments for Tfap4 ..... 34
Figure 2.8. Sequence analysis of the Sp3 locus from sgSp3 derived tumors ..... 35
Figure 2.9. Sequence analysis of the Phip locus from sgPhip-derived tumors ..... 36
Figure 2.10 Functional assessment of a PHIP truncation mutant in the E$\mu$-Myc model 38
Figure 2.11. Frequency of mutations in PHIP (a) and SP3 (b) across human tumor samples as reported from the COSMIC (v77) database ..... 39
Figure 3.1. Inducible and reversible Cas9 Expression in mouse ESCs. ..... 51
Figure 3.2. Inducible Cas9 expression ..... 54
Long Term expression of Cas9 is well tolerated in the mouse..... 55
Figure 3.4. DOX-inducible Genome Editing Ex Vivo ..... 56
Dosage effect of rtTA alleles in the TRE-CiG mouse HSPCs ..... 57
Figure 3.6. Effectiveness of GEMM for in vivo functional assays ..... 60

# List of Tables

Table S1 – List of Genes with Nonsense or Frameshift Mutations in Burkitt's Lymphoma with the Corresponding Murine Orthologs and Designed sgRNAs ..... II
Table S2 – List of sgRNA and shRNAs used to validate candidate tumor suppressor genes.....VII
Table S3 – PCR Primer sequences used in Chapter 2 .....VIII
Table S4 – Blood chemistry analysis of R26-rtTA;TRE-CiG/rtTA mice after 6 months maintenance on 1 mg/mL DOX (n=2).. .....VI
Table S5 - Histopathological analysis of wild-type and R26-rtTA;TRE-CiG/rtTA tissues after 6 month doxycycline induction .....IX

# List of Abbreviations

| | |
|---|---|
| AAV | Adenoassociated Virus |
| ALT | Alanine Aminotransferase |
| APC | Adenomatous Polyposis Coli |
| AST | Aspartate Aminotransferase |
| BCM | B-Cell Medium |
| BL | Burkitt's Lymphoma |
| bp | Base Pair |
| BUN | Blood Urea Nitrogen |
| Cas | CRISPR-associated protein |
| Cas9 | CRISPR-associated protein 9 |
| cDNA | Complementary DNA |
| CK | Creatine Kinase |
| Col1A1 | Collagen Type 1 Alpha 1 |
| COSMIC | Catalogue of Somatic Mutations in Cancer |
| CRISPR | Clustured Regularly Interspaced Palindromic Repeats |
| crRNA | CRISPR-related RNA |
| DMEM | Dulbecco's Modified Eagle's Medium |
| DMSO | Dimethyl Sulfoxide |
| DNA | Deoxyribonucleic Acid |
| DOX | Doxycycline |
| DSB | Double-Stranded Break |
| DSIR | Designer of siRNA |
| *E. coli* | Escherichia coli |
| E13.5 | Embryonic day 13.5 |
| eIF5A | Eukaryotic Initiation Factor 5A |
| EMCV | Encephalomyocarditis Virus |
| ESC | Embryonic Stem Cell |

| | |
|---|---|
| FBS | Fetal Bovine Serum |
| FRT | Flippase Recognition Target |
| GEMM | Genetically Engineered Mouse Model |
| GFP | Green Fluorescent Protein |
| HDR | Homology Directed Repair |
| HSPC | Hematopoietic Stem and Progenitor Cell |
| IL-3 | Interleukin 3 |
| IL-6 | Interleukin 6 |
| IMEM | Iscove's Modified Dulbecco's Medium |
| indels | Insertion Deletion Mutations |
| IRES | Internal Ribosomal Entry Site |
| Lkb1 | Liver Kinase B1 |
| mRNA | Messenger RNA |
| NHEJ | Non-Homologous End Joining |
| NT | Non-Transduced |
| PAM | Protospacer Adjacent Motif |
| PCR | Polymerase Chain Reaction |
| PGK | Phosphoglycerate Kinase |
| PHIP | Pleckstrin Homology Domain Interacting Protein |
| RISC | RNA-Induced Silencing Complex |
| Rluc | Renilla Luciferase |
| RMCE | Recombinase-Mediated Cassette Exchange |
| RNA | Ribonucleic Acid |
| RNAi | RNA interference |
| RT | Room Temperature |
| rtTA3 | Reverse Tetracycline-controlled Transactivator 3 |
| RVD | Repeat Variable Diresidue |
| SCF | Stem Cell Factor |
| sgRNA | single guide RNA |

| | |
|---|---|
| shRNA | short hairpin RNA |
| siRNA | short interfering RNA |
| SP3 | Specificity Protein 3 |
| T7EI | T7 Endonuclease Assay |
| TAL | Transcriptional Activator-Like |
| TALE | Transcriptional Activator-Like Effector |
| TALEN | Transcriptional Activator-Like Effector Nuclease |
| TFAP4 | Transcription Factor Activating Enhancer Binding Protein 4 |
| TLR | Traffic Light Reporter |
| tracrRNA | Trans-acting CRISPR-related RNA |
| TRE | Tetracycline Response Element |
| Tsc1 | Tuberous Sclerosis 1 |
| WT | wild-type |
| ZF | Zinc Finger |
| ZFN | Zinc Finger Nuclease |

# Abstract

The discovery and adaptation of the type II Clustered Regularly Interspaced Palindomic Repeats (CRISPR) prokaryotic immune system has revolutionized the world of targeted genome editing. The programmable, scaleable and multiplexable nature of the CRISPR/Cas9 system makes it amenable to *in vivo* screening applications in a way that its Zinc Finger Nuclease (ZFN) and Transcriptional Activator Like Effector Nuclease (TALEN) predecessors were not. While the use of CRISPR/Cas9 in a screening context has been used to great success, there remains much ground to cover in the development of functional *in vivo* screening frameworks. In Chapter 2, we detail the use of CRISPR/Cas9 to functionally screen for oncogenic drivers of Burkitt's Lymphoma (BL) in the powerful E*μ*-myc mouse model. We identified two genes with novel tumor-suppressor activity: *Phip* and *Sp3.* Since the size of vectors harboring the two CRISPR components can surpass the limits of efficient viral packaging, in Chapter 3, we describe the development of a novel transgenic mouse containing a doxycycline-inducible Cas9 allele. We demonstrated conditional presence of Cas9 protein across a number of tissues and the absence of deleterious effects of long-term induction. Additionally, we developed a novel compact retroviral sgRNA delivery vector, and demonstrated the vector and the mouse's utility for *in vivo* functional studies.

# Résumé

La découverte et l'adaptation du système immunologique prokaryote de courtes répétitions palindromiques groupées et régulièrement espacées (CRISPR) de type II a complètement révolutionné le monde du génie génétique. Avec sa flexibilité, sa facilité de programmation et à être multiplexée, la technologie CRISPR/Cas9 surpasse amplement les autres technologies de génie génétique telles les nucléases de doigts de zinc (ZFNs) et les nucléases effectrices de type activateur de transcription (TALENs). Même si beaucoup de progrès ont été faits dans l'utilisation du système CRISPR pour des criblages génétiques *in vitro*, il reste encore beaucoup de travail pour en développer son plein potentiel à ce niveau. Au Chapitre 2, nous décrivons l'identification de nouveaux gènes impliqués dans la lymphomagènese en combinant l'utilisation de CRISPR/Cas9 et le modèle de lymphome de type Burkitt (BL) E*μ*-myc. Nous avons ainsi identifié deux nouveaux gènes qui protègent contre l'apparition des tumeurs : *Phip* et *Sp3*. Étant donné la taille de la protéine Cas9, il est présentement difficile de bien distribuer ce système dans les divers tissus d'un organisme avec les vecteurs viraux conventionnels. Au Chapitre 3, nous décrivons le développement d'une souris transgénique possédant une allèle de Cas9, dont l'expression est inductible en présence de doxycycline. Nous avons démontré que la protéine Cas9 est bien inductible et que sa production n'entraîne pas d'effets nocifs chez la souris à long terme. De plus, nous avons créé un nouveau vecteur d'expression du sgRNA plus compact et avons démontré qu'il est possible de l'utiliser dans des essais fonctionnels *in vivo*.

# Author Contributions

*Chapter 2*

- Experiments were conceived and designed by myself and my supervisor, Dr. Jerry Pelletier
- I designed the sgRNA and shRNA constructs with help from Dr. Claudio Scuoppo and generated the library and validation constructs.
- I conducted all experiments and generated all reagents with the exception of the initial screen in the E*μ*-myc system which was done with help from Drs. Regina Cencic, Francis Robert and Mr. Patrick Senechal and the Phip cDNA which was a kind gift from Dr. Anne Claude Gingras at the Lunenfeld-Tanenbaum Research Institute in Toronto.
- I conducted the data analysis under supervision of Dr. Jerry Pelletier.

*Chapter 3*

- Experiments were conceived and designed by myself and Dr. Jerry Pelletier.
- I executed all experiments and generated all reagents, with the exception of histologcal analyses, which were conducted by Dr. Marilène Paquet at the Université de Montréal, and the adoptive transplant experiments which were executed with help from Dr. Francis Robert.
- I conducted the data analysis under supervision of Dr. Jerry Pelletier.

# Original Contributions to Knowledge

*Chapter 2:*

- Developed a framework for utilizing the CRISPR/Cas9 system as an approach to functionally screen for rare oncogenic drivers in vivo.
- Conducted a targeted *in vivo* knockout screen for onogenic drivers of Burkitt's lymphoma in the E*μ*-myc mouse model
- Identified 2 genes which had not previously been implicated in lymphomagenesis: *Phip* and *Sp3*

*Chapter 3:*

- Generated a novel transgenic mouse containing a doxycycline-inducible allele encoding Cas9 and green fluorescence protein (GFP)
- Characterized of Cas9 expression in this mouse across a variety of tissues
- Development of a more compact retroviral vector for delivery of sgRNA.
- Demonstrated that this mouse can be used for in vivo functional studies
- Confirmed with histopathological analysis that long-term Cas9 expression shows no deleterious effect on various tissues.

# Acknowledgements

First and foremost, I must acknowledge my supervisor Dr. Jerry Pelletier. Thank you for your patience, guidance and insight and for talking me through even the smallest of concerns and biggest of breakdowns. Without your support, this thesis would not exist. To the members of my research advisory committee, Drs. Philippe Gros and Michel Tremblay, thank you for your guidance, input, and suggestions over the course of my studies. It was greatly appreciated.

To the members of the Pelletier lab, both past and present, thank you for your kindness and generosity. Every incubation started and mouse palpated on my behalf was enormously appreciated. To Regina Cencic, Francis Robert and Patrick Senechal, thank you for all your assistance with the Burkitt's screen. And Francis, our resident French-Canadian, thank you for your help with revision of the French abstract for this thesis. I would also like to thank Drs. Marilène Paquet and Claudio Scuoppo for their expertise and aid in the generation of the two manuscripts included in this work.

To Jennifer Chu, my compatriot in commiseration, purveyor of pints and pastries, and proof-reader of theses and manuscripts alike, thank you for your friendship, guidance and unwavering support in even my most difficult times. Your indefatigable attitude and sense of humor brightened my days in the lab immeasurably. To my friends outside of the lab, Adam and Danielle, thank you for your kindness, encouragement, and companionship. It means the world to me. To my sisters Emily and Kelly, thank you for always filling my life with so much laughter that whatever hardships I encountered never seemed so hard. I love you dearly. Here is to another thousand movie nights in my apartment.

And to my parents, Rick and Suzanne, I owe absolutely everything to you. All of my successes are your successes. I will never be able to return the multitudes that you have given me, but I promise I will never stop trying. I love you both so much.

# Chapter 1: General Introduction

## 1.1 Targeted Genome Editing

### *1.1.1 A Historical Perspective*

The genome is the blueprint for human life but it is only recently that we have developed the tools to read and interpret these plans. The sequencing of the human genome cost hundreds of millions of dollars and took 13 years to complete (National Human Genome Research Institute). Now, genomes of plants, animals, people and diseased tissues are sequenced on a regular basis for several hundred dollars. We are living in an age of unprecedented genetic understanding, with insight into biology and disease mechanisms that would have been unimaginable to researchers less than 20 years ago. However, while genomic sequencing is more accessible than it has ever been, we still lack adequate tools to write, re-write, edit and rearrange eukaryotic genomes. Restriction endonucleases identified in prokaryotes allowed for targeting of specific DNA sequences from 4 to 8 nucleotides, [1] but with the human genome containing ~$3x10^9$ base pairs, this was nowhere near selective enough to be used in the study of human disease, or for use in therapeutics. Over the past 10 years, enormous strides have been made in development of new technologies which could allow for precision genome editing with à la carte design of proteins and complexes capable of targeting specific DNA sequences from 18-36 nucleotides [2], making them suitable for use in highly complex genomes. These technologies largely take advantage of the DNA repair machinery already present in the cell by cleaving target DNA and introducing double stranded breaks (DSBs). Double-stranded breaks are undesirable to the cell as they could lead to dangerous rearrangement of genomic elements and limit the fitness of the cell. Cells therefore seek to repair these breaks through two different mechanisms: Non-Homologous End-Joining (NHEJ) and Homology-Directed Repair (HDR) [3]. NHEJ is an error-prone repair mechanism where non-homologous DNA strands are brought together and ligated [4]. This repair often leads to the introduction of various small insertion or deletion mutations (indels), disrupting the endogenous sequence. (Figure 1.1) HDR occurs when a homologous piece of DNA – usually a sister or daughter chromosome, although researchers introduce exogenous DNA sequences

when they wish to introduce novel sequences or replace existing ones – is available for the cell to use as a “repair template” or “donor”, replacing the damaged DNA with a copy of the sequence present between the homology arms [4](Figure 1.1). While HDR has been used to create genetically modified animals and cells before simply by introducing donor DNA and screening subsequent clones for spontaneous recombination, the rate of conversion is extremely low [5]. It was shown that by inducing DSBs one could significantly increase the rate of clone conversion [6]. The most prominent and commonly-used examples of systems adapted to take advantage of this are: Zinc Finger Nucleases (ZFNs), Transcriptional Activator-Like Effector Nucleases (TALENs) and the Clustered Regularly Interspaced Repeats (CRISPR) Cas9 system.

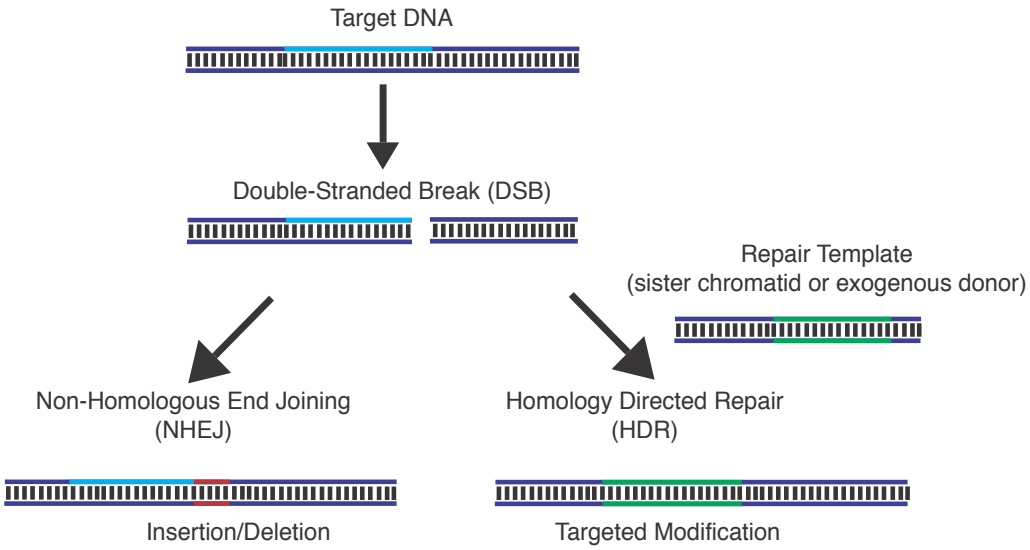


*Figure 1.1. Schematic outlining two DNA repair pathways after induction of a double-stranded break*.

The error-prone NHEJ pathway will lead to random insertions or deletions in the repaired DNA. In the presence of DNA containing sufficient regions of homology, HDR machinery will use this as a template for targeted repair of the endogenous DNA.

*1.1.2 Zinc Finger Nucleases*

Zinc finger nucleases (ZFNs) are engineered proteins made by fusing tandem C2H2 zinc-finger domains to a modified FokI nuclease subunit [7]. Each finger contains amino acid residues that form a DNA-interacting surface and most show trinucleotide specificity [8]. ZFNs are often constructed with 3-6 finger domains, allowing for specific targeting of 9-18 nucleotides [9]. As the modified FokI is an obligate dimer, cleavage requires the assembly of offset ZFNs separated by a short spacer for effective double-stranded cleavage (Figure 1.2). This leads to target specificity of up to a previously unheard of 36 nucleotides, conferring enough specificity for use in mammalian genomes.

Their modular nature made ZFNs an attractive option for researchers. Rearrangement of the zinc-finger domains allowed for targeting of a wide variety of genes in a number of different biological entities including fruit flies[10-12], zebrafish[13, 14], mice[15-18], and human cells [19-21]. However, it became evident that this technology was not without its drawbacks. There was found to be a high level of difficulty in designing ZFNs that would effectively cleave the target sequence of interest, and not all sequences could be targeted with similar efficiency using ZFNs [22, 23]. ZF binding to DNA also appeared to be context-dependent, with different fingers binding more or less efficiently depending on the ZFs which flanked them [24]. It was also reported that introduction of ZFNs could lead to undesirable levels of toxicity in targeted cells, depending on the specificity of the ZFN pair utilized in the experiment [25]. There still remained much room for improvement and development of a more optimal gene editing system.

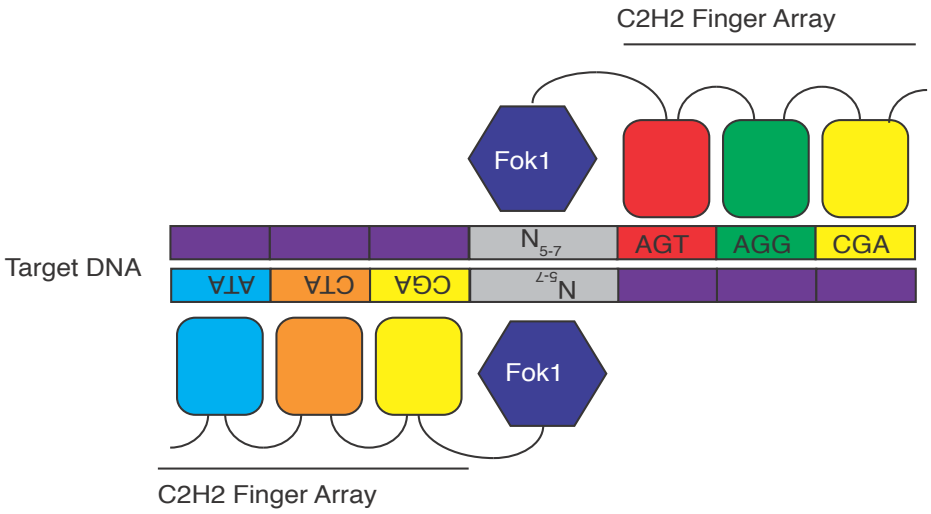


*Figure 1.2. A schematic demonstrating specificity of offset ZFNs.*

Tandem fingers recognize specific trinucleotide sequences. Upon paired recognition of target sites, FokI nuclease domains will dimerize and activate, cleaving the target DNA.

*1.1.3 Transcriptional Activator-Like Effector Nucleases*

Transcriptional Activator-Like Effector Nucleases (TALENs) are another variety of engineered protein that was inspired by naturally-occurring DNA-binding proteins. They are based off of Transcription Activator Like Effectors (TALEs) which were originally identified in plant pathogenic bacteria [26]. Each TALE contains an array of nearly identical 33-35 amino acid repeats (with the exception of the most C-terminal repeat which contains only 20 amino acids and is referred to as a "half repeat") containing two highly variable residues around positions 12 and 13, called Repeat Variable Diresidues (RVDs) [27]. These RVDs provide the TALEs their DNA-binding specificity, with each RVD demonstrating a preference for a single nucleotide [28, 29]. As with ZFNs, their modular nature lent TALEs very well to custom arrangement for à la carte gene targeting, with the added bonus of each repeat showing preference for a single nucleotide rather than a triplet, making them a much more flexible system [29]. Most TALEs generally contain 15.5-19.5 repeats [30] so the fusion of these repeats to the non-specific FokI nuclease domains and creation of paired TALENs would allow for highly specific sequence recognition (Figure 1.3). In addition to their relative ease of assembly, TALENs offered another advantage over their ZFN counterparts: freedom from context dependence. Unlike the zinc-finger modules whose efficiency was found to be highly dependent on its neighbouring fingers, TALE repeats can be arranged in any order and whose targeting capacity is limited only by the need for a thymine or 'T' residue at the 0 position of the target sequence [31].

The relative simplicity and ease of construction made TALENs an attractive option for researchers interested in genome editing but who may have been discouraged by the complexity and difficulty of designing and testing appropriate ZFNs. In the end, TALENs have been successfully implemented in a wide variety of applications and host systems such as the fruit fly[31, 32], zebrafish [33-35], frogs[36-39], rat[40], pig[41], and human cells [42, 43]. Comparing TALENs and ZFNs, it was found that both systems demonstrated similar editing efficiencies, while TALENs appeared to cause less cytotoxicity and more live births, in the case of zygote injections [43-45]. However, this technology is not without its own drawbacks. While the facile

assembly of TAL repeats allowed for unprecedented flexibility in target sequence selection, the DNA encoding the resulting TALEN proteins could be 3-4 times longer than that of ZFNs [46] which limits the delivery systems one can use to administer the proteins.

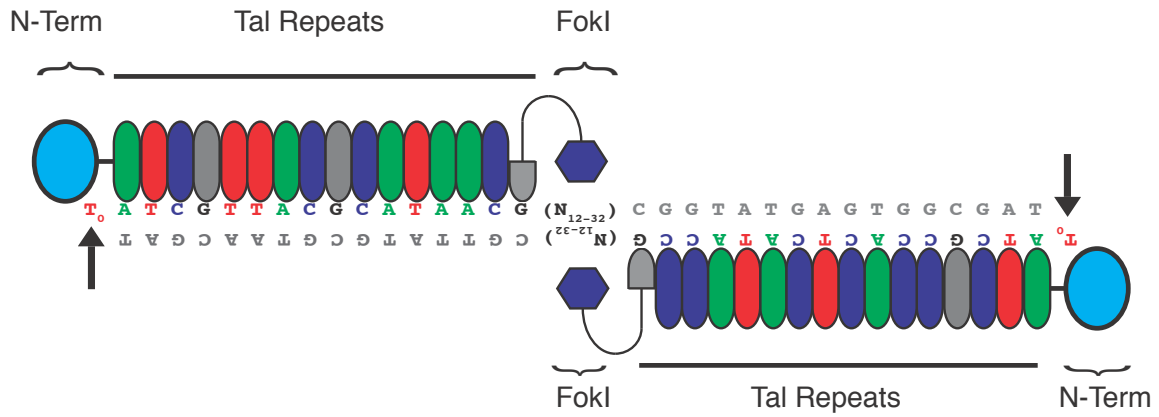


*Figure 1.3. Schematic demonstrating the DNA-targeting specificity of TALENs.*

Each TAL repeat is shown paired with its preferred nucleotide substrate. FokI nuclease domains dimerize and cleave in the 12-32 nucleotide spacer between paired TALENs. Obligate thymines at the 0 position ($T_0$) are indicated by the black arrows.

## 1.2 From Prokaryote Immune System to Eukaryote Genome Editing Revolutionary

### *1.2.1 Quit Bugging Me: CRISPR as defense against foreign viral and plasmid DNA*

The genome-editing revolution that is CRISPR originated in a rather unusual and unassuming manner, with Ishino et al. noticing a cluster of odd palindromic repeat sequences, downstream of an isoenzyme-encoding gene in *Escherichia coli* [47]. These repeats were distributed at regular intervals, with different nucleotide "spacer" sequences separating them, eventually became known as Clustered Regularly Interspaced Palindromic Repeats, or CRISPR (Figure 1.4a). While the exact repeat sequence and length of the intervening spacers vary between species, CRISPR arrays themselves were found to be extremely common, existing in 40% of bacterial genomes and 90% of archaeal genomes [48]. Nearly 20 years after their discovery in *E. coli*, it was proposed that these CRISPR arrays were a part of some sort of prokaryotic immune system providing protection against invading pathogens, as the spacers between repeat sequences were often found to correspond to plasmid or bacteriophage DNA[49-51]. This was soon proven to be true, when Barrangou et al. challenged *Streptococcus thermophilus,* with bacteriophages, sequencing of the CRISPR loci in resistant clones revealed acquisition of one or several new spacers, with level of resistance increasing with the number of novel spacers acquired[52]. Additionally, spacers acquired that contained mismatches of 1 to 15 nucleotides (in a 29-30 nucleotide spacer) conferred no such resistance to the bacteria [52]. Many different arrangements of CRISPR and CRISPR-associated (Cas) proteins were identified, which were then separated into different classes, the simplest of which is the Type II CRISPR system, which required only three components to achieve cleavage and destruction of invading DNA [53]. First, the Cas9 protein – an endonuclease which recognizes and binds to DNA. Second, two small RNAs which together allow the targeting and binding of Cas9 to the target DNA– the CRISPR-related RNA (crRNA) and trans-activating CRISPR-related RNA (tracrRNA). In order to achieve cleavage, two events must occur: the 20 nucleotide targeting sequence within the crRNA must pair with the target DNA

and there must be a short downstream motif called the Protospacer Adjacent Motif (PAM) consisting of an NGG trinucleotide [54, 55] (Figure 1.4b).

### *1.2.2 Adaptation of CRISPR/Cas9 for Targeted Vertebrate Genome Editing*

The simplicity of the type II CRISPR/Cas9 system made it an excellent candidate for adaptation for use in targeted genome editing. In the same way that ZFNs and TALENs were used to introduce double-stranded breaks into eukaryotic DNA, so too would the CRISPR/Cas9 system. In addition to being a highly streamlined system, CRISPR/Cas9 was easily programmable. In the case of ZFNs and TALENs, large complex proteins had to be designed, cloned, and then delivered to cells, with each pair targeting only a single gene. With the CRISPR/Cas9 system, delivery of Cas9 along with two short RNAs would allow for efficient and effective targeting of a locus of choice [55-57]. This system was further simplified by fusing the necessary portions of the crRNA and tracrRNA to form a single chimeric guide RNA (sgRNA) which was sufficient to allow binding and cleavage of target DNA [55] (Figure 1.4c). The CRISPR/Cas9 system quickly sprung to the forefront of the field of genome editing. Researchers studying an enormous variety of organisms quickly put this new tool to use and achieved editing in species across the eukaryotic domain: crop plants[58-61], roundworms[62, 63], frogs[64, 65], fish[66-68] and mice[69-72]. The contribution of CRISPR/Cas9 to the study of human biology and disease has been incredible as well [73-76].

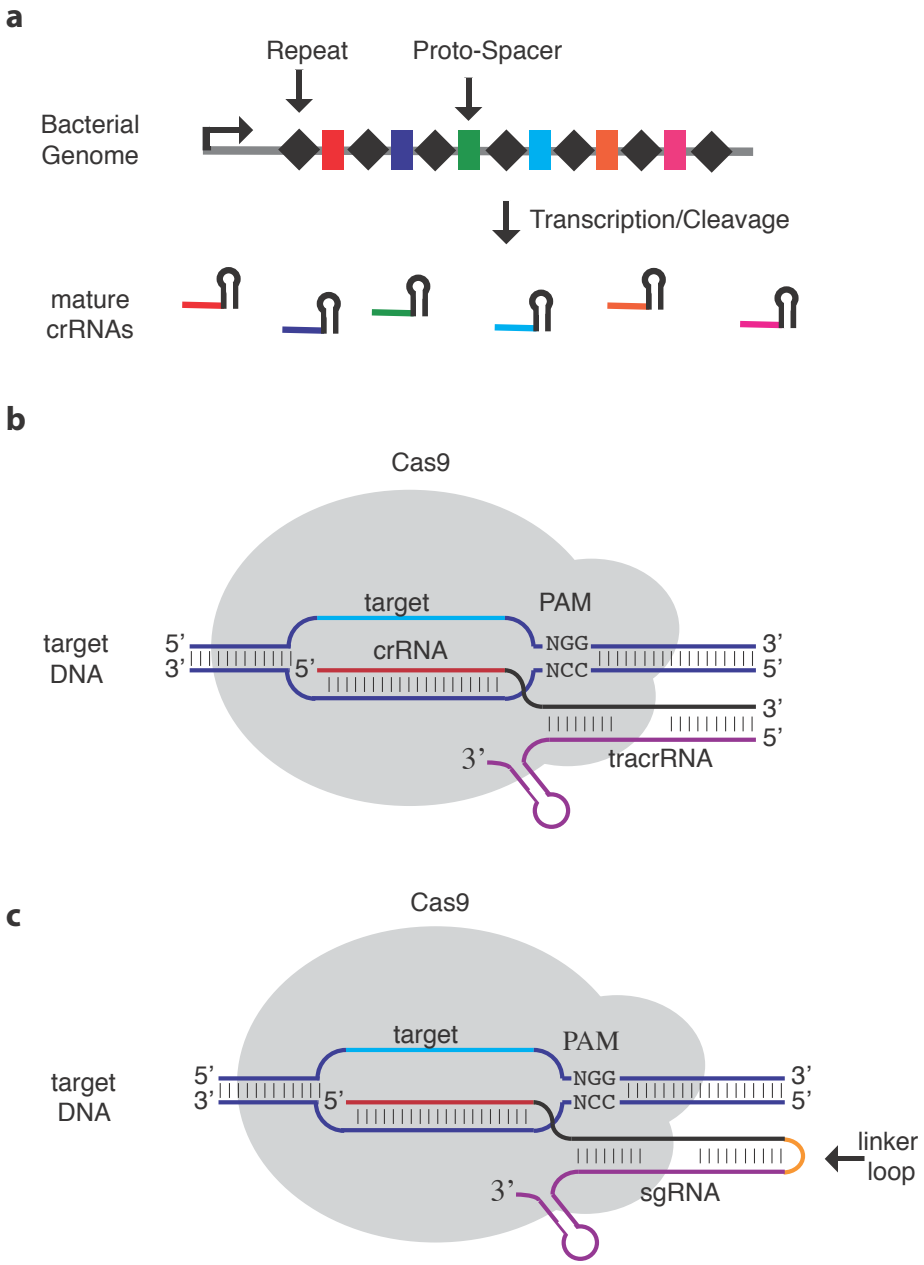


*Figure 1.4. Adaptation of prokaryotic CRISPR system for eukaryotic genome editing*

a) Schematic representing bacterial operon containing the Clustered Regularly Interspaced Repeats and intervening protospacers and how the protospacers are transcribed and processed into targeting crRNAs. b) Representation of the three essential components for DNA targeting by Type II CRISPR/Cas systems and c) subsequent fusion of the two component short RNAs for system streamlining.

*1.2.3 CRISPR as screening tool*

Another major advantage of the CRISPR/Cas9 system was its potential for multiplexing. With the delivery of the single Cas9 protein, one opens up the possibility to target any desired locus or loci within that cell just through delivery of the appropriate sgRNAs [77-82], something that would not have been feasible with TALENs or ZFNs. Not only did this system allow for greater flexibility than previously used genome editing technologies, but it also offered some advantages to the widely implemented RNA-interference (RNAi) high-throughput screening tools: short interfering RNAs (siRNAs) and short hairpin RNAs (shRNAs). Both of these RNAi screening tools take advantage of endogenous RNA-degradation machinery. The siRNA or shRNA contains sequences complementary to a target of choice and upon target recognition and pairing, the duplexed RNAs are recognized by the RNA-induced silencing complex (RISC) and the targeted RNA is degraded [83]. Although this technique has proved highly useful and has contributed greatly to our understanding of different diseases and biological processes, RNAi is not without its limitations. Firstly, as RNAi acts on the mRNA rather than on the gene itself, the amount of translated product is merely reduced and not completely abolished. This can lead to false negatives in a screening context if the amount of targeted gene is not sufficiently reduced[84]. Additionally, off-target knockdown can occur very frequently, so careful assay design is critical for screening and validation [84], although this remains true within the CRISPR/Cas9 system as well. Finally, negative selective pressures can cause the loss of shRNA expression over time, with cells potentially losing the shRNA expression cassette, or shutting down expression through other means. The CRISPR/Cas9 system offers the advantage of permanent editing of the targeted locus. Since the genomic DNA is altered directly, all resulting loss of protein expression will be maintained across generations of cells, even if the targeted cell adapts through silencing or removal of the Cas9/sgRNA-encoding construct, which would not be the case with an shRNA. Genome-scale screening (targeting between 7 000 and 20 000 genes [85]) using CRISPR/Cas9 has been used to great effect by a number of different groups for the study of both biological processes[86-92] and human disease[93-95].

## 1.3 The E*μ*-Myc Mouse Model

The E*μ*-myc mouse model is a transgenic model of Burkitt's and other Non-Hodgkin's lymphomas modeled after the canonical Burkitt's translocation which places oncogene c-*myc* driven by a lymphoid-specific immunoglobulin heavy chain enhancer (*μ*) [96]. This enhancer is highly potent, and mice containing this transgene will often succumb to disseminate B-cell lineage lymphomas within 6 to 15 weeks after birth [96, 97]. Upon transplantation of these tumor cells into wild-type recipients, nearly all will give rise to lymphomas with nearly identical histopathology to the donor animals, confirming the malignant nature of these tumors [97]. This model has proven to be an extremely powerful tool in the study of human cancer. It has been used to evaluate drug response/genotype relationships [98], identify potential new therapeutic targets [99], and identify important new players in lymphomagenesis and drug response through implementation of RNAi screening [100, 101]. The E*μ*-myc mouse is also a highly useful screening tool. Hematopoietic Stem and Progenitor Cells (HSPCs) can be harvested from E*μ*-myc fetal livers, manipulated ex vivo, and transplanted into syngeneic wild-type recipients to assess the effect of genetic alterations on lymphomagenesis [100].

## 1.4 Overview and Basis for Thesis

The CRISPR/Cas9 system has clearly revolutionized the world of targeted genome editing. Although an impressive amount of ground has been covered within the few years since it's implementation, there remains significant potential for expansion. With its potential for multiplexing, CRISPR/Cas9 has proved to be an excellent screening tool. With the advent of next-generation sequencing technology, the availability of high-resolution sequencing data of both normal and diseased tissue has skyrocketed. Determining which reported variants are simply neutral "bystander" mutations and which are disease-drivers remains a struggle. The more frequently mutated genes or "heavy hitters" are most often prioritized for validation, however this

leaves a large bulk of the reported variants uninvestigated, which may leave rare disease drivers undiscovered. In Chapter 2, we sought to identify mutations reported after deep-sequencing of Burkitt's lymphoma (BL) cell lines and patient samples which are not frequently mutated but can contribute to lymphomagenesis by performing an *in vivo* knockout screen in the E*μ*-myc mouse model using CRISPR/Cas9. In order to facilitate *in vivo* screening, we also developed a transgenic mouse with a doxycycline-inducible Cas9 allele, which would allow for development of smaller sgRNA-delivery vectors and open the door to a number a new experimental avenues. This work is detailed in Chapter 3.

# Chapter 2: A Multiplexed CRISPR/Cas9 Functional Screen Identifies Rare Tumor Suppressors

Alexandra Katigbak, Regina Cencic, Francis Robert  Patrick Sénéchal, Claudio Scuoppo, Jerry Pelletier. (2016). A Multiplexed CRISPR/Cas9 Functional Screen Identifies Rare Tumor Suppressors. *Manuscript submitted.*

## 2.1 Preface to the Manuscript

With the recent development of All-in-One retroviral CRISPR/Cas9 delivery vectors [102], the availability of a robust murine model of Burkitt's lymphoma[97], and the recent publication of several deep-sequencing studies of Burkitt's lymphoma cell lines and patient samples[103-105], we sought to conduct a targeted *in vivo* screen to identify rare oncogenic drivers that may otherwise be overlooked in favor of their more frequently-mutated counterparts.

## 2.2 Abstract

An enormous amount of tumor sequencing data has been generated through large scale sequencing consortiums. The functional consequences of the majority of mutations identified by such projects remain an open, unexplored question. This problem is particularly complicated in the case of rare mutations where frequency of occurrence alone or prediction of functional consequences are not insightful in distinguishing driver from passenger or bystander mutations. Here we combine genome editing technology with a powerful mouse cancer model to uncover previously unsuspected rare oncogenic driver mutations in Burkitt's lymphoma. We identify two candidate tumor suppressors, *PHIP* and *SP3*, whose loss cooperates with MYC over-expression to accelerate lymphomagenesis. Our results highlight the utility of *in vivo* CRISPR/Cas9 screens combined with powerful mouse models to identify and validate rare oncogenic driver events from tumor mutational data.

## 2.3 Introduction

The International Cancer Genome Consortium is a colossal tumor sequencing endeavor that has profiled over 10,000 tumors and uncovered ~10 million mutations[106]. Mutation frequency, predicted functional impact, and pan-cancer

analysis of mutated networks are powerful approaches by which to identify oncogenic drivers in order to support diagnostic and therapeutic efforts [107-111]. However, cancers exhibit extensive mutational heterogeneity and in many cases it appears that only a few frequently mutated genes (among all tumor-associated mutations) are significant for initiation and progression. Indeed, the vast proportion of gene mutations within a tumor are thought to represent “passenger” or “bystander” mutations. However, it is unclear whether among these rarer events reside low penetrant oncogenic drivers and this currently constitutes an obstacle to a full understanding of tumor biology.

Burkitt’s lymphoma (BL) is a common B-cell lymphoma, predominantly arising in children, which which is characterized by the hallmark Burkitt translocation t(8;14)(q24;q32) or its variants t(2;8) and t(8:22) – all of which juxtapose the MYC oncogene with one of three immunoglobulin loci [112]. Recent whole genome, exome, and transcriptome sequencing data from 104 sporadic BL patient samples and BL cell lines has defined the mutational landscape in this cancer [103-105]. Among these studies, Schmitz et al. [105] undertook RNA sequencing of 28 sporadic BL samples and 13 cell lines and identified >5000 mutations, Love et al. [103] identified 70 recurrently mutated genes from exome sequencing of 51 primary BL tumors and 8 BL cell lines and Richter et al. [104]sequenced four Burkitt’s lymphomas and identified 119 genes with potentially protein-altering mutations. Within this rich source of BL mutational data lie known oncogenic drivers along side a large number of infrequently mutated genes, leading to a characteristic “long tail” phenomenon when analyzing gene mutation counts in tumors (Figure 2.1a). The significance of this latter class of mutations in BL remains unknown and it is here that functional assays have much to offer.

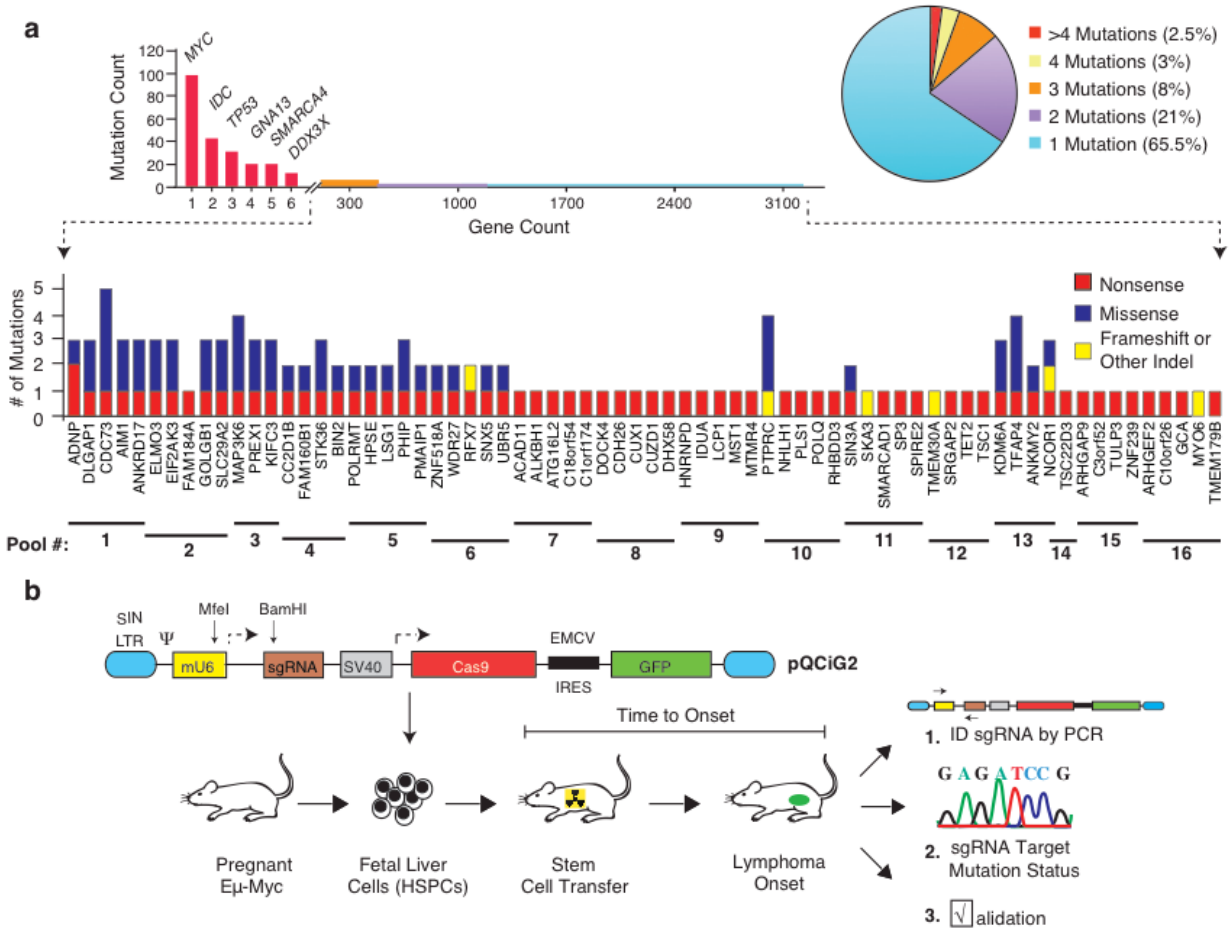


*Figure 2.1 Representation of genes containing rare nonsense or frameshift mutations in BL and design of functional* in vivo *screen.*

**(See following page for legend)**

a) Gene mutation count in BL. The top graph represents all coding region mutations, as reported in Love et al. [103], Richter et al. [104] and Schmitz et al. [105]. The right pie chart denotes the proportion of genes harboring the indicated number of mutations found in the 104 BLs. The bottom graph highlights the frequency and nature of mutations within genes in where at least one nonsense or frameshift mutation was identified in BL mutational studies. Gene names and sgRNA pools are indicated at the bottom. One sgRNA was omitted from pools 2-4, while 3 were omitted from pool 14 as a consequence of quality control experiments revealing that the original vector contained undesired second site mutations. b) Schematic representation of retroviral design and adoptive transfer strategy used for Cas9/sgRNA delivery to HSPCs, followed by transplantation and lymphoma monitoring. Details of pQCiG2 have been previously reported[102]. Accelerated tumors were characterized by: 1) PCR amplification and sequencing of sgRNAs residing in the resulting tumors, 2) the sgRNA targeted loci are probed for mutational status in the obtained tumors, and 3) independent sgRNAs and shRNAs were used in new transplantation experiments for validation of results.

## 2.4 Materials and Methods

### *2.4.1 Retroviral Infections, Stem Cell Isolation, and Adoptive Transfer*

Low passage Phoenix-Eco viral packaging cells were cultured in complete DMEM (10% FBS, 1% Penicillin-Streptomycin, 1% L-Glutamine) at 37˚C in 5% $CO_2$. Twenty four hours prior to transfection, 3.5 x $10^6$ cells were seeded in 10 mL DMEM in 10 cm tissue culture plates. pQCiG2 constructs were pooled in equal molar ratios to a total of 10 $\mu$g and co-transfected into Phoenix-Eco cells with 1 $\mu$g pCL-eco replication-incompetent helper vector[113] using calcium phosphate. Twenty four hours after transfection and twelve hours before the first virus harvest infection, plates were washed with PBS and refreshed with 5 mL complete BCM (45% DMEM, 45% IMEM, 10% FBS, 1% Penicillin-Streptomycin, 1% L-Glutamine). Virus was collected 4 times, every 12 hours starting from 12 hrs after BCM media change.

Hematopoietic stem and progenitor cells (HSPCs) were isolated from fetal livers at E13.5 and frozen until used. Cells were thawed 12 hours before first infection in BCM supplemented with 1 ng/mL IL-3, 10 ng/mL IL-6, 100 ng/mL SCF (stem cell factor) and incubated at 37˚C in 5% $CO_2$. Cultured HSPCs were infected four times at 12h intervals with viral supernatant from transfected Phoenix-Eco cells, supplemented with 1 ng/mL IL-3, 10 ng/mL IL-6, 100 ng/mL SCF and 4 $\mu$g/mL Polybrene, and spinoculated at 950 x g for 1h at 37˚C. Transduction efficiency was assessed by determining the $GFP^+$ population by flow cytometry using a Guava 8HT flow cytometer (Millipore).

For transplantations, 6-8 week old female C57BL/6 mice were placed on 0.125 mg/mL ciprofloxacin + 2% sucrose two days before transplantation. Four hours before transplantation, mice were irradiated with 4 Gy of γ radiation. Approximately 6 x $10^5$ – 8.2 x $10^5$ cells were transplanted into irradiated mice via intravenous tail-vein injection. Mice were maintained on antibiotics for 3 weeks post-transplantation. Mice were palpated twice a week to assess tumor status until the experimental end point at day 120. When tumors arose, mice were sacrificed and the masses harvested. Lymphomas were gently macerated between the frosted ends of two microscope slides and the resulting cell suspension was passed through a 40 $\mu$m cell strainer to isolate single cells.

These cells were then frozen in BCM + 20% FBS + 10% DMSO and stored in liquid $N_2$ until further used. All animal studies were approved by the McGill University Faculty of Medicine Animal Care Committee.

*2.4.2 Recovery of sgRNAs and T7 Endonuclease I Assay (T7EI)*

Genomic DNA was prepared from isolated tumor cells by lysing tumor cell pellets overnight in TNE buffer (10 mM Tris [pH 8.0], 100 mM NaCl, 25 mM EDTA [pH 8.0], 0.25% SDS, 125 $\mu$g/mL Proteinase K, 125 $\mu$g/mL RNase A) at 55˚C. Genomic DNA was deproteinized by extracting once with phenol, twice with phenol:chloroform: (50:50), and once with chloroform and recovered by ethanol precipitation using 0.3M NaOAc [pH 5.2]. PCR amplification of targeted loci was performed using Phusion High-Fidelity DNA polymerase (NEB) according to the manufacturer's recommendations. Amplified DNA was purified using BioBasic EZ-10 spin columns. The T7EI assay was then performed as previously described [72] and the entire reaction was resolved on a 15% 1 x TBE polyacrylamide gel (29:1 acrylamide:bisacrylamide) before staining with ethidium bromide.

*2.4.3 Sequencing of Modified Loci*

Targeted loci were amplified from tumor genomic DNA using primers designed with Primer3[114] and containing adaptor sequences (Table S3). The amplified loci were then cloned into pSKII(+) and inserts sequenced via Sanger sequencing using the T7 sequencing primer.

*2.4.4 Small Hairpin (sh) RNA Design*

The Designer of siRNA (DSIR) algorithm with extended rules described by Fellman et al.[115] was used to generate shRNAs targeting *Phip* and S*p3*. Five shRNAs targeting each gene were generated and cloned into the MLS retroviral backbone using unique *XhoI/EcoRI* restriction sites. After validation *ex vivo* in cell lines, the two most potent shRNAs were chosen for use in HSPC adoptive transfer experiments.

*2.4.5 PHIP and PHIP$^{R1212\Delta}$ Plasmids*

The PHIP cDNA was kindly provided by Dr. Anne-Claude Gingras (The Lunenfeld-Tanenbaum Research Institute, Toronto). From this cDNA, a truncation mutant was generated by excising the C-terminal region of PHIP using unique AgeI/XhoI sites and replacing it with an oligonucleotide containing a premature stop codon to generate PHIP $^{R1212\Delta}$. For insertion into MLS, the proviral backbone was digested with *BglII*, repaired with Klenow, and digested with *XhoI*. PHIP and PHIP $^{R1212\Delta}$) were excised from the parental plasmid by digestion with *AscI*, Klenow repaired, and digested with *XhoI*. Following gel purification, the PHIP cDNAs were ligated into MLS and the integrity of the resulting clones verified by sequencing.

*2.4.6 Antibody Generation and Western Blotting*

The DNA sequence encoding amino acids 661-913 of PHIP (Uniprot: Q8VDD9) were amplified from the complete cDNA with PCR Primers $^{5'}$GAATTCGAAGCAGGTGTTAGTAATGCCAG$^{3'}$ and $^{5'}$CTCGAGTCACTTTGGTGATGTTGGTCCATC$^{3'}$. This product was then cloned into pSKII(+) before subcloning into pGEX6p1 using unique EcoRI/XhoI restriction sites, which allow the in-frame addition of a GST tag to the N-terminus of the protein. The GST-fusion protein was then purified from BL21 *E. coli* induced with 0.3 mM IPTG for 4 hours. Bacteria were lysed in 1M NaCl, 50 mM Tris –HCl [pH 8.0], 1 mM EDTA [pH 8.0], 1 mM EDTA and protein was purified with Gluthatione Sepharose 4B (Amersham) before eluting with 50 mM Tris [pH 7.5], 10 mM reduced Glutathione. Proteins were dialyzed and stored in 50 mM Tris [pH8.0], 150 mM NaCl, 10 mM EDTA,1 mM DTT, and 20% Glycerol. The GST tag was cleaved from the purified PHIP antigen using GST-3C protease followed by subsequent retrieval from the flow-through following passage through a Glutathione Sepharose column. The resulting protein was used antigen for subsequent immunizations.

Protein extracts for immunoblotting were prepared by lysing tumor cell pellets in RIPA buffer (20 mM Tris-HCl [pH 7.5], 150 mM NaCl, 0.1% SDS, 1% NP40, 0.5% sodium deoxycholate, 1 mM β-glycerophosphate, 1 mM PMSF, 1 $\mu$g/ml leupeptin, 10

$\mu$g/ml aprotinin, and 2.5 $\mu$M pepstatin A) on ice for 10 minutes, followed by sonication. Extracts were then boiled for 10 minutes at 95˚C in 1X Laemmli sample buffer and resolved on a 6% or 8% NuPAGE gel. Proteins were transferred to PVDF membranes at 200 mA for 2h. The primary antibodies used in this study were: α-PHIP (1:1000, Bethyl laboratories, A302-055A), α-PHIP-N (1:1000), α-SP3 (1:1000, Santa Cruz, sc-655), α-actin (1:20000, Sigma, A5316), or α-eEF2 (1:1000, Cell Signaling, 2332). Secondary α–rabbit and α-mouse antibodies (Jackson Immunoresearch, 1:5000, 715-035-146/152) were used and the signal was visualized using enhanced chemiluminescence (ECL) (Perkin Elmer).

## 2.5 Results

### *2.5.1 Coupling CRISPR/Cas9 and the Eμ-Myc model to identify rare BL oncogenic drivers*

To functionally screen for rare oncogenic drivers from BL sequencing data, we took advantage of an adoptive transfer strategy utilizing the E$\mu$-Myc genetically engineered mouse model (GEMM) (Figure 2.1b). This GEMM is modeled after the defining Burkitt's translocation and recapitulates typical genetic and pathological features of human non-Hodgkin's lymphomas [96, 97]. It has been extremely useful for unraveling oncogene cooperation, defining pathway addictions, and elucidating drug response/genotype relationships *in vivo* in cancer[98]. From the large number of rarely mutated genes, we focused on genes that had incurred nonsense or frameshift mutations and thus could be engineered using CRISPR/Cas9 (Figure 2.1a, bottom panel and Table S1)[103-105] Perusal of the human BL mutation data identified 91 genes fulfilling these criteria, although in many cases, additional missense mutations were noted in independent BL samples (Figure 2.1a and Table S2). Our screen focused on genes not known to be drivers in this cancer type and that had not been previously characterized in BL. A few known tumor suppressors were retained (e.g. *Tsc1*, *TP53*) and served as positive controls in our assay [116, 117]. In total, 75 sgRNAs targeting the murine orthologs of genes infrequently mutated in BL were generated (Table S2).

We designed the sgRNAs to target their murine counterpart in the vicinity of the nonsense or frameshift mutation that had been documented in the human BL data. Testing of 9 randomly chosen sgRNAs indicated that all displayed significant editing activity, as assessed by the T7EI cleavage assay (Figure 2.2).

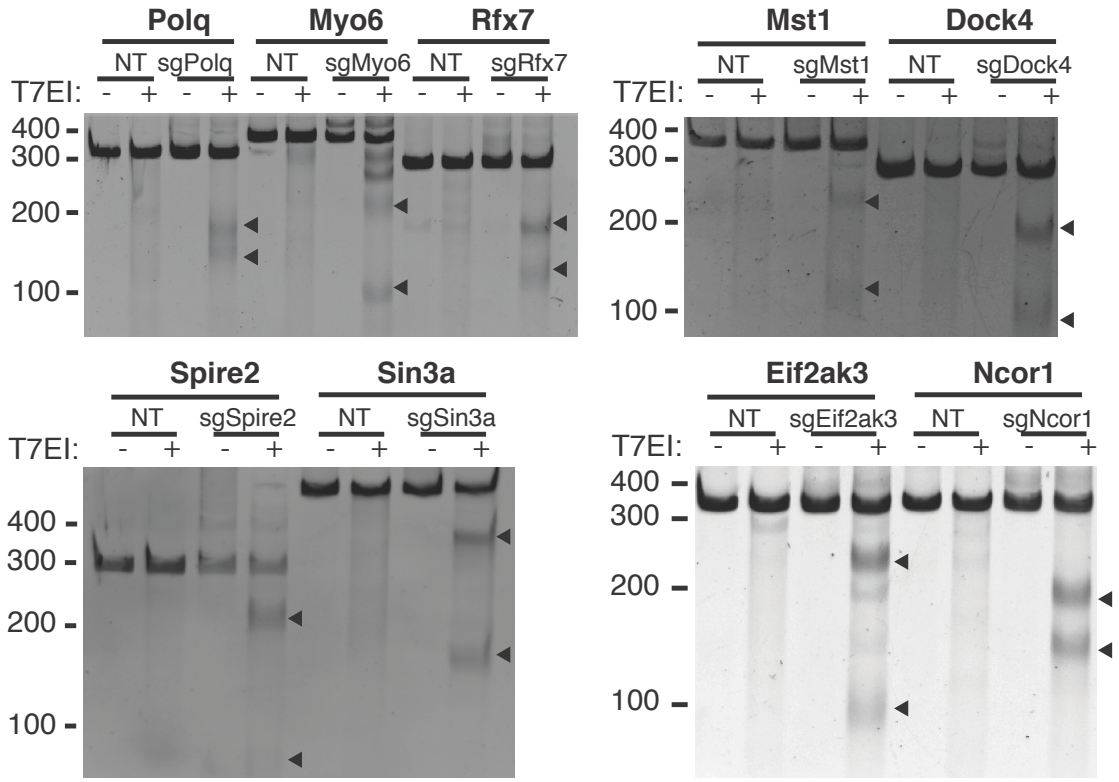


*Figure 2.2. Testing functionality of pQGiG2 constructs*

T7EI assay performed on DNA isolated from NIH 3T3 cells infected with pQCiG2 derivatives harboring sgRNAs to the indicated loci. NT, non-transduced.

One of the parameters that we wished to define before undertaking an *in vivo* screen in the E$\mu$-Myc model was to elucidate the sgRNA pool complexity that would enable identification of "hits" following reconstitution of HSPCs in transplanted recipients (Figure 2.1b). To this end, we used a well-characterized p53-targeting sgRNA, sgp53-1 and an sgRNA targeting the neutral Rosa26 locus as positive and negative controls, respectively [72, 118]. All sgRNAs were co-expressed with Cas9 from a second generation "All-in-One" retroviral vector that also produced green fluorescent protein (GFP), enabling tracking of infected cells by flow cytometry (Figure 2.1b)[102].

E$\mu$-Myc HSPCs transduced with undiluted sgp53-1, or with a 1:5 dilution of sgp53-1 in sgRosa26, produced tumors in recipients by ~25 days with complete penetrance (Figure 2.3a). Mice receiving HSPCs with sgp53-1 diluted 1:20 or 1:100 developed tumors with a slightly longer onset rate and with incomplete penetrance. In contrast, E$\mu$-Myc HSPCs transduced with undiluted sgRosa26 produced tumors with a median onset rate of ~80 days (Figure 2.3a). These results indicate that a functional sgRNA targeting a tumor suppressor gene could be reproducibly enriched from pools containing 5 different sgRNAs.

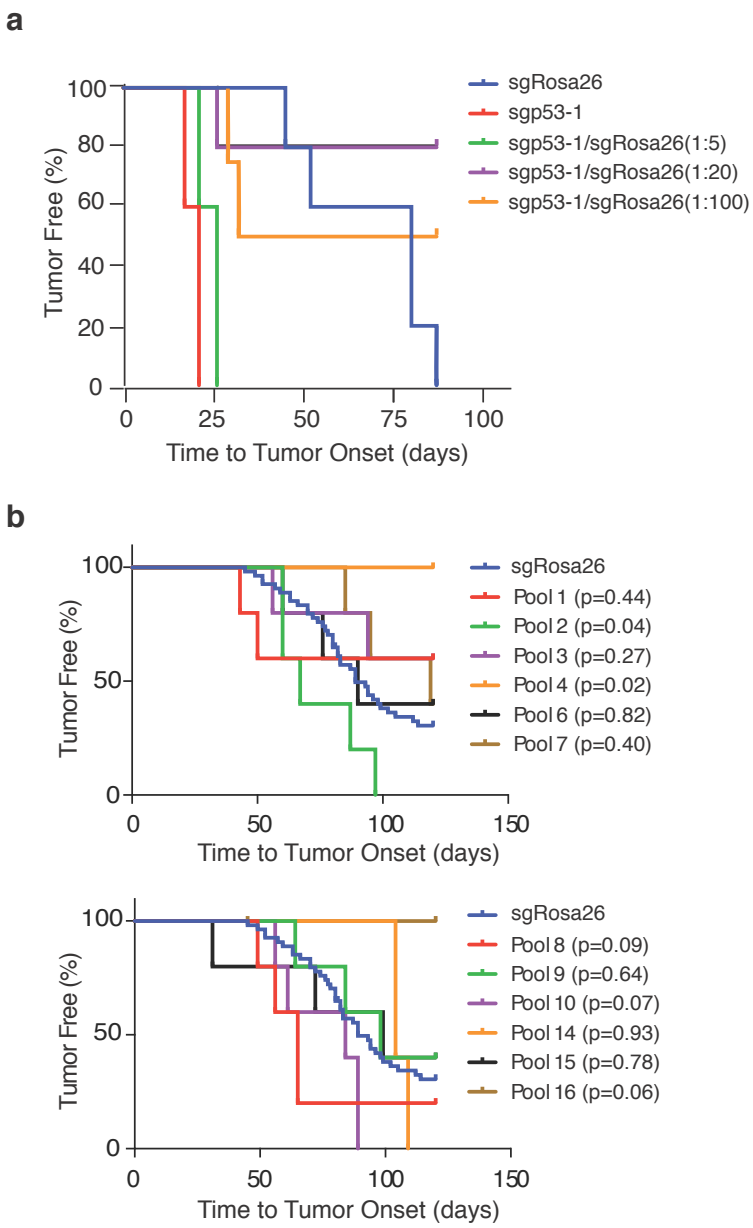


*Figure 2.3 Testing functional pool complexity and onset curves for non-significant pools*

**a)** Kaplan-Meier plot of tumor onset rates in mice transplanted with HSPCs transduced with pQCiG2/sgp53-1, pQCiG2/sgRosa26, and the indicated dilutions of pQCiG2/sgp53-1 with pQCiG2/sgRosa26. **b)** Kaplan-Meier plot of tumor onset rates in mice transplanted with HSPCs infected with the indicated sgRNA pools. Note that data from all cohorts receiving the sgRosa26 pool is combined and used as reference in these plots. In parenthesis are the p values (relative to sgRosa26 cohort) as determined by the Log-Rank Mantel-Cox Test.

*2.5.2 In vivo screening identifies candidate sgRNAs capable of promoting lymphomagenesis*

Based on the results of our dilution experiments, we screened our candidate genes in pools of five sgRNAs or fewer (Figure 2.1a and Table S1). This yielded a total of 16 pools that were used to transduce at least three independent HSPC populations and transplanted into five irradiated recipients. Four of the pools showed significantly increased tumor onset rates compared to mice having received HSPCs infected with pQCiG2/sgRosa26 (Figure 2.4a; $p<0.0001$, (Log-Rank Mantel-Cox Test)). None of the recipients receiving HSPCs infected with the other pools developed lymphomas at rates that were significantly faster than those obtained with pQCiG2/sgRosa26 (Figure 2.3b).

Despite the presence of a GFP reporter within our transduction vector, we found that not all of the recovered tumors were $GFP^+$, which we attribute to the absence of selective pressure to maintain expression from pQCiG2 following locus modification. To identify the tumor-promoting sgRNAs in tumors arising from sgRNA pools 5, 11, 12, and 13, we isolated genomic DNA from all lymphomas, amplified the sgRNA encoding sequences by PCR, and sequenced the amplified products. Two of five tumors from Pool 5 yielded PCR products that, when sequenced, revealed the presence of sgRNAs targeting only *Phip* (data not shown). T7EI analysis of the *Phip* locus in tumors revealed the presence of mutations at the *Phip* locus in those same two tumors (Figure 2.4b, Top panel: T1 and T5). We have not further characterized the three remaining tumors (T2, T3, T4) to determine the underlying oncogenic driver event since we failed to retrieve PCR products from these tumors. From Pool 11, 5/5 tumors revealed the presence of only *Sp3*-targeting sgRNA and T7EI analysis of these 5 tumors confirmed modification at the endogenous *Sp3* locus (Figure 2.4b, Middle panel). All tumors from Pool 12 harbored an sgRNA targeting *Tsc1* and indeed all 5 tumors showed evidence of mutagenesis at this locus (Figure 2.4b, Bottom panel). All tumors from Pool 13 revealed the presence of an sgRNA targeting *Tfap4* (data not shown).

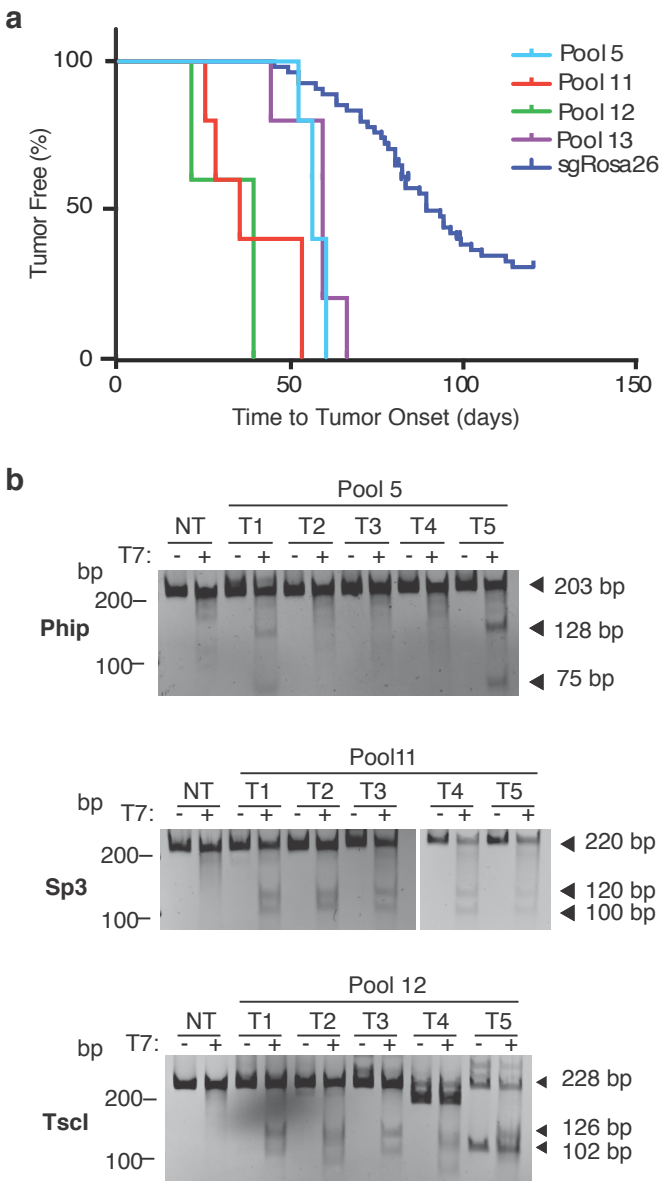


*Figure 2.4 Analysis of sgRNA pools exhibiting accelerated tumorigenesis.*

**a.** Kaplan-Meier plot of tumor onset rates in mice transplanted with HSPCs infected with the indicated sgRNA pools. Note that data from all cohorts receiving sgRosa26 are combined and used as reference in these plots. **b.** T7EI assay from individual tumors of the indicated pools or non-targeted (NT) control cells. The locus targeted for amplification is shown to the left of each gel.

*2.5.3 In vivo validation of candidate tumor suppressors*

We undertook to validate these results by repeating the HSPC adoptive transfer experiment using the original sgRNA on its own as well as a second independent, non-overlapping sgRNA (Figures 2.5 and 2.6 and Table S2). For *Sp3* and *Phip*, both sgRNAs lead to increased lymphoma onset compared to the Rosa26 cohort (Figs. 2.5b and 2.6b). For *Tfap4*, we were able to recapitulate accelerated tumorigenesis with the original sgRNA, but not with a second independent sgRNA (Figure 2.7) and thus did not further pursue *Tfap4* characterization. Sequencing of cloned amplicons obtained from PCR amplification across the sgRNA targeted loci for *Sp3* and *Phip* from tumors obtained in the validation experiment revealed indel mutations (Figures 2.8 and 2.9). We also noted considerable sequence heterogeneity at the *Sp3* or *Phip* loci within any given lymphoma indicating that the tumors that arose were polyclonal in nature and thus unlikely to be due to rare integration events that happened to inactivate a tumor suppressor locus. Western blot analysis of tumors obtained generated by CRISPR/Cas9 targeting of *Sp3* and *Phip* indicated significant reductions in levels of both proteins in all tumors analyzed (Figures 2.5c and 2.6c). We attribute the small residual protein levels to normal cells contaminating the tumor samples.

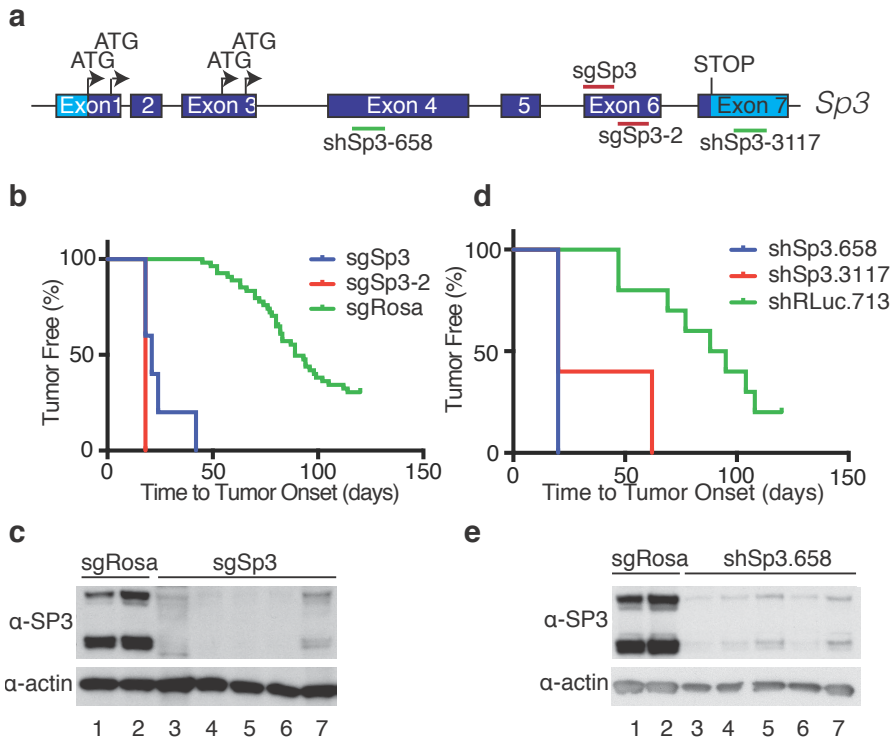


*Figure 2.5. Validation of Sp3 as a tumor suppressor.*

**a)** Schematic of the *Sp3* gene denoting targeted regions by the sgRNAs and shRNAs used in this study. Note that 4 protein isoforms are generated from the *Sp3* gene as a result of alternative translation initiation events[119]. The light blue shading represents untranslated regions whereas dark blue denotes coding exons. **b)** Kaplan-Meier plot of tumor onset rates in mice receiving HSPCs infected with retroviruses expressing the indicated sgRNAs. Data from all cohorts receiving sgRosa26 are combined and used as reference in this plot. **c)** Immunoblots comparing SP3 levels in tumors obtained from mice transplanted with HSPCs infected with Cas9/sgRosa26 or Cas9/sgSp3. **d)** Kaplan-Meier plot of tumor onset rates in mice receiving HSPCs transduced with retroviruses expressing the shRNAs targeting RLuc (neutral control) or *Sp3*. Data from all cohorts receiving shRLuc.713 were pooled and used as reference. **e)** Immunoblots assessing SP3 protein levels in sgRosa26- or shSp3.658-derived tumors

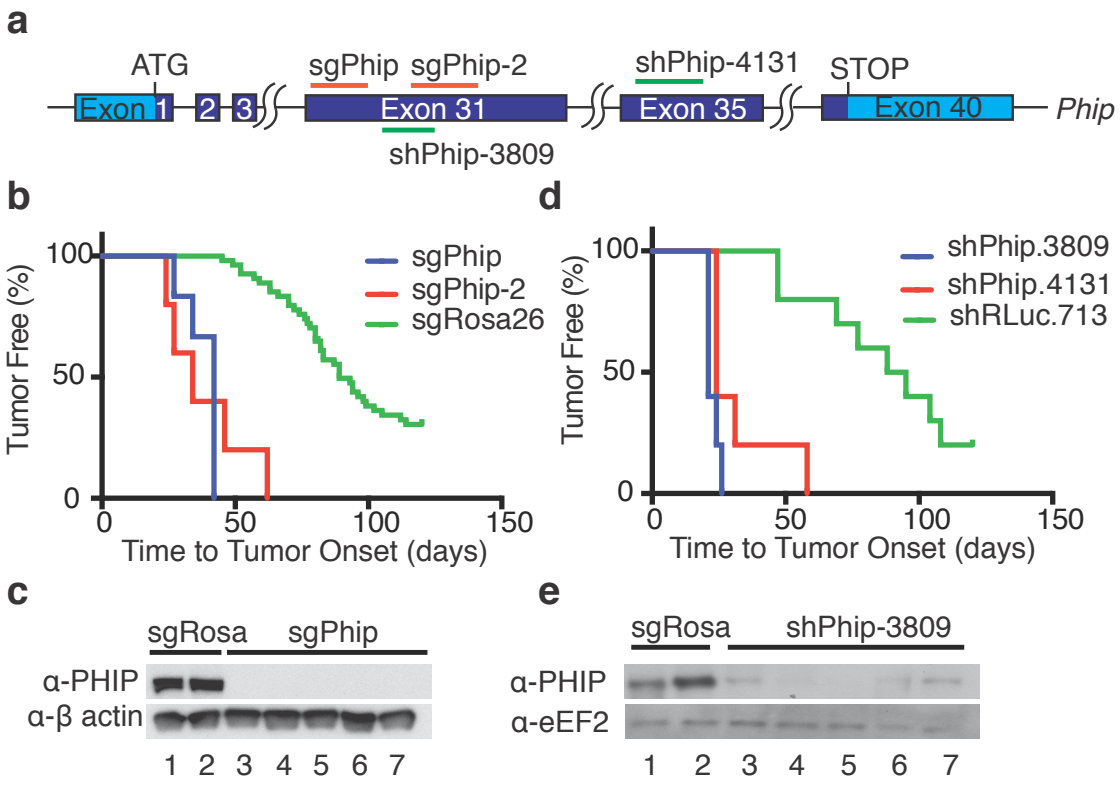


*Figure 2.6. Validation of Phip as a tumor suppressor.*

**a)** Schematic diagram of the *Phip* gene indicating the sgRNA and shRNA targeted sites. The light blue shading represents untranslated regions whereas dark blue denotes coding exons. **b)** Kaplan-Meier plot of tumor onset rates in mice receiving HSPCs infected with retroviruses expressing the indicated sgRNAs. Data from all cohorts receiving sgRosa26 are combined and used as reference in this plot. **c)** Immunoblots comparing Phip levels in sgPhip and sgRosa26 derived tumors. **d)** Kaplan-Meier plot of tumor onset rates in mice receiving HSPCs transduced with retroviruses expressing shRNAs targeting *Phip*. Data from all cohorts receiving shRLuc.713 were pooled and used as reference. **e)** Immunoblots comparing PHIP levels in sgRosa26- or shPhip.3809-derived tumors.

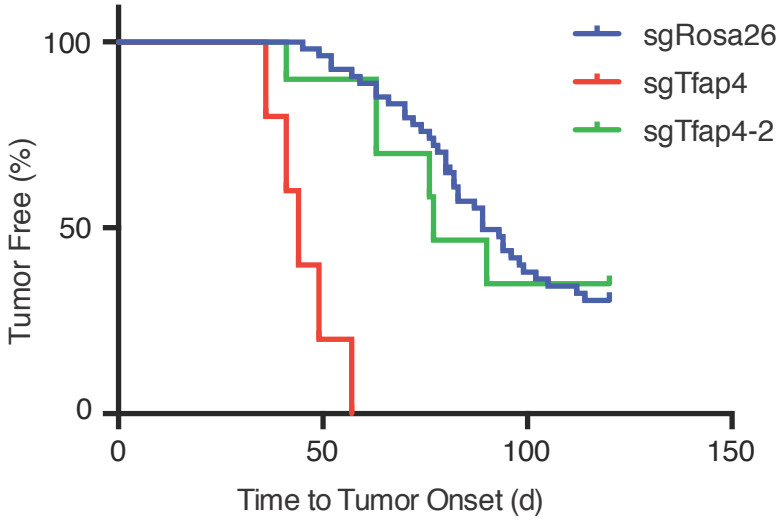


*Figure 2.7. Validation experiments for Tfap4*

Kaplan-Meier plot of tumor onset rates in mice transplanted with HSPCs transduced with pQCiG2/sgTfap4 and pQCiG2/sgTfap4-2. Compiled pQCiG2/sgRosa26 cohort data is used for comparison.

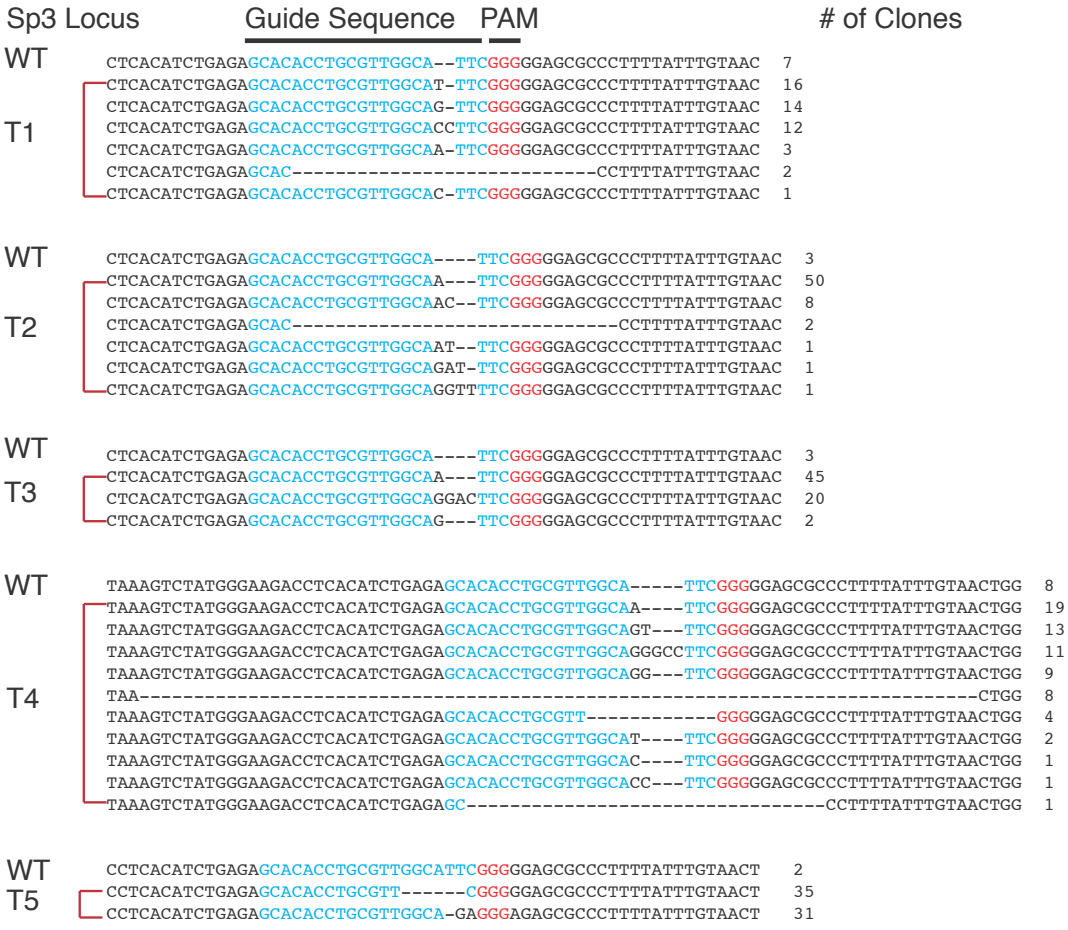


*Figure 2.8. Sequence analysis of the Sp3 locus from sgSp3 derived tumors.*

PCR products obtained following amplification of the *Sp3* locus were cloned into pSKII(+) and sequenced. The region targeted by the sgRNA is highlight in light blue and the PAM motif is denoted in red. Dashes represent deleted nucleotides and the number of clones harboring the indicated lesions is denoted to the right. The presence of wild-type alleles likely reflect contamination of the tumor by infiltrating wild-type cells or hemizygous inactivation being sufficient to drive tumor initiation.

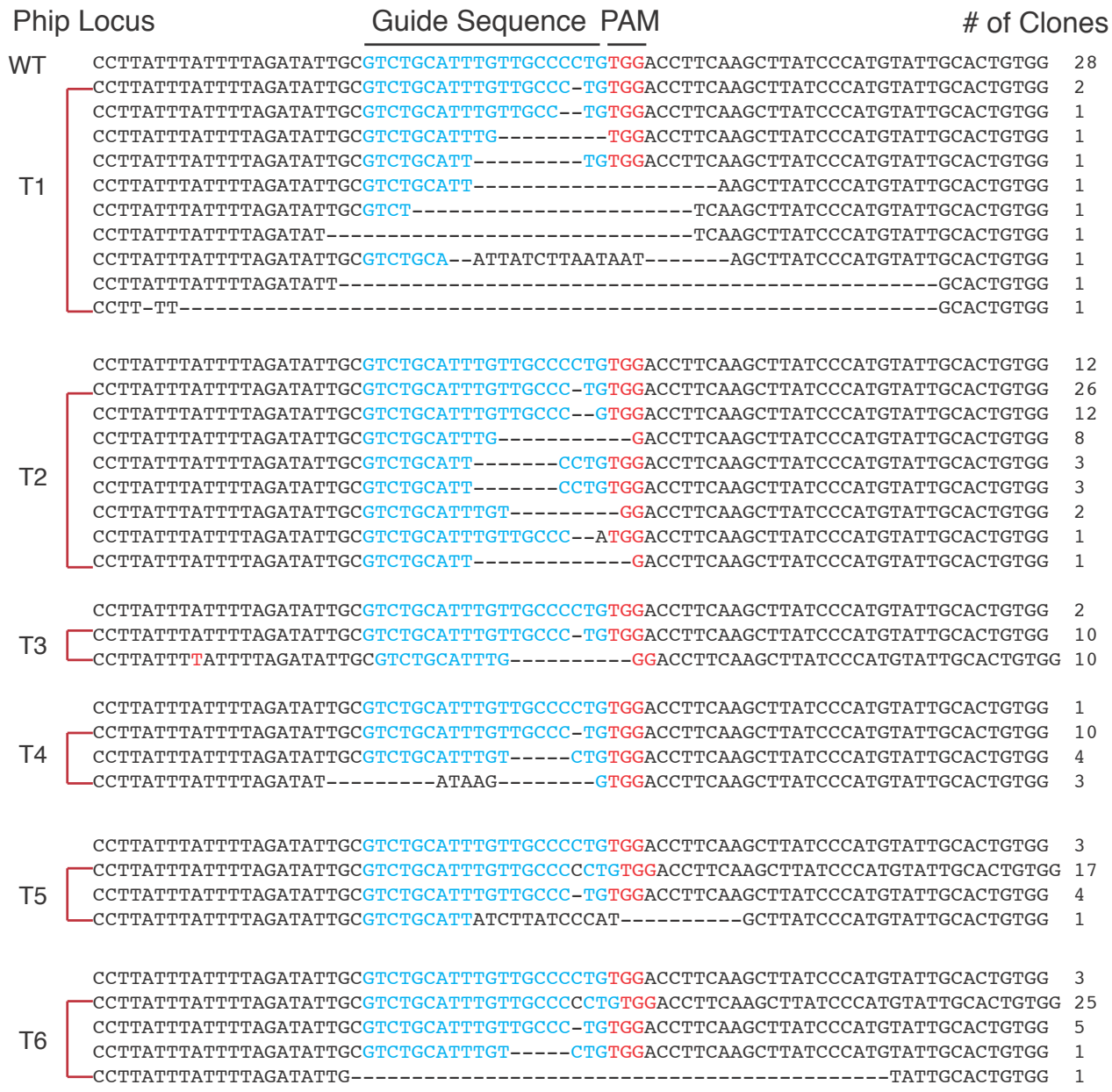


*Figure 2.9. Sequence analysis of the Phip locus from sgPhip-derived tumors.*

PCR products obtained following amplification of the *Phip* locus were cloned into pSKII(+) and sequenced. The region targeted by the sgRNA is highlighted in light blue and the PAM motif is denoted in red. Dashes represent deleted nucleotides and the number of clones harboring the indicated lesions is denoted to the right. The presence of wild-type alleles may reflect contamination of the tumor by infiltrating normal cells or hemizygous inactivation being sufficient to drive tumor initiation.

*2.5.4 SP3 and PHIP display tumor suppressive activity in vivo*

Both SP3 and PHIP have been reported to exhibit pro-oncogenic activity in other contexts. Reduced SP3 expression in the rat small intestinal cell line IEC-6 is associated with decreased apoptosis-related caspase activity, a phenomenon that is recapitulated using siRNAs[120]. Induction of SP3 expression in LS174 modified colon carcinoma cells leads to increased apoptosis and prevents tumor formation in nude mice[121], whereas in other situations, loss of SP3 is associated with reduced oncogenicity[122-124]. Similar conflicting data exists for PHIP[125]. Although predominantly a nuclear protein, over-expression of PHIP profoundly inhibits IRS-1 tyrosine phosphorylation levels[126], potently stimulates a mitogenic response mediated in part through transcriptional induction of cyclin D2[127], and inhibits caspase-9 and -3 activation in pancreatic b cells[127].

Therefore, to exclude the possibility that modification of the *Sp3* or *Phip* loci by CRISPR/Cas9 had led to the generation of gain-of-function truncation mutants, we targeted *Sp3* and *Phip* for knockdown using two independently generated shRNAs. Our rationale was that if loss of function was truly responsible for tumor initiation in our Cas9-based experiments (Figures 2.4b and 2.5b), we should be able to phenocopy this using shRNAs that reduce gene activity. In both cases, using two independent shRNAs, we observed significantly accelerated tumor onset as compared to a neutral control shRNA targeting renilla luciferase (Figures 2.4d and 2.5d). As expected, the resulting tumors showed significant reductions in target protein expression levels (Figures 2.4e and 2.5e). As well, ectopic expression of a PHIP C-terminal truncation mutant, lacking the same functional regions as expected from the human mutation identified in BL, did not lead to accelerated tumorigenesis following infection of E$\mu$-Myc HSPCs (Figure 2.10) In sum, our results demonstrate that both *Sp3* and *Phip* behave as tumor suppressors in E$\mu$-Myc driven lymphomas.

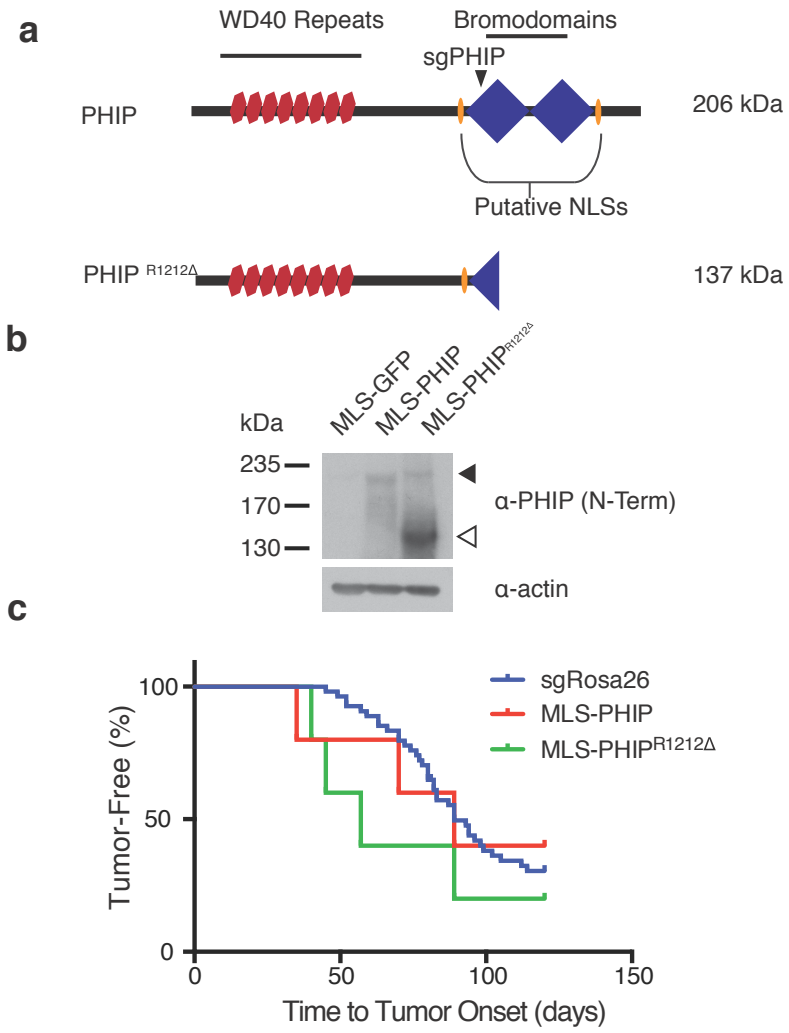


*Figure 2.10 Functional assessment of a PHIP truncation mutant in the Eμ-Myc model.*

**a)** Schematic diagram showing functional domains of PHIP and the site of the PHIP$^{R1212\Delta}$truncation mutation. **b)** Immunoblot illustrating ectopic expression of full-length PHIP and PHIP$^{R1212\Delta}$ in NIH 3T3 cells following retroviral transduction. Solid and white arrowheads indicate the position of migration of PHIP and PHIP$^{R1212\Delta}$, respectively. **c.** Kaplan-Meier plot of tumor onset in mice receiving HSPCs transduced with retrovirus expressing PHIP or PHIP$^{R1212\Delta}$.

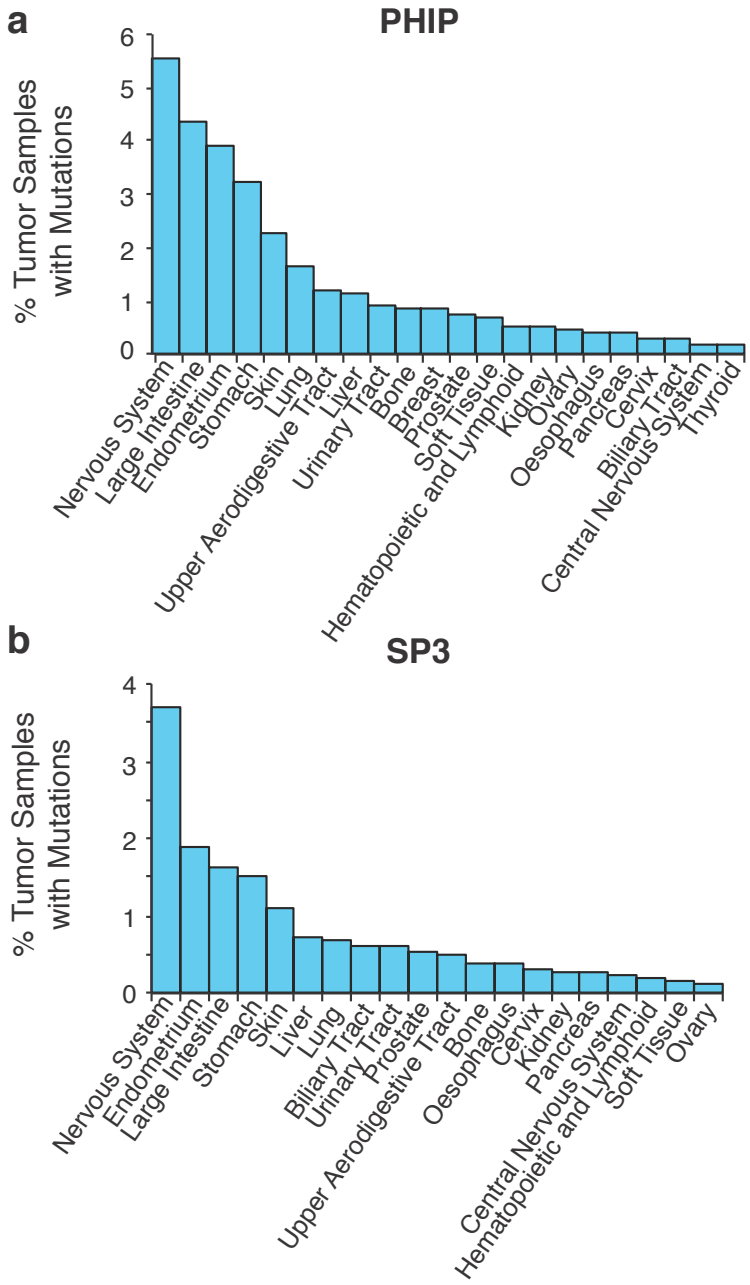


*Figure 2.11. Frequency of mutations in PHIP (**a**) and SP3 (**b**) across human tumor samples as reported from the COSMIC (v77) database* (http://cancer.sanger.ac.uk/cosmic).

## 2.6 Discussion

Our results provide a framework for identifying functionally relevant rare mutations in human tumor sequencing data. Our approach is complementary to bioinformatics initiatives that score for mutation frequency and predicted gene function to identify oncogenic drivers among tumor mutation data. Interestingly, perusal of the Catalogue of Somatic Mutations in Cancer (COSMIC) database revealed that *PHIP* and *SP3* are found mutated in other human cancers, including a small fraction of hematopoietic and lymphoid cancers (Figure 2.11). In the absence of our functional data and solely based on *in vitro* cell-based assays, the role of *Sp3* and *Phip* in tumorigenesis would have been difficult to assess or could have been misclassified. SP family members SP1/3/4 have been implicated as non-oncogenic addiction events in pancreatic cancer xenograft experiments[127]. *Sp3* null mice are not viable, succumbing to respiratory failure shortly after birth[128] and are impaired in hematopoiesis[129]. On the other hand, increased *Phip* copy number is correlated with ulceration in melanoma[130] and increased PHIP expression is linked to increased likelihood of metastasis and poor prognosis in melanoma patients whereas knockdown of *Phip* in mouse models prolongs survival and has been reported to protect against metastasis[125]. In embryogenesis, *Phip* is required for post-natal development in mice and its loss in the mouse leads to hypoglycemia, poorly developed lung epithelia, and death within 4-5 weeks after birth[131]. In the E$\mu$-Myc model, PHIP and SP3 demonstrated clear *in vivo* tumor suppressor activity (Figures 2.4 and 2.5). This may reflect context-dependency of tumor-suppressor activity as highlighted by eIF5A, which acts as a promoter of oncogenesis in a liver cancer model[132], but when knocked-down in the E$\mu$-Myc system, acts as a potent tumor suppressor[100]. CRISPR/Cas9 in concert with available deep-sequencing data and appropriate GEMM is thus a powerful approach to identify context-dependent lesions.

CRISPR/Cas9 is well-suited for the type of *in vivo* loss-of-function screens undertaken herein, but we note that our screen was not exhaustive: expanding the number of sgRNAs used per gene, increasing the animal cohort size, and technological improvements should improve the discovery rate and throughput of the screen. Related

to the latter point - an obvious limitation of this screen is the fairly low complexity of sgRNA screening pools used herein as compared to previously published shRNA screens[100]. One limitation is the large size of the pQCiG2 sgRNA/Cas9 retroviral delivery vector (~8 kbp) which leads to reduced viral titers and subsequent lower infection efficiencies[133]. Hence the incorporation of Cas9 alleles into cancer GEMMs[134] will allow the use of smaller sgRNA delivery vectors with higher viral titers and hence, transduction efficiencies.

Although BL and the E$\mu$-Myc model share the same initiating genetic lesion (i.e. a translocation leading to elevated MYC expression), the etiology of the murine and human diseases differ. As the translocation is present in the germline in the E$\mu$-Myc model, transformation arises in pro- and pre-B cells in the bone marrow at a time when the E$\mu$ enhancer becomes activated and begins driving MYC expression. Human BL however arises as a consequence of a *Myc* translocation occurring in more mature B cells present in lymph node germinal centers. This may be a limitation of the E$\mu$-Myc model and we may be under-estimating the number of oncogenic lesions in BL if any of these are B cell-stage specific. None-the-less the E$\mu$-Myc model has proven itself as an excellent genetic system for identifying lesions that co-operate with MYC *in vivo*[116]. This model has correctly reported on the ability of *p53* suppression[135] or *Tsc1 and Tsc2* loss[117] to accelerate tumorigenesis - two genes mutated in human BL.

In the era of personalized medicine, the identification of rare alleles that restrict tumorigenesis has important therapeutic implications. If some of the identified genes are pro-oncogenic in certain settings and are targets for drug development, defining context is critical to supporting correct clinical development. Also, understanding downstream networks perturbed by loss of PHIP or SP3 could lead to identification of new therapeutic targets. As well, rare mutational events may dilute the response to therapeutics targeting the more frequent mutational events and a better understanding of these rare events will enable better clinical stratification. If loss of PHIP or SP3 is also required for tumor maintenance, then this would support the rationale for biotherapeutic development, such as approaches aiming to systemically deliver wild-type protein[136]. The priority placed on developing tailored therapeutics to rare mutations that can drive

tumorigenesis will ultimate be determined by their relevance to tumor biology.

## 2.7 Acknowledgements

AK is supported by a Lymphoma Research Foundation Fellowship. This research was supported by a Canadian Cancer Society Research Institute (CCSRI) grant (#702778) to JP.

# Chapter 3: Inducible Genome Editing with Conditional CRISPR/Cas9 Mice

Alexandra Katigbak, Francis Robert, Marilène Paquet, Jerry Pelletier. (2016) Inducible Genome Editing with Conditional CRISPR/Cas9 Mice. *Manuscript in preparation.*

## 3.1 Preface to the Manuscript

Although CRISPR/Cas9 has shown remarkable utility in a plethora of investigations, advances in *in vivo* gene editing remain hampered by the question of delivery. Adenoassociated virus (AAV) vectors remain the delivery method of choice in mammals, however they are limited by their packaging capacity of ~4.9 kb and the expression of the most commonly used Cas9 variant requires a 4.2 kb cDNA [137]. We have also noted rather poor transduction efficiency of E$\mu$-myc HSPCs using an All-in-One CRISPR/Cas9 retroviral vector, which allowed only for the interrogation of rather low-complexity pools in a screening context [138]. We therefore decided to develop a transgenic mouse which would contain a germline doxycycline-inducible Cas9 allele, thereby allowing the development of smaller sgRNA delivery vectors and exploration of new experimental avenues.

## 3.2 Abstract

Genetically engineered mouse models (GEMMs) are powerful tools by which to elucidate gene function *in vivo*, provide insight into disease etiology, and identify modifiers of drug response. Increased sophistication of GEMMs has lead to the design of tissue-specific and/or inducible models in which genes of interest are expressed or ablated in defined tissues or cellular subtypes. Here we describe the generation of a transgenic mouse harboring a doxycycline-inducible Cas9 allele. Genome editing is achieved by exogenous delivery of sgRNAs and should allow for the modelling of a range of biological and pathological processes.

## 3.3 Introduction

Rapid and facile genome editing has been enabled through the use of type II bacterial CRISPR (clustered, regularly interspaced, short palindromic repeats)/Cas9 (CRISPR-associated protein) systems. By taking advantage of RNA-directed targeting, the Cas9 endonuclease is used to induce DNA breaks at a given locus. These are subsequently repaired by either the mutagenic NHEJ (non-homologous end joining) pathway or, if a template complementary to the targeted region is available, by HDR

(homology-directed repair). This game changing technology has been used in a myriad of applications; including *ex vivo* and *in vivo* genome editing and the rapid development of novel animal models for disease.

Genetically engineered mouse models (GEMMs) are powerful tools with which one can elucidate gene function *in vivo*, provide insight into disease etiology, and identify modifiers of drug response. Increased sophistication of GEMMs has lead to the design of tissue-specific and/or inducible systems in which genes of interest can be expressed or ablated in defined tissues or cellular subtypes. Indeed, to extend the utility of the mouse for CRISPR/Cas9-based functional genomic studies, transgenic mice expressing Cas9 in their germline have been developed. A Cre-dependent Cas9 knock-in mouse in which Cas9 expression is activated in a tissue-specific manner has been used to model lung adenocarcinoma by simultaneously inactivating *p53* and *Lkb1* by NHEJ, while generating $Kras^{G12D}$ alleles by HDR[134]. Prolonged expression of Cas9 in constitutively expressing mice is well tolerated [134]. Dow *et al.* [139] used a different approach and produced GEMMs co-expressing sgRNAs and DOX (doxycycline)-inducible Cas9 (as well as the nickase variant $Cas9^{D10A}$) in their germline. This platform illustrated the feasibility of inducible *in vivo* genome editing at multiple loci (*p53* and *Apc*) to model cancer progression[139]. A third Cas9 transgenic mouse strain was recently described harboring a Cre/loxP-dependent conditional Cas9 allele engineered into the *Rosa26* locus[140]. These powerful models are enabling the application of Cas9 editing technology to a number of tissue- and embryo-based settings.

Here, we report on the generation of a DOX-inducible Cas9 mouse in which we placed a TRE (tetracycline responsive element)-inducible Cas9 allele into the *Col1A1* locus. This mouse overcomes the *in vivo* delivery challenges of Cas9, avoids potential genotoxicity associated with *Cre* recombinase[141], and maintains flexibility with respect to choice of sgRNA delivery. We demonstrate viral-mediated sgRNA delivery achieves efficient editing in adoptive stem cell transfer experiments.

## 3.4 Materials And Methods

### *3.4.1 Generating Col1A1 Knock-in Cas9 Mice*

A pUC57 derivative (pUC57a) with appropriate linker sequences tailored for multi-component assembly of the donor template was purchased from GenScript and contained the following adaptor sequence: $^{5'}$CCATGGTGATGCATATGGCCGTGAAGAGACCCGCCGCCACCAAGAAGGCCGGCC TTAATTAAACGCGTTGAGAACTTCAGGGTGAGTTTGGGGACCCTTGATTGTTCTTTC TTTTTCGCTATTGTAAAATTCATGTTATATGGAGGGGGCAAAGTTTTCAGGGTGTTG TTTAGAATGGGAAGATGTCCCTTGTATCACCATGG$^{3'}$. Using unique FseI/PacI (NEB; New England Biolabs) restriction sites, the Flag-Cas9-IRES-GFP fragment from pQCiG2[102] was cloned into pUC57a. GFP was transferred from pUC57a-Cas9-IRES-GFP into pCol-TGM-p53.1224 [142] using NcoI (NEB). The resulting plasmid was partially cleaved with NcoI and the Cas9-IRES fragment from the parental pUC57a-Cas9-IRES-GFP vector transferred to generate pCol-Tre-Cas9-iG. Unique AscI/XmnI restriction sites were then used to transfer the CAGs-rtTA3-SAdpA cassette [143] [143] into pCol-Tre-Cas9-iG, downstream of GFP to generate the knock-in donor template, pCol-TCiG-rtTA3.

C10 ES cells were cultured in complete Knock-out DMEM (15% ESC Qualified Serum, 1% Penicillin-Streptomycin, 1% Non-Essential Amino Acids, 1% L-Glutamine, 0.1% BME, 0.01% LIF) on gelatinized plates with PMEF-N Feeders (Millipore). Fifty micrograms of pCol-TCiG-rtTA3 was electroporated with 25 $\mu$g of Flpe recombinase expression plasmid (pCAGs-Flpe) as previously described[144]. After 2 days of recovery, recombinant clones were selected using 140 $\mu$g/mL hygromycin, assessed for DOX inducibility, and used to generate chimeras. The TRE-Cas9 allele has been crossed onto the C57BL/6 background for 6 generations. All animal studies were approved by the McGill University Faculty of Medicine Animal Care Committee.

*3.4.2 Genotyping*

Cas9 allele status was assessed with primers Col1A1-F: $^{5'}$AATCATCCCAGGTGCACAGC$^{3'}$, SAdpA-R (from Mirimus, NY): $^{5'}$CTTTGAGGGCTCATGAACCTCCCAGG$^{3'}$, Col1A1-R: $^{5'}$ACCGCGAAGAGTTTGTCCTCAAC$^{3'}$. Primers Col1A1-F and Col1A1-R provided a characteristic 379 bp band indicative of the presence of Cas9, whereas Col1A1-F and SAdpA-R generated a 239 bp band indicative of a wt *Col1A1* locus. The *Rosa26* locus status was assessed using the following primers: Rosa-A: $^{5'}$AAAGTCGCTCTGAGTTGTTAT$^{3'}$, Rosa-B: $^{5'}$GCGAAGAGTTTGTCCTCAACC$^{3'}$, Rosa-C: $^{5'}$GGAGCGGGAGAAATGGATATG$^{3'}$. Rosa-A and Rosa-B produce a ~500 bp band, indicative of a wild-type *Rosa26* allele, while Rosa-A and Rosa-C produce a ~300 bp band, indicating the presence of the rtTA allele. E*μ*-Myc allele status was assessed using primers 5'E*μ*-Myc: $^{5'}$GGACAGTGCTTAGATCCAAGGTGA$^{3'}$, and 3'E*μ*-Myc: $^{5'}$CCTCTGTCTCTCGCTGGAATTACT$^{3'}$ which produce a 600 bp band when the E*μ*-Myc allele is present.

*3.4.3 Construction of pUSPPC sgRNA-expression Vectors*

To generate pUSPPC, we first replaced GFP in pQCiG2 with mCherry by digesting with EcoRV/ClaI to remove the IRES-GFP sequence. This was replaced with the EMCV IRES which was PCR amplified from pQCiG2 using primers "IRES-F" $^{5'}$AGTACGTAGATATCCCCATTAATCGATTTGAATTCCG$^{3'}$ and "IRES-R" $^{5'}$AGTACGTAATCGATACTAGTGTGGCCATATTATCATCG$^{3'}$ and digested with ClaI/EcoRV and ligated into the gutted pQCiG2 vector to produce 'pQCi'. The mCherry coding region sequence was amplified using PCR with primers "mCherry-F" $^{5'}$ATATCGCCTAGGCTTTTGCAAAAAGC$^{3'}$ and "mCherry-R" $^{5'}$ATATCGCCTAGGTTACTTGTACAGCTCGTCCATG$^{3'}$ using Vent polymerase according to manufacturer's instructions. This amplicon was then digested with AvrII and cloned into pQCi, which had been linearized with SpeI, to form 'pQCiC'. The Cas9 expression cassette was then removed from this vector using unique XhoI/EcoRV sites. The PGK-Puromycin cassette from pPrime-shRNA [145] was excised by first digesting

with PacI, repaired with T4 DNA polymerase, and cleaved with XhoI. The resulting product was ligated into pQCiC vector to generate pUSPPC.

*3.4.4 T7 Endonuclease I (T7EI) Cleavage Assay*

Genomic DNA from pUSPPC-transduced HSPCs was prepared using a Zymo Research Quick-gDNA MiniPrep kit (D3006). PCR amplification of the sgP53-3 targeted region of *Trp53* was performed using Primer F: $^{5'}$CTGTGCAGTTGTGGGTCAG$^{3'}$ and Primer R: $^{5'}$GGAGGCTGCCAGTCCTAAC$^{3'}$ with A-Key ($^{5'}$CCATCTCATCCCTGCGTGTCTCCGACTCAG$^{3'}$) and Tr-P1 ($^{5'}$CCTCTCTATGGGCAGTCGGTGAT$^{3'}$) adaptor sequences using Phusion High-Fidelity polymerase according to manufacturer's recommendations. The T7EI assay was then performed as previously described[72] [72] and the entire reaction resolved on a 15% 1x TBE polyacrylamide gel (29:1 acrylamide:bisacrylamide) before staining with SybrGold (ThermoFisher).

*3.4.5 HSPC Adoptive Transfers*

Low passage Phoenix-Eco packaging cells were cultured in complete DMEM (10% FBS, 1% Penicillin-Streptomycin, 1% L-Glutamine) and grown at 37˚C/5% $CO_2$. Twenty four hours prior to transfection, 3.5 million Phoenix-Eco cells were seeded in 10 cm tissue culture plates. Plasmids (10 $\mu$g) were co-transfected with 1$\mu$g pCL-eco replication-incompetent helper vector using calcium phosphate[113]. Twenty-four hours after transfection and 12h before the first virus harvest infection, plates were washed with PBS and refreshed with 5 mL complete BCM (45% DMEM, 45% IMEM, 10% FBS, 1% Penicillin-Streptomycin, 1% L-Glutamine). 12h after refreshing media, virus was then collected every 12 h for a period of 48h

R26-rtTA;TRE-CiG/rtTA;E$\mu$-Myc HSPCs were isolated from fetal livers at E13.5 days as previously described [146]. Cells were placed in culture 12 hours before first infection in BCM supplemented with 1 ng/mL IL-3, 10 ng/mL IL-6, 100 ng/mL SCF and incubated at 37˚C/5% $CO_2$. Cultured HSPCs were infected four times at 12h intervals with viral supernatant from transfected Phoenix-Eco cells, supplemented with 1 ng/mL

IL-3, 10 ng/mL IL-6, 100 ng/mL SCF and 4 $\mu$g/mL polybrene, and spinoculated at 950 xg for 1 hour at 32˚C. To induce Cas9 expression, cells were treated with 1$\mu$g/mL doxycycline. Transduction and GFP-induction efficiency was assessed by flow-cytometry prior to transplantation (Guava EasyCyte 8HT).

For transplantations, 6-8 week old female C57BL/6 mice were placed on 0.125 mg/mL ciprofloxacin/2% sucrose two days before transplantation. Four hours before transplantation, mice were irradiated with 4 Gy γ radiation. Approximately 6 x $10^5$ HSPCs were transplanted into irradiated mice via intravenous tail-vein injection. Mice were palpated bi-weekly to assess tumor status until the experimental end point at day 120.

*3.4.6 Immunoblotting*

Extracts were prepared from frozen cell pellets. Pellets were resuspended in RIPA buffer (20 mM Tris-HCl [pH 7.5], 150 mM NaCl, 0.1% SDS, 1% NP40, 0.5% sodium deoxycholate, 1 mM β-glycerophosphate, 1 mM PMSF, 1 mg/ml leupeptin, 10 mg/ml aprotinin, and 2.5 mM pepstatin A) on ice for 10 minutes. Lysates were denatured in Laemmli sample buffer by heating to 90$^o$C for 10 minutes. Proteins were resolved on 10% NuPAGE gels and transferred to PVDF membranes by electroblotting at 200 mA/gel for 2 hours. Antibodies used were: α-Flag (1:5000, Sigma), α-Cas9 (1:1000, Abcam ab191468), α-GAPDH (1:1000, Abcam ab8245), α-eEF2 (1:1000, Cell Signaling, 2332).

*3.4.7 Southern Blot Analysis of the Col1A1 Locus*

Genomic DNA was isolated from ES cell clones, digested with EcoRI, and fractionated on a 0.8% TBE agarose gel [147]. After transfer to Hybond N+ membranes, the DNA was interrogated using a probe targeting the hygromycin gene outside of the region targeted by the donor template. The probe was generated by PCR amplification using primers A ($^{5'}$ATGAAAAAGCCTGAACTCACCG$^{3'}$) and B ($^{5'}$CCAATGTCAAGCACTTCCG$^{3'}$) and labeled using ThermoFisher DecaLabel DNA Labeling Kit (K0662) with $^{32}$P-dCTP (New England Nuclear, MA). Following hybridization,

membranes were washed in 2x SSC/0.1% SDS once at 25˚C, twice at 55˚C, and then once with 1x SSC/0.1% SDS at 55˚C.

*3.4.8 Immunophenotyping and Immunohistochemical Analysis*

Spleens were harvested from mice, macerated, and passed through a 40 $\mu$m cell strainer to create single-cell suspensions. Red blood cells were eliminated by lysis in ACK lysis buffer (150 mM $NH_4Cl$, 10 mM $KHCO_3$, 0.1 mM EDTA) [pH 7.2] for 5 minutes on ice, before neutralizing with PBS. 300,000 cells were stained either with 0.06 $\mu$g PE-conjugated α-CD4 (BD Pharmigen 553652) or α-B220 (BD Pharmigen 553090) for 30 minutes before washing with PBS. $PE^+$ and $GFP^+$ populations were analyzed by flow cytometry (Guava EasyCyte 8HT, Millipore).

Tissues were harvested from mice and fixed in 10% buffered formalin for 48 h before embedding in paraffin. Sections (4 $\mu$m) were de-paraffinized using xylene and rehydrated through a series of decreasing ethanol washes, followed by a final water wash. Antigen retrieval was performed in a pressure cooker for 15 min in 10 mM sodium citrate (pH 6.0)/ 0.05% Tween-20. After washing, samples were blocked using TBS [pH 7.5]/ 10% FBS/ 1% BSA for 2h at RT and incubated with a-GFP antibodies (1:500, Cell Signaling, 2555) overnight at 4˚C. Slides were blocked with hydrogen peroxide for 10 minutes, incubated for 30 minutes with biotinylated goat anti-rabbit IgG and then streptavidin peroxidase (Anti-rabbit HRP/DAB detection kit, Abcam). Staining was performed using DAB chromogen and substrate from Abcam and counterstained using IHC-optimized hematoxylin (Vector Labs). Sections were dehydrated, mounted using permount, and slides scanned using an Aperio XT slide scanner with the resultant images analyzed using Aperio ScanScope.

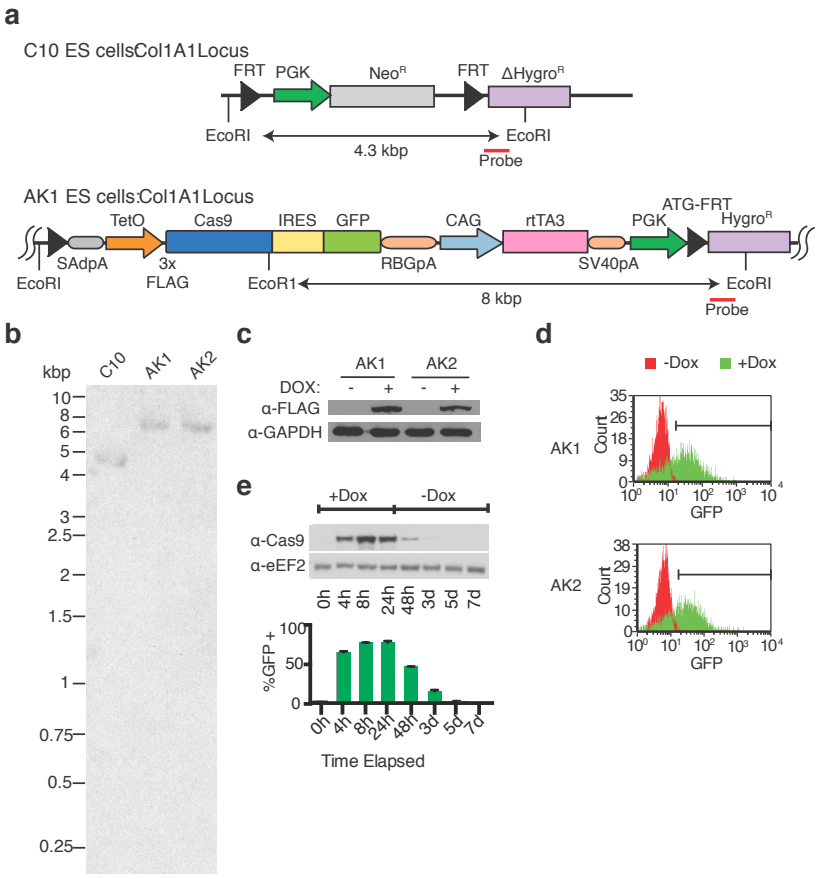


*Figure 3.1. Inducible and reversible Cas9 Expression in mouse ESCs.*

**a)** Configuration of the *Col1A1* locus in C10 ESCs as well as following Flpe-mediated recombination. Denoted are the diagnostic EcoR1 sites and region outside of the targeting vector used for probe generation (red bar) to confirm integration by Southern blotting. **b)** Southern blot analysis of the parental C10 ES cell line and two hygromycin-resistant clones (AK1 and AK2) using a downstream probe external to the FRT site (see panel A, red bar). **c)** Western blot indicating Cas9 induction in ESC clones 48 h following 1 ug/ml DOX treatment. Blots were probed with antibodies directed to the indicated proteins. **d)** GFP induction in ESC clones 48 h following 1 ug/ml DOX treatment as assessed by flow cytometry. **e)** Western blot illustrating reversible Cas9 expression in AK1 cells. AK1 cells were treated with 1 ug/ml DOX for 24 h, after which time fresh media lacking DOX was added. At the indicated time points, one aliquot of cells was taken to prepare extracts for Western blot analysis and another analyzed by flow cytometry.

## 3.5 RESULTS

### *3.5.1 Generation of a Doxycyline (DOX)-Inducible Cas9 Mouse*

Recombinase-mediated cassette exchange (RMCE) is a rapid method by which to generate transgenic mice with DOX-inducible cDNAs or shRNAs. This approach is facilitate by the existence of pre-engineered C10 ES cells containing a FRT-hygro-pA "homing" cassette downstream of the *Col1A1* locus [142, 148] (Figure 3.1a, top panel). We took advantage of the ease of manipulation of these cells and used FLPe recombinase to mediate recombination between the FRT sites at the *Col1A1* locus and a site present in the pCol-TCiG-rtTA3 targeting vector[142, 148]. In this vector, we placed Cas9 and GFP under regulation of the tetracycline response elements (TRE) and positioned a second transcriptional unit downstream with the CAGs promoter[149] driving reverse tet-transactivator (rtTA3) expression (Figure 3.1a, bottom panel). Following ES cell electroporation and RMCE, two hygromycin resistant cells (AK1 and AK2) were clonally expanded and characterized by Southern blotting to confirm correct integration at the desired locus, as revealed by the presence of an 8 kbp DNA fragment (Figure 3.1a and b). Both AK1 and AK2 showed DOX-dependent induction of Cas9 and GFP expression (Figure 3.1c and d). Expression of both proteins was reversible (Figure 3.1e).

### *3.5.2 Characterization of Inducible Cas9 Expression in Mice*

Transgenic mice were produced from AK1 ESCs, referred to henceforth as TRE-CiG/rtTA, and their preliminary characterization revealed weak global GFP induction in a large number of tissues following DOX treatment (data not shown). We reasoned that one possibility for this could be limiting rtTA3 activity and/or levels. Indeed, DOX induction of the TRE promoter *in vivo* can be restricted by limiting rtTA levels – as documented in GEMMs harboring conditional shRNAs[150]. Specifically, shRNA-mediated suppression of Replication Protein A, subunit 3 (Rpa3) *in vivo* has been shown to be more potent when two rtTA expressing alleles are present in the germline of shRpa3-bearing mice, compared to mice expressing only one rtTA allele[150]. We therefore crossed Rosa26(R26)-rtTA mice to the TRE-CiG/rtTA GEMM and found that

the resulting R26-rtTA;TRE-CiG/rtTA offsprings displayed higher induced levels of Cas9 and GFP in a number of analyzed tissues compared to TRE-CiG/rtTA mice following DOX exposure (eg, skin, spleen, thymus, small and large intestine, liver) (Figure 3.2a and b). Robust induction of GFP was also observed in B cells isolated from spleen and thymus of R26-rtTA;TRE-CiG/rtTA mice (Figure 3.2c).

We did not notice any evidence of toxicity associated with expression of the Cas9 transgene. Mice harboring the TRE-CiG/rtTA allele were fertile, had normal litters, and appeared morphologically normal. The TRE-CiG/rtTA allele was inherited at the expected Mendelian frequency with no significant associated sex effects in the inheritance pattern (Figure 3.3a). Long-term (6 months) treatment of R26-rtTA;TRE-CiG/rtTA mice with DOX did not affect weight gain (Figure 3.3b) nor overall general behavior. Cas9 was still expressed in tissues of mice continuously receiving DOX for 6 months and in many, levels appeared even higher than in tissues from R26-rtTA;TRE-CiG/rtTA mice that had been on DOX for only 1 week (Figure 3.3c). Tissue analysis showed no discernible histological changes and we found no significant pathology (Figure 3.3d and Table S5). Additionally, blood chemistry from R26-rtTA;TRE-CiG/rtTA mice after 6 months of DOX treatment showed almost all values within normal range, with the values of blood cholesterol and potassium being the only parameters only slightly outside the norm (Table S4). Thus, consistent with what was reported for mice constitutively expressing Cas9[134], long term sustained Cas9 expression is not associated with any overt detrimental phenotype or negative impact on the animal's well being.

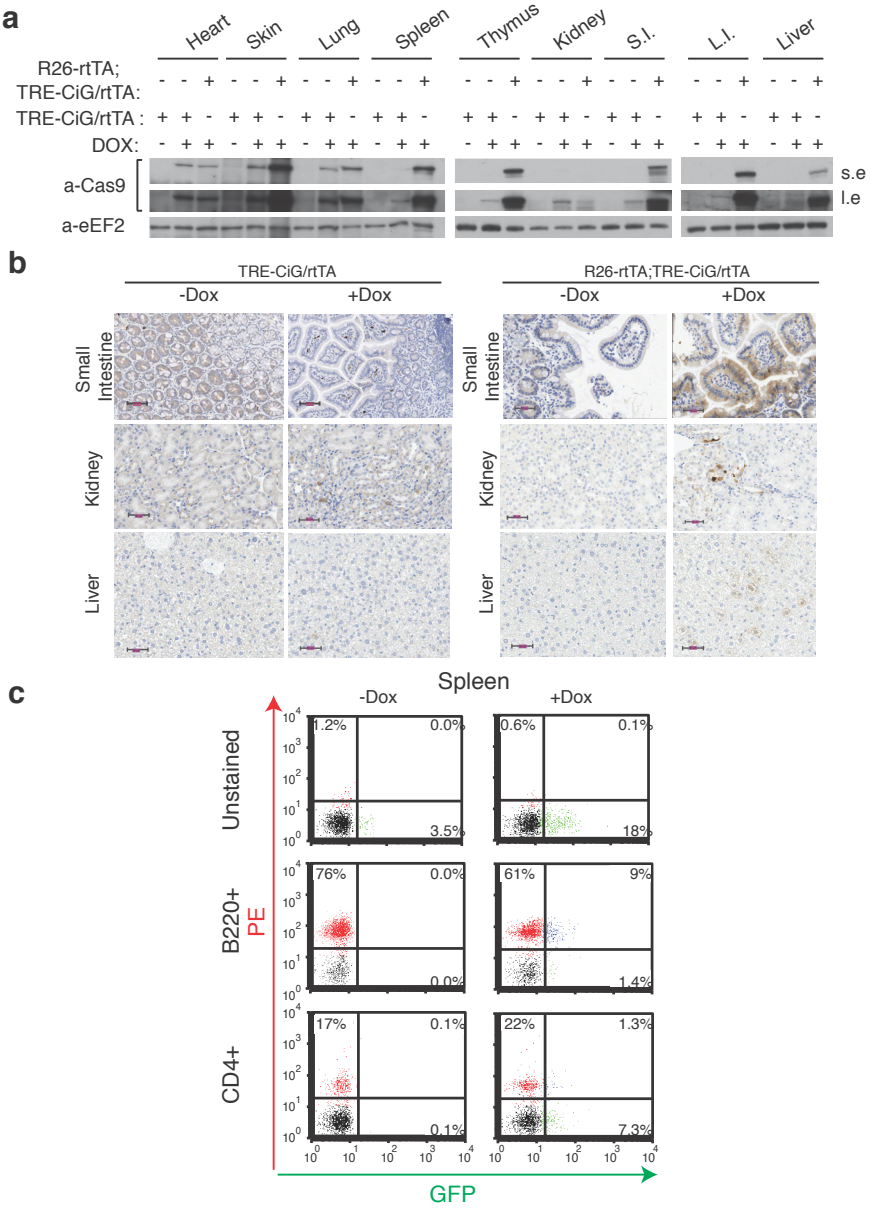


*Figure 3.2. Inducible Cas9 expression*

**a)** Western blot of Cas9 from the indicated tissues harvested from TRE-CiG/rtTA mice treated with vehicle (-) or DOX (+) and from R26-rtTA;TRE-CiG/rtTA mice treated with DOX for 1 week. s.e., short exposure; l.e., long exposure. **b)** Immunohistochemical staining for GFP expression in the small intestine, kidney, and liver from the indicated mice (+/- DOX). Magnification bars denote 50 um. **c)** Quantitation of B220+ cells isolated from the spleen and thymus of R26-rtTA;TRE-CiG/rtTA mice that had been treated with DOX for 1 week.

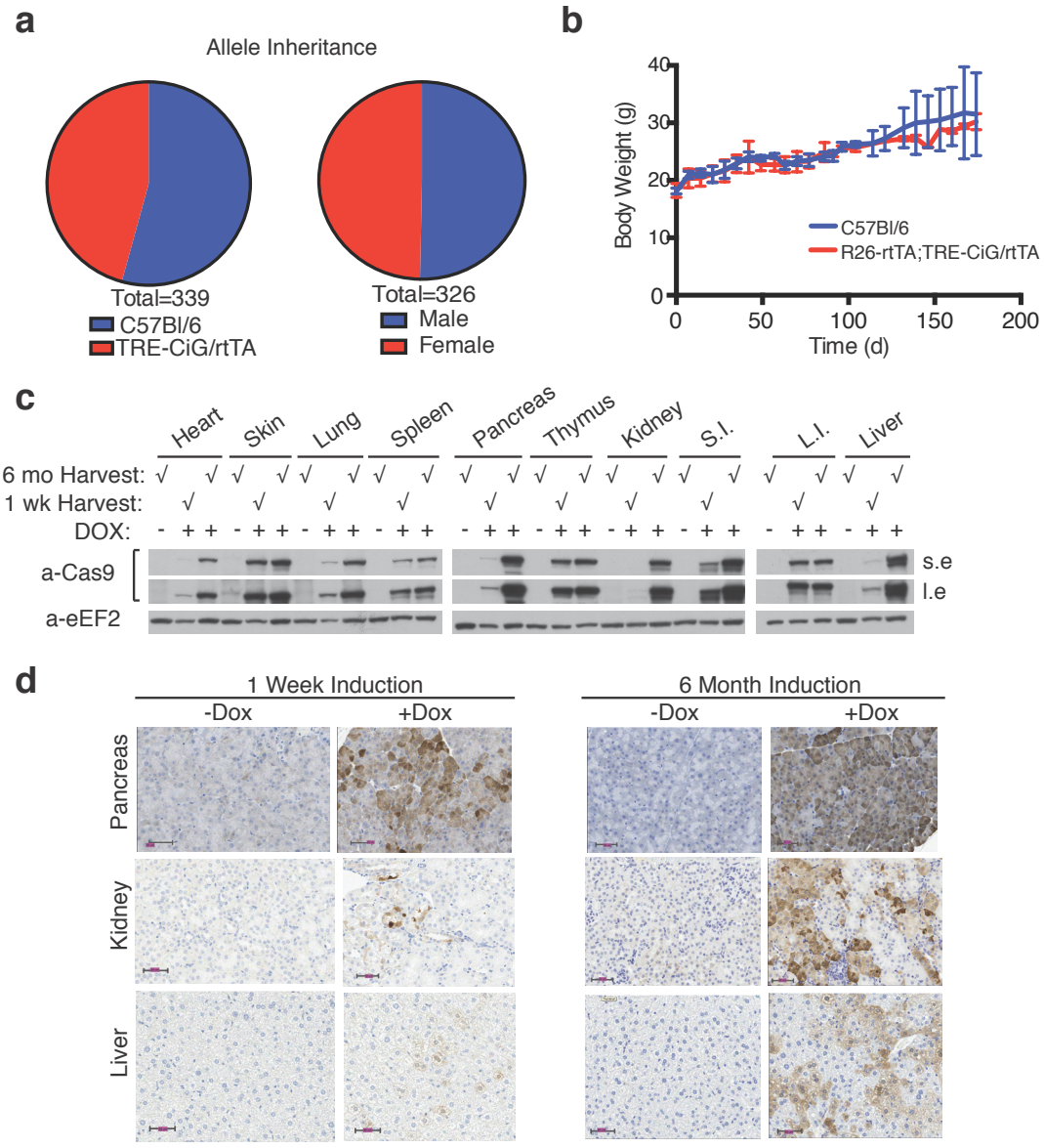


*Figure 3.3. Long Term expression of Cas9 is well tolerated in the mouse*

**a)** Mendelian inheritance frequency of the TRE-CiG/rtTA allele, as well as sex distribution of the inheritance frequency. **b)** Body weight of the indicated mice that had been treated with DOX or vehicle for 6 months. N= 2 mice +/- SD. **c)** Western blot of Cas9 from the indicated tissues harvested from R26-rtTA;TRE-CiG/rtTA mice treated with vehicle (-) or DOX (+) for 1 week (wk) or 6 months (mo). **d)** Immunohistochemical analysis of GFP expression in the pancreas, kidney, and liver from R26-rtTA;TRE-CiG/rtTA mice exposed to vehicle or DOX for 1 week (left) or 6 months (right). Magnification bars denote 50 um.

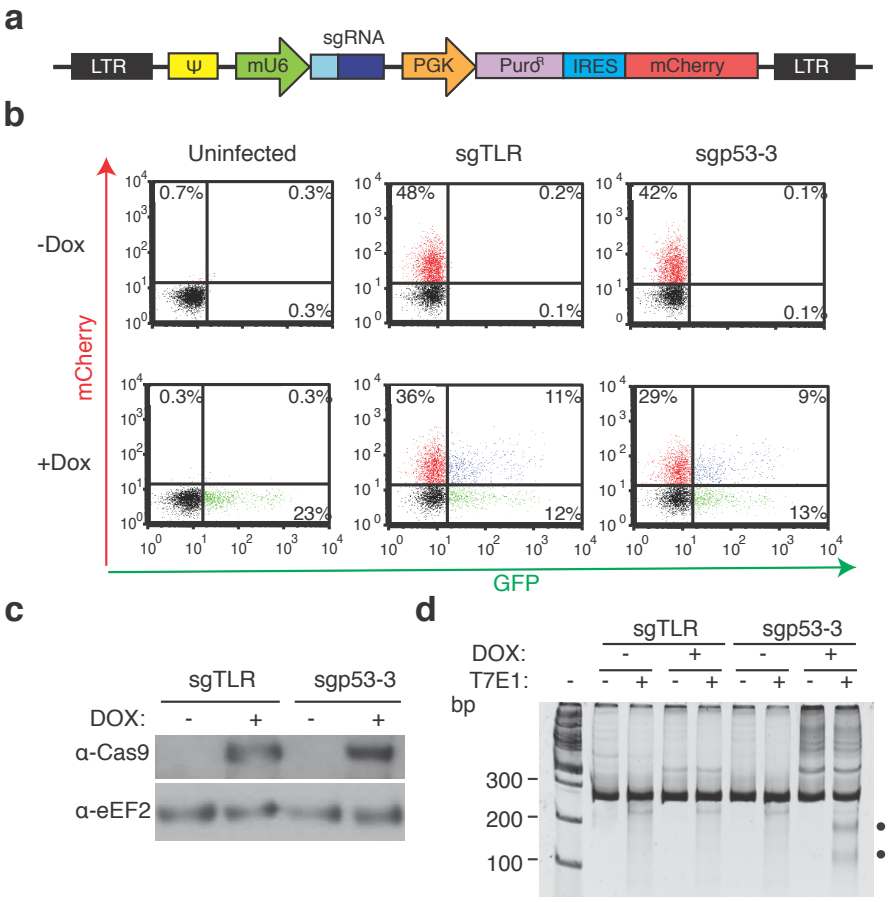


*Figure 3.4. DOX-inducible Genome Editing* Ex Vivo

**a)** Schematic representation of pUSPPC sgRNA vector. **b)** Flow cytometry analysis of R26-rtTA;TRE-CiG/rtTA HSPCs infected with pUSPPC expressing a neutral sgRNA (sgTLR: $^{5'}$AGCAGCGTCTTCGAGAGTG$^{3'}$ ) or targeting p53 (sgp53-3: $^{5'}$AAGUCACAGCACAUGACGG$^{3'}$). Following infection, cells were exposed to vehicle or DOX (1 ug/ml) for 3 days. Infected cells are mCherry+ and those responsive to DOX are mCherry+/GFP+. **c)** Western blot showing induction of Cas9 expression in R26-rtTA;TRE-CiG/rtTA HSPCs exposed to DOX for 3 days. **d)** T7E1 assay from DNA isolated from the indicated HSPCs. The dark circles denote the position of migration of cleaved products observed with DNA from pUSPPC-sgp53-3 infected R26-rtTA;TRE-CiG/rtTA HSPCs exposed to DOX for 2 days.

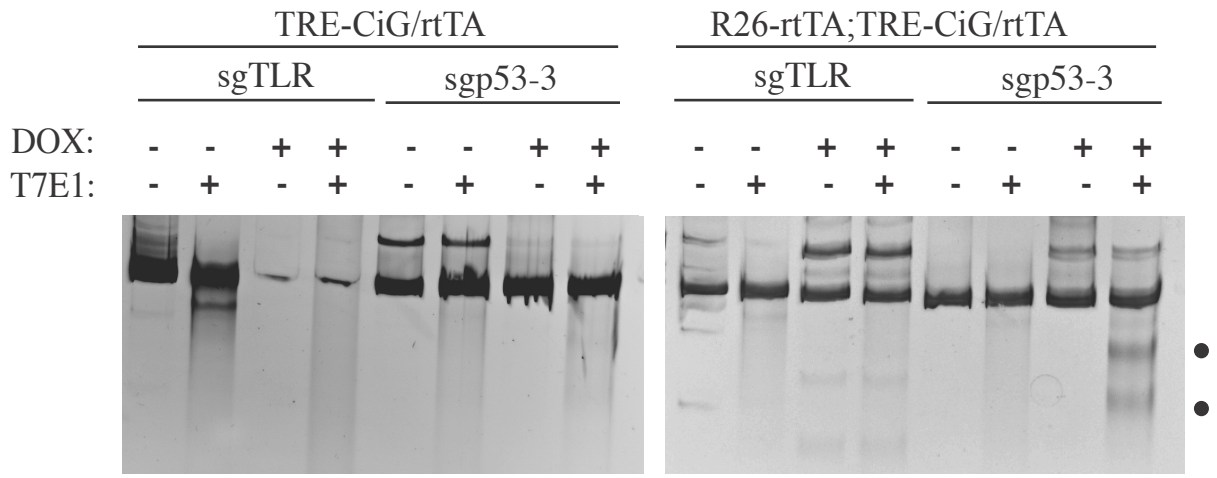


*Figure 3.5. Dosage effect of rtTA alleles in the TRE-CiG mouse HSPCs*

Two rtTA Alleles drive stronger Cas9-mediated editing than a single rtTA allele in HSPCs. T7E1 assay from DNA isolated from the indicated HSPCs. The dark circles denote the position of migration of cleaved products observed with DNA from pUSPPC-sgp53-3 infected R26-rtTA;TRE-CiG/rtTA HSPCs exposed to DOX for 2 days.

*3.5.3 Ex Vivo Genome Editing in Primary Hematopoietic Stem and Progenitor Cells (HSPCs)*

In our mouse, the spatial induction of Cas9 is determined by the sites of expression of the rtTA alleles. Very powerful genetic screens for novel oncogenic drivers have utilized the E*μ*-Myc model, a GEMM that predisposes mice to lymphomagenesis. For example, the approach has identified novel oncogenic drivers by infecting E*μ*-Myc HSPCs with libraries of shRNAs followed by transplantation into normal recipients and monitoring for tumor onset[100]. As a prelude to future experiments in which sgRNAs could be used for *in vivo* screens in the E*μ*-Myc model[151], we sought to assess if we could obtain Cas9-mediated editing in HSPCs that had been isolated from R26-rtTA;TRE-CiG/rtTA mice. For this, we tailored a retroviral delivery vector, pUSPPC, to constitutively express sgRNAs as well as puromycin and mCherry selectable markers (Figure 3.4a). Infection of HSPCs derived from R26-rtTA;TRE-CiG/rtTA mice with pUSPPC lead to infection rates ranging from 30-48% (mCherry$^{+}$ cells) (Figure 3.4b). Cas9 expression was induced upon exposure of HSPCs to DOX *ex vivo* (Figure 3.4c). Infection of these with pUSPPC-sgp53-3 revealed editing at the p53 locus 2 days later (Figure 3.4d). Consistent with our previous findings (Figure 3.2), significantly higher levels of modification were observed when two rtTA alleles [R26-rtTA;TRE-CiG/rtTA] were present in HSPCs compared to only one [TRE-CiG/rtTA] (Figure 3.5). These results show that Cas9 is inducible and functional in HSPCs and that conditional editing can be achieved in HSPCs *in vitro*.

*3.5.4 Ex vivo manipulation of HSPCs and adoptive transfer experiment in the Eμ-Myc GEMM*

The E*μ*-Myc mouse model is a robust and malleable model of non-Hodgkin's lymphomas [97]. We have previously demonstrate that delivery of Cas9 with an sgRNA targeting p53 to E*μ*-Myc HSPCs *ex vivo* accelerated tumor onset rates in transplanted recipients compared to recipients who received HSPCs infected with Cas9/sgRosa26[97]. However, transduction efficiencies of HSPCs with an All-In-One vector was disappointing low, precluding screens involving high complexity pools[138].

We compared the ability of HSPCs isolated from E$\mu$-Myc mice (infected with the All-In-One vector, pQCiG2, expressing sgTLR (a neutral sgRNA) or sgp53-3) to form tumors compared to HSPCs isolated from R26-rtTA;TRE-CiG/rtTA;E$\mu$-Myc mice (transduced with pUSPPC expressing sgTLR or sgp53-3) (Figure 3.6). The results indicated that pUSPPC driven sgp53-3 was as efficient at driving tumorigenesis in R26-rtTA;TRE-CiG/rtTA;E$\mu$-Myc HSPCs as pQCiG2 driving sgp53-3 production in E$\mu$-Myc HSPCs, as was a 1:5 dilution of sgP53-3. A further dilution of pUSPPC-sgP53-3 to 1:50 also accelerated tumor onset .

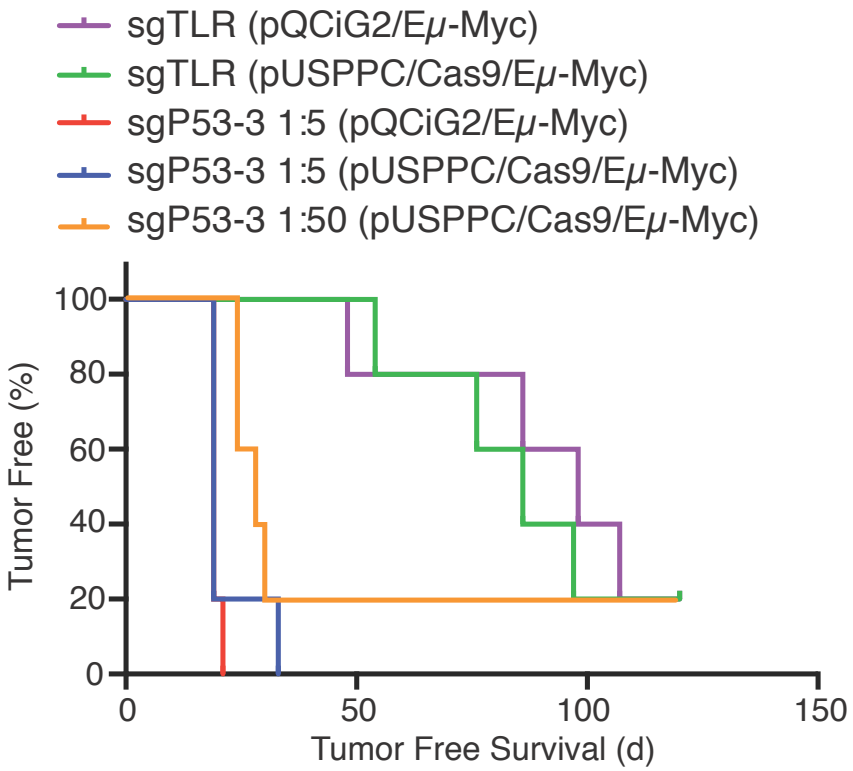


*Figure 3.6. Effectiveness of GEMM for* in vivo *functional assays*

Kaplan-Meier plot indicating tumor-free survival of C57B/6 mice receiving either Eμ-Myc HSPCs transduced with the All-in-One pQCiG2 system, or Eμ-Myc;R26-rtTA;TRE-CiG/rtTA HSPCs transduced with the more compact pUSPPC system. Tumor onset curves for pUSPPC-sgP53-3 diluted in pUSPPC-sgTLR 1:5 or 1:50 are overlaid.

## 3.6 DISCUSSION

Herein, we describe the generation of a mouse model that inducibly expresses Cas9 across a wide range of tissues upon administration of doxycycline. Although Cas9-expressing mice exist, our iteration distinguishes itself in a number of ways. Platt et al.[134] developed a Cre-dependent CRISPR-Cas9 mouse which constitutively expresses Cas9 in tissues expressing Cre-recombinase. Although in their model (as in ours) long-term Cas9 expression was not deleterious at an organismal level, Cas9 is a foreign antigen and one concern is generating an immune response that could target for elimination cells from the edited pool. Indeed, experiments with adenovirus-mediated delivery of Cas9 and sgRNA to the liver resulted in a Cas9-specific immune response [152]. Similar findings were also reported following delivery of split-Cas9 moieties via adeno-associated virus (AAV) vectors[153]. As well, given that off-target effects are an ever-present concern when it comes to genome editing, constitutive Cas9 expression is unwanted, especially since longer-term expression of Cas9 is associated with more off-target damage than transient Cas9 expression [154] [155]. Dow et al.[139] have successfully generated transgenic mice that demonstrate inducible CRISPR/Cas9 editing upon doxycycline administration. This inducible system is quite powerful but limited in that the sgRNA expression cassette is co-integrated with Cas9, therefore necessitating generation of a new strain for every target. The TRE-CiG/rtTA mice we describe here addressed these issues. It is a doxycycline inducible system, which allows for controlled, short-term induction of Cas9 expression, which should decrease off-target mutagenesis and mitigate host immune responses against Cas9. Additionally, any sgRNA of choice can be introduced into these mice, allowing for flexibility and facile multiplexing, making it a robust addition to the CRISPR/Cas9 toolbox.

## 3.7 ACKNOWLEDGEMENTS

AK is supported by a Lymphoma Research Foundation Fellowship. This research was supported by a James McGill Professor Award, a Merck, Sharp & Dohme Corp/McGill Faculty of Medicine Grant for Translational Research grant, and a grant from the Richard and Edith Strauss Canada Foundation to JP.

# Chapter 4: General Discussion

### 4.1 CRISPR/Cas9 in functional in vivo screening

With the ready availability of high-resolution genome sequencing data of both normal and disease tissues, there is great interest in using this data to identify which reported variants are important drivers of disease. Most often, this involves bioinformatics approaches where the most frequently mutated gene or sets of genes are identified and then queried with functional assays. However, what we often see in disease sequencing data is a handful of frequently mutated genes and a vastly larger number of infrequently mutated ones. Additionally, there are samples where the more frequent mutations are not present. To address this discrepancy, we demonstrate in Chapter 2 a complementary application of the CRISPR/Cas9 system in a functional *in vivo* screens to identify rare drivers of oncogenesis. By targeting sgRNAs to those infrequently mutated genes reported in three deep sequencing studies [103-105] we identified two genes with novel tumor suppressor function: *Phip* and *Sp3.* These genes are reported in the Catalogue of Somatic Mutations in Cancer (COSMIC) to be mutated in a number of different human tumor types, including a small number of hematopoietic or lymphoid malignancies (Figure 2.11). Additionally, *Sp3-/-* embryos have been shown to have impaired hematopoiesis *[129].* Using the more conventional bioinformatics approach, these genes likely would have notbeen investigated, leaving our knowledge of the system incomplete. Interestingly, both Phip and Sp3 have been reported to have either pro- and anti-cancer properties in a number of different cancers and cancer models. Increased *PHIP* copy number and PHIP expression are correlated with severity of melanoma in human patients [125, 130], whereas knockdown of Phip in a mouse model reduces metastatic potential and promotes survival [125]. Similarly, exogenous expression of SP3 in LS174 modified colon carcinoma cells leads to increased apoptotic events as well as abrogating the ability of these cells to form tumors in nude mouse xenograft experiments [121]. However, loss of SP3 expression has also been demonstrated to reduce oncogenic potential in through a number of different processes such as through regulation of histone deacetylases [122], regulation of proteins that are known metastatic markers [123], and regulation of proteins involved in the regulation of cell death [124]. However, in the E$\mu$-myc model, both Phip and Sp3 demonstrate clear

tumor suppressor function. This again highlights the utility of developing in vivo assays with functional significance, as bioinformatics and cell culture-based approaches cannot give a complete view of biological systems and thus can be limited in what they can uncover. CRISPR/Cas9 offers a great deal of potential for exploration in this area.

### 4.2 Improvements on the E*μ*-Myc Screen

There are clearly several limitations on the screen we have performed and there remains much room for improvement. First, expanding the number of sgRNAs targeting each candidate gene could have increased the power of our screen, providing a safeguard against false negatives resulting from inefficient sgRNA activity, or disruption of the target gene which is well tolerated. Additionally, expanding the animal cohort size would have increased the statistical power of our screen. However, one of the greatest limitations of our screen in comparison to previous shRNA screens in the same model is the relatively low complexity of pools from which we can successfully identify a positive hit. We established that we could identify an sgRNA which promotes lymphomagenesis diluted in equal molar ratios with four other neutral sgRNAs (Figure 2.3a). This is a far cry from the effective pools of 200 shRNAs that had previously been reported [100]. One contributor to this issue is the large size of our All-in-One pQCiG2 vector (~8 kb) which approaches the packaging capacity of retroviruses. This large size reduces the packaging efficiency of our virus, leading to reduced viral titers and resulting in poor transduction efficiency [133]. The most commonly used Cas9 cDNA alone accounts for 4.2 kb, therefore the development of genetically engineered mice which already express Cas9 protein in the desired tissues would allow for development of more compact sgRNA delivery vectors, thereby increasing viral titers, transduction efficiency and, ultimately, effective pool size.

### 4.3 Utility of a Genetically Engineered Inducible Cas9 Mouse

Delivery of the CRISPR/Cas9 system to the target tissue remains one of the largest obstacles in *in vivo* genome editing. As has been previously mentioned, the most commonly used variant of Cas9 has a cDNA of 4.2 kb. This is problematic when

considering viral administration routes. Adding on regulatory components and an sgRNA expression cassette to a Cas9 vector stretches the limit of lenti- and retroviral packaging, and is completely beyond the capacity of a single AAV vector. Various approaches have been taken in order to address these difficulties. Most commonly, the sgRNA and Cas9 protein will be delivered in two separate viruses. Other groups have created split-Cas9 systems wherein Cas9 is split into two domains and delivered independently of one another and self-assemble once expressed in cells [153, 156, 157]. Additionally, smaller Cas9 orthologs are being examined and characterized. One such ortholog from *Staphylococcus aureus,* whose cDNA is >1kb shorter than that of the most commonly used Cas9, has been characterized and successfully used for *in vivo* editing[158]. However, one approach summarily removes the question of Cas9 delivery altogether: generation of a genetically engineered Cas9 mouse. Several such mice have already been described. Platt et al. [134] developed a genetically engineered Cre-dependent mouse where Cas9 protein will be constitutively expressed in any tissue also expressing Cre-recombinase. Though highly powerful, this mouse is not without its limitations. Cas9 is a foreign bacterial protein against which an immune response could be elicited. In the case of an *in vivo* screen, this could negatively impact targeted cells, affecting the readout of the screen. Expression of Cas9, while not deleterious at the organismal level, has been reported to elicit an immune response specific to the Cas9 protein in both adenoviral and AAV-based administration routes [152, 153]. Additionally, it has been demonstrated that prolonged expression of CRISPR/Cas9 machinery can increase the ratio of off-target to on-target editing [154, 155, 159], therefore making it desirable to limit the duration of expression of Cas9. Dow et al. [139] have described a doxycycline-inducible CRISPR/Cas9 mouse which constitutively expresses an sgRNA, but inducibly expresses Cas9 upon administration of doxycycline. However, this system is limited in that the sgRNA is included in the transgene, therefore requiring the generation of a new strain for every new target of interest. The system which we describe in Chapter 3 addresses each of these issues. We have developed a more compact sgRNA delivery vector with which we achieve much higher transduction efficiencies of HSPCs  than we do with the previously used All-in-One construct (Figure

3.4, data not shown). Although we did not see significant acceleration of tumorigenesis in a 50-fold dilution of our sgP53-3 sgRNA, there is potential to further increase the transduction efficiency by further reducing the size of our pUSPPC vector by excising the PGK-Puromycin cassette. Our system also has inducible, controllable expression of Cas9 across a variety of tissues. And finally, we have the flexibility to introduce any sgRNA of interest, with the potential for facile multiplexing. All of these suggest that our TRE-CiG/rtTA is a welcome expansion on the current CRISPR/Cas9 technology.

# References


1. Pingoud A, Wilson GG, Wende W. Type II restriction endonucleases--a historical perspective and more. Nucleic Acids Res. 2014;42(12):7489-527. doi: 10.1093/nar/gku447. PubMed PMID: 24878924; PubMed Central PMCID: PMCPMC4081073.
2. Handel EM, Cathomen T. Zinc-finger nuclease based genome surgery: it's all about specificity. Curr Gene Ther. 2011;11(1):28-37. PubMed PMID: 21182467.
3. Iliakis G, Wang H, Perrault AR, Boecker W, Rosidi B, Windhofer F, et al. Mechanisms of DNA double strand break repair and chromosome aberration formation. Cytogenet Genome Res. 2004;104(1-4):14-20. doi: 10.1159/000077461. PubMed PMID: 15162010.
4. Stella S, Montoya G. The genome editing revolution: A CRISPR-Cas TALE off-target story. Bioessays. 2016;38 Suppl 1:S4-S13. doi: 10.1002/bies.201670903. PubMed PMID: 27417121.
5. Capecchi MR. Altering the genome by homologous recombination. Science. 1989;244(4910):1288-92. PubMed PMID: 2660260.
6. Rouet P, Smih F, Jasin M. Introduction of double-strand breaks into the genome of mouse cells by expression of a rare-cutting endonuclease. Molecular and cellular biology. 1994;14(12):8096-106. PubMed PMID: 7969147; PubMed Central PMCID: PMCPMC359348.
7. Kim YG, Shi Y, Berg JM, Chandrasegaran S. Site-specific cleavage of DNA-RNA hybrids by zinc finger/FokI cleavage domain fusions. Gene. 1997;203(1):43-9. PubMed PMID: 9426005.
8. Le Provost F, Lillico S, Passet B, Young R, Whitelaw B, Vilotte J-L. Zinc finger nuclease technology heralds a new era in mammalian transgenesis. Trends in Biotechnology. 2010;28(3):134-41. doi: http://dx.doi.org/10.1016/j.tibtech.2009.11.007.
9. Chandrasegaran S, Carroll D. Origins of Programmable Nucleases for Genome Engineering. J Mol Biol. 2016;428(5 Pt B):963-89. doi: 10.1016/j.jmb.2015.10.014. PubMed PMID: 26506267; PubMed Central PMCID: PMCPMC4798875.
10. Bibikova M, Golic M, Golic KG, Carroll D. Targeted chromosomal cleavage and mutagenesis in Drosophila using zinc-finger nucleases. Genetics. 2002;161(3):1169-75. PubMed PMID: 12136019; PubMed Central PMCID: PMCPMC1462166.
11. Bibikova M, Beumer K, Trautman JK, Carroll D. Enhancing gene targeting with designed zinc finger nucleases. Science. 2003;300(5620):764. doi: 10.1126/science.1079512. PubMed PMID: 12730594.
12. Beumer KJ, Trautman JK, Bozas A, Liu JL, Rutter J, Gall JG, et al. Efficient gene targeting in Drosophila by direct embryo injection with zinc-finger nucleases. Proceedings of the National Academy of Sciences of the United States of America. 2008;105(50):19821-6. doi: 10.1073/pnas.0810475105. PubMed PMID: 19064913; PubMed Central PMCID: PMCPMC2604940.
13. Doyon Y, McCammon JM, Miller JC, Faraji F, Ngo C, Katibah GE, et al. Heritable targeted gene disruption in zebrafish using designed zinc-finger nucleases. Nat Biotechnol. 2008;26(6):702-8. doi: 10.1038/nbt1409. PubMed PMID: 18500334; PubMed Central PMCID: PMCPMC2674762.

14. Meng X, Noyes MB, Zhu LJ, Lawson ND, Wolfe SA. Targeted gene inactivation in zebrafish using engineered zinc-finger nucleases. Nat Biotechnol. 2008;26(6):695-701. doi: 10.1038/nbt1398. PubMed PMID: 18500337; PubMed Central PMCID: PMCPMC2502069.
15. Carbery ID, Ji D, Harrington A, Brown V, Weinstein EJ, Liaw L, et al. Targeted genome modification in mice using zinc-finger nucleases. Genetics. 2010;186(2):451-9. doi: 10.1534/genetics.110.117002. PubMed PMID: 20628038; PubMed Central PMCID: PMCPMC2954478.
16. Meyer M, de Angelis MH, Wurst W, Kuhn R. Gene targeting by homologous recombination in mouse zygotes mediated by zinc-finger nucleases. Proceedings of the National Academy of Sciences of the United States of America. 2010;107(34):15022-6. doi: 10.1073/pnas.1009424107. PubMed PMID: 20686113; PubMed Central PMCID: PMCPMC2930558.
17. Cui X, Ji D, Fisher DA, Wu Y, Briner DM, Weinstein EJ. Targeted integration in rat and mouse embryos with zinc-finger nucleases. Nat Biotechnol. 2011;29(1):64-7. doi: 10.1038/nbt.1731. PubMed PMID: 21151125.
18. Meyer M, Ortiz O, Hrabe de Angelis M, Wurst W, Kuhn R. Modeling disease mutations by gene targeting in one-cell mouse embryos. Proceedings of the National Academy of Sciences of the United States of America. 2012;109(24):9354-9. doi: 10.1073/pnas.1121203109. PubMed PMID: 22660928; PubMed Central PMCID: PMCPMC3386067.
19. Lombardo A, Genovese P, Beausejour CM, Colleoni S, Lee YL, Kim KA, et al. Gene editing in human stem cells using zinc finger nucleases and integrase-defective lentiviral vector delivery. Nat Biotechnol. 2007;25(11):1298-306. doi: 10.1038/nbt1353. PubMed PMID: 17965707.
20. Hockemeyer D, Soldner F, Beard C, Gao Q, Mitalipova M, DeKelver RC, et al. Efficient targeting of expressed and silent genes in human ESCs and iPSCs using zinc-finger nucleases. Nat Biotechnol. 2009;27(9):851-7. doi: 10.1038/nbt.1562. PubMed PMID: 19680244; PubMed Central PMCID: PMCPMC4142824.
21. Zou J, Maeder ML, Mali P, Pruett-Miller SM, Thibodeau-Beganny S, Chou BK, et al. Gene targeting of a disease-related gene in human induced pluripotent stem and embryonic stem cells. Cell Stem Cell. 2009;5(1):97-110. doi: 10.1016/j.stem.2009.05.023. PubMed PMID: 19540188; PubMed Central PMCID: PMCPMC2720132.
22. Kim HJ, Lee HJ, Kim H, Cho SW, Kim JS. Targeted genome editing in human cells with zinc finger nucleases constructed via modular assembly. Genome Res. 2009;19(7):1279-88. doi: 10.1101/gr.089417.108. PubMed PMID: 19470664; PubMed Central PMCID: PMCPMC2704428.
23. Ramirez CL, Foley JE, Wright DA, Muller-Lerch F, Rahman SH, Cornu TI, et al. Unexpected failure rates for modular assembly of engineered zinc fingers. Nat Methods. 2008;5(5):374-5. doi: 10.1038/nmeth0508-374. PubMed PMID: 18446154.
24. Sander JD, Dahlborg EJ, Goodwin MJ, Cade L, Zhang F, Cifuentes D, et al. Selection-free zinc-finger-nuclease engineering by context-dependent assembly (CoDA). Nat Methods. 2011;8(1):67-9. doi: 10.1038/nmeth.1542. PubMed PMID: 21151135; PubMed Central PMCID: PMCPMC3018472.
25. Cornu TI, Thibodeau-Beganny S, Guhl E, Alwin S, Eichtinger M, Joung JK, et al. DNA-binding specificity is a major determinant of the activity and toxicity of zinc-finger

nucleases. Mol Ther. 2008;16(2):352-8. doi: 10.1038/sj.mt.6300357. PubMed PMID: 18026168.
26. Bogdanove AJ, Schornack S, Lahaye T. TAL effectors: finding plant genes for disease and defense. Curr Opin Plant Biol. 2010;13(4):394-401. doi: 10.1016/j.pbi.2010.04.010. PubMed PMID: 20570209.
27. Joung JK, Sander JD. TALENs: a widely applicable technology for targeted genome editing. Nat Rev Mol Cell Biol. 2013;14(1):49-55. doi: 10.1038/nrm3486. PubMed PMID: 23169466; PubMed Central PMCID: PMCPMC3547402.
28. Boch J, Scholze H, Schornack S, Landgraf A, Hahn S, Kay S, et al. Breaking the code of DNA binding specificity of TAL-type III effectors. Science. 2009;326(5959):1509-12. doi: 10.1126/science.1178811. PubMed PMID: 19933107.
29. Moscou MJ, Bogdanove AJ. A simple cipher governs DNA recognition by TAL effectors. Science. 2009;326(5959):1501. doi: 10.1126/science.1178817. PubMed PMID: 19933106.
30. Boch J, Bonas U. Xanthomonas AvrBs3 family-type III effectors: discovery and function. Annu Rev Phytopathol. 2010;48:419-36. doi: 10.1146/annurev-phyto-080508-081936. PubMed PMID: 19400638.
31. Katsuyama T, Akmammedov A, Seimiya M, Hess SC, Sievers C, Paro R. An efficient strategy for TALEN-mediated genome engineering in Drosophila. Nucleic Acids Res. 2013;41(17):e163. doi: 10.1093/nar/gkt638. PubMed PMID: 23877243; PubMed Central PMCID: PMCPMC3783190.
32. Liu J, Li C, Yu Z, Huang P, Wu H, Wei C, et al. Efficient and specific modifications of the Drosophila genome by means of an easy TALEN strategy. J Genet Genomics. 2012;39(5):209-15. doi: 10.1016/j.jgg.2012.04.003. PubMed PMID: 22624882.
33. Sander JD, Cade L, Khayter C, Reyon D, Peterson RT, Joung JK, et al. Targeted gene disruption in somatic zebrafish cells using engineered TALENs. Nat Biotechnol. 2011;29(8):697-8. doi: 10.1038/nbt.1934. PubMed PMID: 21822241; PubMed Central PMCID: PMCPMC3154023.
34. Bedell VM, Wang Y, Campbell JM, Poshusta TL, Starker CG, Krug RG, 2nd, et al. In vivo genome editing using a high-efficiency TALEN system. Nature. 2012;491(7422):114-8. doi: 10.1038/nature11537. PubMed PMID: 23000899; PubMed Central PMCID: PMCPMC3491146.
35. Cade L, Reyon D, Hwang WY, Tsai SQ, Patel S, Khayter C, et al. Highly efficient generation of heritable zebrafish gene mutations using homo- and heterodimeric TALENs. Nucleic Acids Res. 2012;40(16):8001-10. doi: 10.1093/nar/gks518. PubMed PMID: 22684503; PubMed Central PMCID: PMCPMC3439908.
36. Ishibashi S, Cliffe R, Amaya E. Highly efficient bi-allelic mutation rates using TALENs in Xenopus tropicalis. Biol Open. 2012;1(12):1273-6. doi: 10.1242/bio.20123228. PubMed PMID: 23408158; PubMed Central PMCID: PMCPMC3558749.
37. Lei Y, Guo X, Deng Y, Chen Y, Zhao H. Generation of gene disruptions by transcription activator-like effector nucleases (TALENs) in Xenopus tropicalis embryos. Cell Biosci. 2013;3(1):21. doi: 10.1186/2045-3701-3-21. PubMed PMID: 23663889; PubMed Central PMCID: PMCPMC3665704.
38. Nakade S, Sakuma T, Sakane Y, Hara Y, Kurabayashi A, Kashiwagi K, et al. Homeolog-specific targeted mutagenesis in Xenopus laevis using TALENs. In Vitro Cell Dev Biol Anim. 2015;51(9):879-84. doi: 10.1007/s11626-015-9912-0. PubMed PMID: 25920501.

39. Liu Y, Zhao H, Cheng CH. Mutagenesis in Xenopus and Zebrafish using TALENs. Methods Mol Biol. 2016;1338:207-27. doi: 10.1007/978-1-4939-2932-0_16. PubMed PMID: 26443224.
40. Tesson L, Usal C, Menoret S, Leung E, Niles BJ, Remy S, et al. Knockout rats generated by embryo microinjection of TALENs. Nat Biotechnol. 2011;29(8):695-6. doi: 10.1038/nbt.1940. PubMed PMID: 21822240.
41. Carlson DF, Tan W, Lillico SG, Stverakova D, Proudfoot C, Christian M, et al. Efficient TALEN-mediated gene knockout in livestock. Proceedings of the National Academy of Sciences of the United States of America. 2012;109(43):17382-7. doi: 10.1073/pnas.1211446109. PubMed PMID: 23027955; PubMed Central PMCID: PMCPMC3491456.
42. Cermak T, Doyle EL, Christian M, Wang L, Zhang Y, Schmidt C, et al. Efficient design and assembly of custom TALEN and other TAL effector-based constructs for DNA targeting. Nucleic Acids Res. 2011;39(12):e82. doi: 10.1093/nar/gkr218. PubMed PMID: 21493687; PubMed Central PMCID: PMCPMC3130291.
43. Hockemeyer D, Wang H, Kiani S, Lai CS, Gao Q, Cassady JP, et al. Genetic engineering of human pluripotent cells using TALE nucleases. Nat Biotechnol. 2011;29(8):731-4. doi: 10.1038/nbt.1927. PubMed PMID: 21738127; PubMed Central PMCID: PMCPMC3152587.
44. Mussolino C, Morbitzer R, Lutge F, Dannemann N, Lahaye T, Cathomen T. A novel TALE nuclease scaffold enables high genome editing activity in combination with low toxicity. Nucleic Acids Res. 2011;39(21):9283-93. doi: 10.1093/nar/gkr597. PubMed PMID: 21813459; PubMed Central PMCID: PMCPMC3241638.
45. Wood AJ, Lo TW, Zeitler B, Pickle CS, Ralston EJ, Lee AH, et al. Targeted genome editing across species using ZFNs and TALENs. Science. 2011;333(6040):307. doi: 10.1126/science.1207773. PubMed PMID: 21700836; PubMed Central PMCID: PMCPMC3489282.
46. Miller JC, Tan S, Qiao G, Barlow KA, Wang J, Xia DF, et al. A TALE nuclease architecture for efficient genome editing. Nat Biotechnol. 2011;29(2):143-8. doi: 10.1038/nbt.1755. PubMed PMID: 21179091.
47. Ishino Y, Shinagawa H, Makino K, Amemura M, Nakata A. Nucleotide sequence of the iap gene, responsible for alkaline phosphatase isozyme conversion in Escherichia coli, and identification of the gene product. J Bacteriol. 1987;169(12):5429-33. PubMed PMID: 3316184; PubMed Central PMCID: PMCPMC213968.
48. Sorek R, Kunin V, Hugenholtz P. CRISPR--a widespread system that provides acquired resistance against phages in bacteria and archaea. Nat Rev Microbiol. 2008;6(3):181-6. doi: 10.1038/nrmicro1793. PubMed PMID: 18157154.
49. Bolotin A, Quinquis B, Sorokin A, Ehrlich SD. Clustered regularly interspaced short palindrome repeats (CRISPRs) have spacers of extrachromosomal origin. Microbiology. 2005;151(Pt 8):2551-61. doi: 10.1099/mic.0.28048-0. PubMed PMID: 16079334.
50. Mojica FJ, Diez-Villasenor C, Garcia-Martinez J, Soria E. Intervening sequences of regularly spaced prokaryotic repeats derive from foreign genetic elements. J Mol Evol. 2005;60(2):174-82. doi: 10.1007/s00239-004-0046-3. PubMed PMID: 15791728.
51. Pourcel C, Salvignol G, Vergnaud G. CRISPR elements in Yersinia pestis acquire new repeats by preferential uptake of bacteriophage DNA, and provide additional tools for evolutionary studies. Microbiology. 2005;151(Pt 3):653-63. doi: 10.1099/mic.0.27437-0. PubMed PMID: 15758212.

52. Barrangou R, Fremaux C, Deveau H, Richards M, Boyaval P, Moineau S, et al. CRISPR provides acquired resistance against viruses in prokaryotes. Science. 2007;315(5819):1709-12. doi: 10.1126/science.1138140. PubMed PMID: 17379808.
53. Makarova KS, Haft DH, Barrangou R, Brouns SJ, Charpentier E, Horvath P, et al. Evolution and classification of the CRISPR-Cas systems. Nat Rev Microbiol. 2011;9(6):467-77. doi: 10.1038/nrmicro2577. PubMed PMID: 21552286; PubMed Central PMCID: PMCPMC3380444.
54. Mojica FJ, Diez-Villasenor C, Garcia-Martinez J, Almendros C. Short motif sequences determine the targets of the prokaryotic CRISPR defence system. Microbiology. 2009;155(Pt 3):733-40. doi: 10.1099/mic.0.023960-0. PubMed PMID: 19246744.
55. Jinek M, Chylinski K, Fonfara I, Hauer M, Doudna JA, Charpentier E. A programmable dual-RNA-guided DNA endonuclease in adaptive bacterial immunity. Science. 2012;337(6096):816-21. doi: 10.1126/science.1225829. PubMed PMID: 22745249.
56. Deltcheva E, Chylinski K, Sharma CM, Gonzales K, Chao Y, Pirzada ZA, et al. CRISPR RNA maturation by trans-encoded small RNA and host factor RNase III. Nature. 2011;471(7340):602-7. doi: 10.1038/nature09886. PubMed PMID: 21455174; PubMed Central PMCID: PMCPMC3070239.
57. Sapranauskas R, Gasiunas G, Fremaux C, Barrangou R, Horvath P, Siksnys V. The Streptococcus thermophilus CRISPR/Cas system provides immunity in Escherichia coli. Nucleic Acids Res. 2011;39(21):9275-82. doi: 10.1093/nar/gkr606. PubMed PMID: 21813460; PubMed Central PMCID: PMCPMC3241640.
58. Jia H, Wang N. Targeted genome editing of sweet orange using Cas9/sgRNA. PloS one. 2014;9(4):e93806. doi: 10.1371/journal.pone.0093806. PubMed PMID: 24710347; PubMed Central PMCID: PMCPMC3977896.
59. Xu R, Wei P, Yang J. Use of CRISPR/Cas Genome Editing Technology for Targeted Mutagenesis in Rice. Methods Mol Biol. 2017;1498:33-40. doi: 10.1007/978-1-4939-6472-7_3. PubMed PMID: 27709567.
60. Zhang Y, Liang Z, Zong Y, Wang Y, Liu J, Chen K, et al. Efficient and transgene-free genome editing in wheat through transient expression of CRISPR/Cas9 DNA or RNA. Nature communications. 2016;7:12617. doi: 10.1038/ncomms12617. PubMed PMID: 27558837; PubMed Central PMCID: PMCPMC5007326.
61. Andersson M, Turesson H, Nicolia A, Falt AS, Samuelsson M, Hofvander P. Efficient targeted multiallelic mutagenesis in tetraploid potato (Solanum tuberosum) by transient CRISPR-Cas9 expression in protoplasts. Plant Cell Rep. 2016. doi: 10.1007/s00299-016-2062-3. PubMed PMID: 27699473.
62. Xu S. The application of CRISPR-Cas9 genome editing in Caenorhabditis elegans. J Genet Genomics. 2015;42(8):413-21. doi: 10.1016/j.jgg.2015.06.005. PubMed PMID: 26336798; PubMed Central PMCID: PMCPMC4560834.
63. Li W, Ou G. The application of somatic CRISPR-Cas9 to conditional genome editing in Caenorhabditis elegans. Genesis. 2016;54(4):170-81. doi: 10.1002/dvg.22932. PubMed PMID: 26934570.
64. Schmitt SM, Gull M, Brandli AW. Engineering Xenopus embryos for phenotypic drug discovery screening. Adv Drug Deliv Rev. 2014;69-70:225-46. doi: 10.1016/j.addr.2014.02.004. PubMed PMID: 24576445.
65. Liu Z, Cheng TT, Shi Z, Liu Z, Lei Y, Wang C, et al. Efficient genome editing of genes involved in neural crest development using the CRISPR/Cas9 system in Xenopus embryos.

Cell Biosci. 2016;6:22. doi: 10.1186/s13578-016-0088-4. PubMed PMID: 27042291; PubMed Central PMCID: PMCPMC4818404.
66. De Santis F, Di Donato V, Del Bene F. Clonal analysis of gene loss of function and tissue-specific gene deletion in zebrafish via CRISPR/Cas9 technology. Methods Cell Biol. 2016;135:171-88. doi: 10.1016/bs.mcb.2016.03.006. PubMed PMID: 27443925.
67. Zhang Y, Huang H, Zhang B, Lin S. TALEN- and CRISPR-enhanced DNA homologous recombination for gene editing in zebrafish. Methods Cell Biol. 2016;135:107-20. doi: 10.1016/bs.mcb.2016.03.005. PubMed PMID: 27443922.
68. Shah AN, Moens CB, Miller AC. Targeted candidate gene screens using CRISPR/Cas9 technology. Methods Cell Biol. 2016;135:89-106. doi: 10.1016/bs.mcb.2016.01.008. PubMed PMID: 27443921.
69. Li D, Qiu Z, Shao Y, Chen Y, Guan Y, Liu M, et al. Heritable gene targeting in the mouse and rat using a CRISPR-Cas system. Nat Biotechnol. 2013;31(8):681-3. doi: 10.1038/nbt.2661. PubMed PMID: 23929336.
70. Wang H, Yang H, Shivalila CS, Dawlaty MM, Cheng AW, Zhang F, et al. One-step generation of mice carrying mutations in multiple genes by CRISPR/Cas-mediated genome engineering. Cell. 2013;153(4):910-8. doi: 10.1016/j.cell.2013.04.025. PubMed PMID: 23643243; PubMed Central PMCID: PMCPMC3969854.
71. Wu Y, Liang D, Wang Y, Bai M, Tang W, Bao S, et al. Correction of a genetic disease in mouse via use of CRISPR-Cas9. Cell Stem Cell. 2013;13(6):659-62. doi: 10.1016/j.stem.2013.10.016. PubMed PMID: 24315440.
72. Malina A, Mills JR, Cencic R, Yan Y, Fraser J, Schippers LM, et al. Repurposing CRISPR/Cas9 for in situ functional assays. Genes Dev. 2013;27(23):2602-14. doi: 10.1101/gad.227132.113. PubMed PMID: 24298059; PubMed Central PMCID: PMCPMC3861673.
73. Kannan R, Ventura A. The CRISPR revolution and its impact on cancer research. Swiss Med Wkly. 2015;145:w14230. doi: 10.4414/smw.2015.14230. PubMed PMID: 26661454.
74. Muffat J, Li Y, Jaenisch R. CNS disease models with human pluripotent stem cells in the CRISPR age. Curr Opin Cell Biol. 2016;43:96-103. doi: 10.1016/j.ceb.2016.10.001. PubMed PMID: 27768957.
75. Hu X. CRISPR/Cas9 system and its applications in human hematopoietic cells. Blood Cells Mol Dis. 2016;62:6-12. doi: 10.1016/j.bcmd.2016.09.003. PubMed PMID: 27736664.
76. Zhang H, McCarty N. CRISPR-Cas9 technology and its application in haematological disorders. Br J Haematol. 2016;175(2):208-25. doi: 10.1111/bjh.14297. PubMed PMID: 27619566.
77. Sakuma T, Nishikawa A, Kume S, Chayama K, Yamamoto T. Multiplex genome engineering in human cells using all-in-one CRISPR/Cas9 vector system. Sci Rep. 2014;4:5400. doi: 10.1038/srep05400. PubMed PMID: 24954249; PubMed Central PMCID: PMCPMC4066266.
78. Kabadi AM, Ousterout DG, Hilton IB, Gersbach CA. Multiplex CRISPR/Cas9-based genome engineering from a single lentiviral vector. Nucleic Acids Res. 2014;42(19):e147. doi: 10.1093/nar/gku749. PubMed PMID: 25122746; PubMed Central PMCID: PMCPMC4231726.
79. Ousterout DG, Kabadi AM, Thakore PI, Majoros WH, Reddy TE, Gersbach CA. Multiplex CRISPR/Cas9-based genome editing for correction of dystrophin mutations that

cause Duchenne muscular dystrophy. Nature communications. 2015;6:6244. doi: 10.1038/ncomms7244. PubMed PMID: 25692716; PubMed Central PMCID: PMCPMC4335351.
80. Yin L, Maddison LA, Li M, Kara N, LaFave MC, Varshney GK, et al. Multiplex Conditional Mutagenesis Using Transgenic Expression of Cas9 and sgRNAs. Genetics. 2015;200(2):431-41. doi: 10.1534/genetics.115.176917. PubMed PMID: 25855067; PubMed Central PMCID: PMCPMC4492370.
81. Weber J, Ollinger R, Friedrich M, Ehmer U, Barenboim M, Steiger K, et al. CRISPR/Cas9 somatic multiplex-mutagenesis for high-throughput functional cancer genomics in mice. Proceedings of the National Academy of Sciences of the United States of America. 2015;112(45):13982-7. doi: 10.1073/pnas.1512392112. PubMed PMID: 26508638; PubMed Central PMCID: PMCPMC4653208.
82. Cong L, Ran FA, Cox D, Lin S, Barretto R, Habib N, et al. Multiplex genome engineering using CRISPR/Cas systems. Science. 2013;339(6121):819-23. doi: 10.1126/science.1231143. PubMed PMID: 23287718; PubMed Central PMCID: PMCPMC3795411.
83. Adams R, Steckel M, Nicke B. Functional Genomics in Pharmaceutical Drug Discovery. Handbook of experimental pharmacology. 2016;232:25-41. Epub 2015/09/04. doi: 10.1007/164_2015_27. PubMed PMID: 26330261.
84. Sigoillot FD, King RW. Vigilance and validation: Keys to success in RNAi screening. ACS Chem Biol. 2011;6(1):47-60. doi: 10.1021/cb100358f. PubMed PMID: 21142076; PubMed Central PMCID: PMCPMC3306249.
85. McDade JR, Waxmonsky NC, Swanson LE, Fan M. Practical Considerations for Using Pooled Lentiviral CRISPR Libraries. Curr Protoc Mol Biol. 2016;115:31 5 1- 5 13. doi: 10.1002/cpmb.8. PubMed PMID: 27366891.
86. Koike-Yusa H, Li Y, Tan EP, Velasco-Herrera Mdel C, Yusa K. Genome-wide recessive genetic screening in mammalian cells with a lentiviral CRISPR-guide RNA library. Nat Biotechnol. 2014;32(3):267-73. doi: 10.1038/nbt.2800. PubMed PMID: 24535568.
87. Shalem O, Sanjana NE, Hartenian E, Shi X, Scott DA, Mikkelsen TS, et al. Genome-scale CRISPR-Cas9 knockout screening in human cells. Science. 2014;343(6166):84-7. doi: 10.1126/science.1247005. PubMed PMID: 24336571; PubMed Central PMCID: PMCPMC4089965.
88. Hart T, Chandrashekhar M, Aregger M, Steinhart Z, Brown KR, MacLeod G, et al. High-Resolution CRISPR Screens Reveal Fitness Genes and Genotype-Specific Cancer Liabilities. Cell. 2015;163(6):1515-26. doi: 10.1016/j.cell.2015.11.015. PubMed PMID: 26627737.
89. Parnas O, Jovanovic M, Eisenhaure TM, Herbst RH, Dixit A, Ye CJ, et al. A Genome-wide CRISPR Screen in Primary Immune Cells to Dissect Regulatory Networks. Cell. 2015;162(3):675-86. doi: 10.1016/j.cell.2015.06.059. PubMed PMID: 26189680; PubMed Central PMCID: PMCPMC4522370.
90. Wang T, Birsoy K, Hughes NW, Krupczak KM, Post Y, Wei JJ, et al. Identification and characterization of essential genes in the human genome. Science. 2015;350(6264):1096-101. doi: 10.1126/science.aac7041. PubMed PMID: 26472758; PubMed Central PMCID: PMCPMC4662922.

91. Arroyo JD, Jourdain AA, Calvo SE, Ballarano CA, Doench JG, Root DE, et al. A Genome-wide CRISPR Death Screen Identifies Genes Essential for Oxidative Phosphorylation. Cell Metab. 2016. doi: 10.1016/j.cmet.2016.08.017. PubMed PMID: 27667664.
92. Schmid-Burgk JL, Chauhan D, Schmidt T, Ebert TS, Reinhardt J, Endl E, et al. A Genome-wide CRISPR (Clustered Regularly Interspaced Short Palindromic Repeats) Screen Identifies NEK7 as an Essential Component of NLRP3 Inflammasome Activation. J Biol Chem. 2016;291(1):103-9. doi: 10.1074/jbc.C115.700492. PubMed PMID: 26553871; PubMed Central PMCID: PMCPMC4697147.
93. Chen S, Sanjana NE, Zheng K, Shalem O, Lee K, Shi X, et al. Genome-wide CRISPR screen in a mouse model of tumor growth and metastasis. Cell. 2015;160(6):1246-60. doi: 10.1016/j.cell.2015.02.038. PubMed PMID: 25748654; PubMed Central PMCID: PMCPMC4380877.
94. Ma H, Dang Y, Wu Y, Jia G, Anaya E, Zhang J, et al. A CRISPR-Based Screen Identifies Genes Essential for West-Nile-Virus-Induced Cell Death. Cell Rep. 2015;12(4):673-83. doi: 10.1016/j.celrep.2015.06.049. PubMed PMID: 26190106; PubMed Central PMCID: PMCPMC4559080.
95. Tao L, Zhang J, Meraner P, Tovaglieri A, Wu X, Gerhard R, et al. Frizzled proteins are colonic epithelial receptors for C. difficile toxin B. Nature. 2016;538(7625):350-5. doi: 10.1038/nature19799
http://www.nature.com/nature/journal/v538/n7625/abs/nature19799.html - supplementary-information.
96. Adams JM, Harris AW, Pinkert CA, Corcoran LM, Alexander WS, Cory S, et al. The c-myc oncogene driven by immunoglobulin enhancers induces lymphoid malignancy in transgenic mice. Nature. 1985;318(6046):533-8. PubMed PMID: 3906410.
97. Harris AW, Pinkert CA, Crawford M, Langdon WY, Brinster RL, Adams JM. The E mu-myc transgenic mouse. A model for high-incidence spontaneous lymphoma and leukemia of early B cells. J Exp Med. 1988;167(2):353-71. PubMed PMID: 3258007; PubMed Central PMCID: PMCPMC2188841.
98. Schmitt CA, Lowe SW. Apoptosis and chemoresistance in transgenic cancer models. J Mol Med (Berl). 2002;80(3):137-46. doi: 10.1007/s00109-001-0293-3. PubMed PMID: 11894140.
99. Cencic R, Robert F, Galicia-Vazquez G, Malina A, Ravindar K, Somaiah R, et al. Modifying chemotherapy response by targeted inhibition of eukaryotic initiation factor 4A. Blood Cancer J. 2013;3:e128. doi: 10.1038/bcj.2013.25. PubMed PMID: 23872707; PubMed Central PMCID: PMCPMC3730203.
100. Scuoppo C, Miething C, Lindqvist L, Reyes J, Ruse C, Appelmann I, et al. A tumour suppressor network relying on the polyamine-hypusine axis. Nature. 2012;487(7406):244-8. doi: 10.1038/nature11126. PubMed PMID: 22722845; PubMed Central PMCID: PMCPMC3530829.
101. Mills JR, Malina A, Lee T, Di Paola D, Larsson O, Miething C, et al. RNAi screening uncovers Dhx9 as a modifier of ABT-737 resistance in an Emu-myc/Bcl-2 mouse model. Blood. 2013;121(17):3402-12. doi: 10.1182/blood-2012-06-434365. PubMed PMID: 23440244; PubMed Central PMCID: PMCPMC3637015.
102. Malina A, Katigbak A, Cencic R, Maiga RI, Robert F, Miura H, et al. Adapting CRISPR/Cas9 for functional genomics screens. Methods Enzymol. 2014;546:193-213. doi: 10.1016/B978-0-12-801185-0.00010-6. PubMed PMID: 25398342.

103. Love C, Sun Z, Jima D, Li G, Zhang J, Miles R, et al. The genetic landscape of mutations in Burkitt lymphoma. Nat Genet. 2012;44(12):1321-5. doi: 10.1038/ng.2468. PubMed PMID: 23143597; PubMed Central PMCID: PMCPMC3674561.
104. Richter J, Schlesner M, Hoffmann S, Kreuz M, Leich E, Burkhardt B, et al. Recurrent mutation of the ID3 gene in Burkitt lymphoma identified by integrated genome, exome and transcriptome sequencing. Nat Genet. 2012;44(12):1316-20. doi: 10.1038/ng.2469. PubMed PMID: 23143595.
105. Schmitz R, Young RM, Ceribelli M, Jhavar S, Xiao W, Zhang M, et al. Burkitt lymphoma pathogenesis and therapeutic targets from structural and functional genomics. Nature. 2012;490(7418):116-20. doi: 10.1038/nature11378. PubMed PMID: 22885699; PubMed Central PMCID: PMCPMC3609867.
106. Ledford H. End of cancer-genome project prompts rethink. Nature. 2015;517(7533):128-9. doi: 10.1038/517128a. PubMed PMID: 25567260.
107. Futreal PA, Coin L, Marshall M, Down T, Hubbard T, Wooster R, et al. A census of human cancer genes. Nat Rev Cancer. 2004;4(3):177-83. doi: 10.1038/nrc1299. PubMed PMID: 14993899; PubMed Central PMCID: PMCPMC2665285.
108. Pon JR, Marra MA. Driver and passenger mutations in cancer. Annu Rev Pathol. 2015;10:25-50. doi: 10.1146/annurev-pathol-012414-040312. PubMed PMID: 25340638.
109. Leiserson MD, Vandin F, Wu HT, Dobson JR, Eldridge JV, Thomas JL, et al. Pan-cancer network analysis identifies combinations of rare somatic mutations across pathways and protein complexes. Nat Genet. 2015;47(2):106-14. doi: 10.1038/ng.3168. PubMed PMID: 25501392; PubMed Central PMCID: PMCPMC4444046.
110. Niu B, Scott AD, Sengupta S, Bailey MH, Batra P, Ning J, et al. Protein-structure-guided discovery of functional mutations across 19 cancer types. Nat Genet. 2016;48(8):827-37. doi: 10.1038/ng.3586. PubMed PMID: 27294619.
111. Alvarez MJ, Shen Y, Giorgi FM, Lachmann A, Ding BB, Ye BH, et al. Functional characterization of somatic mutations in cancer using network-based inference of protein activity. Nat Genet. 2016;48(8):838-47. doi: 10.1038/ng.3593. PubMed PMID: 27322546.
112. Boerma EG, Siebert R, Kluin PM, Baudis M. Translocations involving 8q24 in Burkitt lymphoma and other malignant lymphomas: a historical review of cytogenetics in the light of todays knowledge. Leukemia. 2009;23(2):225-34. doi: 10.1038/leu.2008.281. PubMed PMID: 18923440.
113. Naviaux RK, Costanzi E, Haas M, Verma IM. The pCL vector system: rapid production of helper-free, high-titer, recombinant retroviruses. J Virol. 1996;70(8):5701-5. PubMed PMID: 8764092; PubMed Central PMCID: PMCPMC190538.
114. Untergasser A, Cutcutache I, Koressaar T, Ye J, Faircloth BC, Remm M, et al. Primer3--new capabilities and interfaces. Nucleic Acids Res. 2012;40(15):e115. doi: 10.1093/nar/gks596. PubMed PMID: 22730293; PubMed Central PMCID: PMCPMC3424584.
115. Fellmann C, Zuber J, McJunkin K, Chang K, Malone CD, Dickins RA, et al. Functional identification of optimized RNAi triggers using a massively parallel sensor assay. Mol Cell. 2011;41(6):733-46. doi: 10.1016/j.molcel.2011.02.008. PubMed PMID: 21353615; PubMed Central PMCID: PMCPMC3130540.
116. Bric A, Miething C, Bialucha CU, Scuoppo C, Zender L, Krasnitz A, et al. Functional identification of tumor-suppressor genes through an in vivo RNA interference screen in a

mouse lymphoma model. Cancer Cell. 2009;16(4):324-35. doi: 10.1016/j.ccr.2009.08.015. PubMed PMID: 19800577; PubMed Central PMCID: PMCPMC2829755.
117. Mills JR, Hippo Y, Robert F, Chen SM, Malina A, Lin CJ, et al. mTORC1 promotes survival through translational control of Mcl-1. Proceedings of the National Academy of Sciences of the United States of America. 2008;105(31):10853-8. doi: 10.1073/pnas.0804821105. PubMed PMID: 18664580; PubMed Central PMCID: PMCPMC2504845.
118. Cencic R, Miura H, Malina A, Robert F, Ethier S, Schmeing TM, et al. Protospacer adjacent motif (PAM)-distal sequences engage CRISPR Cas9 DNA target cleavage. PloS one. 2014;9(10):e109213. doi: 10.1371/journal.pone.0109213. PubMed PMID: 25275497; PubMed Central PMCID: PMCPMC4183563.
119. Kennett SB, Udvadia AJ, Horowitz JM. Sp3 encodes multiple proteins that differ in their capacity to stimulate or repress transcription. Nucleic Acids Res. 1997;25(15):3110-7. PubMed PMID: 9224612; PubMed Central PMCID: PMCPMC146854.
120. Ban K, Kozar RA. Glutamine protects against apoptosis via downregulation of Sp3 in intestinal epithelial cells. Am J Physiol Gastrointest Liver Physiol. 2010;299(6):G1344-53. doi: 10.1152/ajpgi.00334.2010. PubMed PMID: 20884886; PubMed Central PMCID: PMCPMC3006244.
121. Essafi-Benkhadir K, Grosso S, Puissant A, Robert G, Essafi M, Deckert M, et al. Dual role of Sp3 transcription factor as an inducer of apoptosis and a marker of tumour aggressiveness. PloS one. 2009;4(2):e4478. doi: 10.1371/journal.pone.0004478. PubMed PMID: 19212434; PubMed Central PMCID: PMCPMC2636865.
122. Yang H, Salz T, Zajac-Kaye M, Liao D, Huang S, Qiu Y. Overexpression of histone deacetylases in cancer cells is controlled by interplay of transcription factors and epigenetic modulators. FASEB J. 2014;28(10):4265-79. doi: 10.1096/fj.14-250654. PubMed PMID: 24948597; PubMed Central PMCID: PMCPMC4202103.
123. Kajita Y, Kato T, Jr., Tamaki S, Furu M, Takahashi R, Nagayama S, et al. The transcription factor Sp3 regulates the expression of a metastasis-related marker of sarcoma, actin filament-associated protein 1-like 1 (AFAP1L1). PloS one. 2013;8(1):e49709. doi: 10.1371/journal.pone.0049709. PubMed PMID: 23326307; PubMed Central PMCID: PMCPMC3541374.
124. Huang Y, Shen P, Chen X, Chen Z, Zhao T, Chen N, et al. Transcriptional regulation of BNIP3 by Sp3 in prostate cancer. Prostate. 2015;75(14):1556-67. doi: 10.1002/pros.23029. PubMed PMID: 26012884.
125. De Semir D, Nosrati M, Bezrookove V, Dar AA, Federman S, Bienvenu G, et al. Pleckstrin homology domain-interacting protein (PHIP) as a marker and mediator of melanoma metastasis. Proceedings of the National Academy of Sciences of the United States of America. 2012;109(18):7067-72. doi: 10.1073/pnas.1119949109. PubMed PMID: 22511720; PubMed Central PMCID: PMCPMC3344978.
126. Farhang-Fallah J, Yin X, Trentin G, Cheng AM, Rozakis-Adcock M. Cloning and characterization of PHIP, a novel insulin receptor substrate-1 pleckstrin homology domain interacting protein. J Biol Chem. 2000;275(51):40492-7. doi: 10.1074/jbc.C000611200. PubMed PMID: 11018022.
127. Podcheko A, Northcott P, Bikopoulos G, Lee A, Bommareddi SR, Kushner JA, et al. Identification of a WD40 repeat-containing isoform of PHIP as a novel regulator of beta-cell growth and survival. Molecular and cellular biology. 2007;27(18):6484-96. doi:

10.1128/MCB.02409-06. PubMed PMID: 17636024; PubMed Central PMCID: PMCPMC2099606.
128. Bouwman P, Gollner H, Elsasser HP, Eckhoff G, Karis A, Grosveld F, et al. Transcription factor Sp3 is essential for post-natal survival and late tooth development. The EMBO journal. 2000;19(4):655-61. doi: 10.1093/emboj/19.4.655. PubMed PMID: 10675334; PubMed Central PMCID: PMCPMC305603.
129. Van Loo PF, Bouwman P, Ling KW, Middendorp S, Suske G, Grosveld F, et al. Impaired hematopoiesis in mice lacking the transcription factor Sp3. Blood. 2003;102(3):858-66. doi: 10.1182/blood-2002-06-1848. PubMed PMID: 12676787.
130. Bezrookove V, De Semir D, Nosrati M, Tong S, Wu C, Thummala S, et al. Prognostic impact of PHIP copy number in melanoma: linkage to ulceration. The Journal of investigative dermatology. 2014;134(3):783-90. doi: 10.1038/jid.2013.369. PubMed PMID: 24005052; PubMed Central PMCID: PMCPMC3945648.
131. Li S, Francisco AB, Han C, Pattabiraman S, Foote MR, Giesy SL, et al. The full-length isoform of the mouse pleckstrin homology domain-interacting protein (PHIP) is required for postnatal growth. FEBS letters. 2010;584(18):4121-7. doi: 10.1016/j.febslet.2010.08.042. PubMed PMID: 20816727; PubMed Central PMCID: PMCPMC2965186.
132. Zender L, Xue W, Zuber J, Semighini CP, Krasnitz A, Ma B, et al. An oncogenomics-based in vivo RNAi screen identifies tumor suppressors in liver cancer. Cell. 2008;135(5):852-64. doi: 10.1016/j.cell.2008.09.061. PubMed PMID: 19012953; PubMed Central PMCID: PMCPMC2990916.
133. Gelinas C, Temin HM. Nondefective spleen necrosis virus-derived vectors define the upper size limit for packaging reticuloendotheliosis viruses. Proceedings of the National Academy of Sciences of the United States of America. 1986;83(23):9211-5. PubMed PMID: 3024171; PubMed Central PMCID: PMCPMC387105.
134. Platt RJ, Chen S, Zhou Y, Yim MJ, Swiech L, Kempton HR, et al. CRISPR-Cas9 knockin mice for genome editing and cancer modeling. Cell. 2014;159(2):440-55. doi: 10.1016/j.cell.2014.09.014. PubMed PMID: 25263330; PubMed Central PMCID: PMCPMC4265475.
135. Hemann MT, Bric A, Teruya-Feldstein J, Herbst A, Nilsson JA, Cordon-Cardo C, et al. Evasion of the p53 tumour surveillance network by tumour-derived MYC mutants. Nature. 2005;436(7052):807-11. doi: 10.1038/nature03845. PubMed PMID: 16094360; PubMed Central PMCID: PMCPMC4599579.
136. Sharma R, Anguela XM, Doyon Y, Wechsler T, DeKelver RC, Sproul S, et al. In vivo genome editing of the albumin locus as a platform for protein replacement therapy. Blood. 2015;126(15):1777-84. doi: 10.1182/blood-2014-12-615492. PubMed PMID: 26297739; PubMed Central PMCID: PMCPMC4600017.
137. Schmidt F, Grimm D. CRISPR genome engineering and viral gene delivery: A case of mutual attraction. Biotechnology Journal. 2015;10(2):258-72. doi: 10.1002/biot.201400529.
138. Katigbak A, Cencic R, Robert F, Sénéchal P, Scuoppo C, Pelletier J. A CRISPR/Cas9 Functional Screen Identifies Rare Tumor Suppressors. Submitted. 2016.
139. Dow LE, Fisher J, O'Rourke KP, Muley A, Kastenhuber ER, Livshits G, et al. Inducible in vivo genome editing with CRISPR-Cas9. Nat Biotechnol. 2015;33(4):390-4. doi: 10.1038/nbt.3155. PubMed PMID: 25690852; PubMed Central PMCID: PMCPMC4390466.

140. Chu VT, Weber T, Graf R, Sommermann T, Petsch K, Sack U, et al. Efficient generation of Rosa26 knock-in mice using CRISPR/Cas9 in C57BL/6 zygotes. BMC Biotechnol. 2016;16:4. doi: 10.1186/s12896-016-0234-4. PubMed PMID: 26772810; PubMed Central PMCID: PMCPMC4715285.
141. Loonstra A, Vooijs M, Beverloo HB, Allak BA, van Drunen E, Kanaar R, et al. Growth inhibition and DNA damage induced by Cre recombinase in mammalian cells. Proceedings of the National Academy of Sciences of the United States of America. 2001;98(16):9209-14. doi: 10.1073/pnas.161269798. PubMed PMID: 11481484; PubMed Central PMCID: PMCPMC55399.
142. Premsrirut PK, Dow LE, Kim SY, Camiolo M, Malone CD, Miething C, et al. A rapid and scalable system for studying gene function in mice using conditional RNA interference. Cell. 2011;145(1):145-58. doi: 10.1016/j.cell.2011.03.012. PubMed PMID: 21458673; PubMed Central PMCID: PMCPMC3244080.
143. Dow LE, Nasr Z, Saborowski M, Ebbesen SH, Manchado E, Tasdemir N, et al. Conditional reverse tet-transactivator mouse strains for the efficient induction of TRE-regulated transgenes in mice. PloS one. 2014;9(4):e95236. doi: 10.1371/journal.pone.0095236. PubMed PMID: 24743474; PubMed Central PMCID: PMCPMC3990578.
144. Lin CJ, Nasr Z, Premsrirut PK, Porco JA, Jr., Hippo Y, Lowe SW, et al. Targeting synthetic lethal interactions between Myc and the eIF4F complex impedes tumorigenesis. Cell Rep. 2012;1(4):325-33. doi: 10.1016/j.celrep.2012.02.010. PubMed PMID: 22573234; PubMed Central PMCID: PMCPMC3346676.
145. Lee T, Di Paola D, Malina A, Mills JR, Kreps A, Grosse F, et al. Suppression of the DHX9 helicase induces premature senescence in human diploid fibroblasts in a p53-dependent manner. J Biol Chem. 2014;289(33):22798-814. doi: 10.1074/jbc.M114.568535. PubMed PMID: 24990949; PubMed Central PMCID: PMCPMC4132785.
146. McCurrach ME, Lowe SW. Chapter 9 Methods for studying pro- and antiapoptotic genes in nonimmortal cells. Methods in Cell Biology. Volume 66: Academic Press; 2001. p. 197-227.
147. Sambrook J. Molecular cloning : a laboratory manual / Joseph Sambrook, David W. Russell. Russell DW, Cold Spring Harbor L, editors. Cold Spring Harbor, N.Y: Cold Spring Harbor Laboratory; 2001.
148. Beard C, Hochedlinger K, Plath K, Wutz A, Jaenisch R. Efficient method to generate single-copy transgenic mice by site-specific integration in embryonic stem cells. Genesis. 2006;44(1):23-8. doi: 10.1002/gene.20180. PubMed PMID: 16400644.
149. Okabe M, Ikawa M, Kominami K, Nakanishi T, Nishimune Y. 'Green mice' as a source of ubiquitous green cells. FEBS letters. 1997;407(3):313-9. PubMed PMID: 9175875.
150. McJunkin K, Mazurek A, Premsrirut PK, Zuber J, Dow LE, Simon J, et al. Reversible suppression of an essential gene in adult mice using transgenic RNA interference. Proceedings of the National Academy of Sciences of the United States of America. 2011;108(17):7113-8. doi: 10.1073/pnas.1104097108. PubMed PMID: 21482754; PubMed Central PMCID: PMCPMC3084121.
151. Wendel HG, Silva RL, Malina A, Mills JR, Zhu H, Ueda T, et al. Dissecting eIF4E action in tumorigenesis. Genes Dev. 2007;21(24):3232-7. doi: 10.1101/gad.1604407. PubMed PMID: 18055695; PubMed Central PMCID: PMCPMC2113024.

152. Wang D, Mou H, Li S, Li Y, Hough S, Tran K, et al. Adenovirus-Mediated Somatic Genome Editing of Pten by CRISPR/Cas9 in Mouse Liver in Spite of Cas9-Specific Immune Responses. Hum Gene Ther. 2015;26(7):432-42. doi: 10.1089/hum.2015.087. PubMed PMID: 26086867; PubMed Central PMCID: PMCPMC4509492.
153. Chew WL, Tabebordbar M, Cheng JK, Mali P, Wu EY, Ng AH, et al. A multifunctional AAV-CRISPR-Cas9 and its host response. Nat Methods. 2016. doi: 10.1038/nmeth.3993. PubMed PMID: 27595405.
154. Zuris JA, Thompson DB, Shu Y, Guilinger JP, Bessen JL, Hu JH, et al. Cationic lipid-mediated delivery of proteins enables efficient protein-based genome editing in vitro and in vivo. Nat Biotechnol. 2015;33(1):73-80. doi: 10.1038/nbt.3081. PubMed PMID: 25357182; PubMed Central PMCID: PMCPMC4289409.
155. Do MH, Kim T, He F, Dave H, Intriago RE, Astorga UA, et al. Polyribosome and ribonucleoprotein complex redistribution of mRNA induced by GnRH involves both EIF2AK3 and MAPK signaling. Mol Cell Endocrinol. 2014;382(1):346-57. doi: 10.1016/j.mce.2013.10.007. PubMed PMID: 24161835; PubMed Central PMCID: PMCPMC4042833.
156. Truong DJ, Kuhner K, Kuhn R, Werfel S, Engelhardt S, Wurst W, et al. Development of an intein-mediated split-Cas9 system for gene therapy. Nucleic Acids Res. 2015;43(13):6450-8. doi: 10.1093/nar/gkv601. PubMed PMID: 26082496; PubMed Central PMCID: PMCPMC4513872.
157. Wright AV, Sternberg SH, Taylor DW, Staahl BT, Bardales JA, Kornfeld JE, et al. Rational design of a split-Cas9 enzyme complex. Proceedings of the National Academy of Sciences of the United States of America. 2015;112(10):2984-9. doi: 10.1073/pnas.1501698112. PubMed PMID: 25713377; PubMed Central PMCID: PMCPMC4364227.
158. Ran FA, Cong L, Yan WX, Scott DA, Gootenberg JS, Kriz AJ, et al. In vivo genome editing using Staphylococcus aureus Cas9. Nature. 2015;520(7546):186-91. doi: 10.1038/nature14299. PubMed PMID: 25830891; PubMed Central PMCID: PMCPMC4393360.
159. Chen Y, Liu X, Zhang Y, Wang H, Ying H, Liu M, et al. A Self-restricted CRISPR System to Reduce Off-target Effects. Mol Ther. 2016;24(9):1508-10. doi: 10.1038/mt.2016.172. PubMed PMID: 27687135.

# Appendices

*Table S1 - List of Genes with Nonsense or Frameshift Mutations in Burkitt's Lymphoma with the Corresponding Murine Orthologs and Designed sgRNAs*



| *Gene* | *Murine Ortholog* | *Reference* | *sgRNA Name* | *sgRNA Sequence* | *Nonsense* | *Frameshift* | *Missense* | *Total* | *Pool Number* |
|---|---|---|---|---|---|---|---|---|---|
| DLGAP1 | Dlgap1 | Love *et al.* | sgDLGAP1 | GTGAGCGAGATGGAGGTGAA | 1 | 0 | 2 | 3 | 1 |
| CDC73 | Cdc73 | Love *et al.*;Schmitz *et al.* | sgCDC73 | GAGGAGTTTTGTGGATGCTG | 1 | 0 | 4 | 5 | 1 |
| ADNP | Adnp | Richter *et al.*; Schmitz *et al.* | sgADNP | GTTCATATTGATGAAGAGAT | 2 | 0 | 1 | 3 | 1 |
| AIM1 | Aim1 | Schmitz *et al.* | sgAIM1 | GACCAAGTCTTGCAGAGTTT | 1 | 0 | 2 | 3 | 1 |
| ANKRD17 | Ankrd17 | Schmitz *et al.* | sgANKRD17 | GGTTCTCAGGTGAATTCAGC | 1 | 0 | 2 | 3 | 1 |
| EIF2AK3 | Eif2ak3 | Schmitz *et al.* | sgEIF2AK3 | GCAGATCACAGTCAGGTTCC | 1 | 0 | 2 | 3 | 2 |
| ELMO3 | Elmo3 | Schmitz *et al.* | sgELMO3 | GGCTCTGAAGCCCACCTCCC | 1 | 0 | 2 | 3 | 2 |
| FAM184A | Fam184a | Schmitz *et al.* | sgFAM184A | GGTGGAGGCCTTGAACAACA | 1 | 0 | 0 | 1 | 2 |
| GOLGB1 | Golgb1 | Schmitz *et al.* | sgGOLGB1 | GATGAAGGAACAGTTCCTCA | 1 | 0 | 2 | 3 | 2 |
| SLC29A2 | Slc29a2 | Love *et al.* | sgSLC29A2 | GATGCCCAGACCTCTGCTCT | 1 | 0 | 2 | 3 | 3 |
| MAP3K6 | Map3k6 | Love *et al.*;Schmitz *et al.* | sgMAP3K6 | GTGGAGCCCAGCCTGCACTC | 1 | 0 | 3 | 4 | 3 |
| RP11.269H4.1 (PREX1) | Prex1 | Love *et al.* | sgPREX1 | GAAAGTGTGCTTCAAGGTGT | 1 | 0 | 2 | 3 | 3 |
| KIFC3 | Kifc3 | Love *et al.* | sgKIFC3 #2 | GACCCGGAACCAGCACCTGC | 1 | 0 | 2 | 3 | 3 |
| CC2D1B | Cc2d1b | Schmitz et al. | sgCC2D1B | GGAGCAGGTGACACTGCTGG | 1 | 0 | 1 | 2 | 4 |
| FAM160B1 | Fam160b1 | Schmitz *et al.* | sgFAM160B1 #1 | GATTTTGTTTATCACTGGA | 1 | 0 | 1 | 2 | 4 |
| STK36 | Stk36 | Schmitz *et al.* | sgSTK36 | GGCGCTCAGAGAAAGAGCTG | 1 | 0 | 2 | 3 | 4 |
| BIN2 | Bin2 | Schmitz *et al.* | sgBIN2 | GGGCAGAGGTCAGACAGGGA | 1 | 0 | 1 | 2 | 4 |
| POLRMT | Polrmt | Love *et al.*;Schmitz *et al.* | sgPOLRMT | GCGTGTAAACGGGCATCTGC | 1 | 0 | 1 | 2 | 5 |
| HSPE | Hspe | Schmitz *et al.* | sgHPSE | GAACGGTCAAATTCTGAAGA | 1 | 0 | 1 | 2 | 5 |
| LSG1 | Lsg1 | Schmitz *et al.* | sgLSG1 | GCCACCGTCATACTGACTCC | 1 | 0 | 1 | 2 | 5 |
| PHIP | Phip | Love *et al.*;Schmitz *et al.* | sgPHIP | GTCTGCATTTGTTGCCCCTG | 1 | 0 | 2 | 3 | 5 |
| PMAIP1 | Pmaip1 | Schmitz *et al.* | sgPMAIP1 | GGACGAGTGTGCTCAACTC | 1 | 0 | 1 | 2 | 5 |
| ZNF518A | Zfp518a | Schmitz *et al.* | sgZNF518A | GTTCATCCCCTGTGCTTGCC | 1 | 0 | 1 | 2 | 6 |
| WDR27 | Wdr27 | Schmitz *et al.* | sgWDR27 | GTCTGAAGACCGAAGCTTTA | 1 | 0 | 1 | 2 | 6 |
| RFX7 | Rfx7 | Schmitz *et al.*;Richter *et al.* | sgRFX7 | GACCGTGAGTCAAAATCAGA | 1 | 1 | 0 | 2 | 6 |
| SNX5 | Snx5 | Schmitz *et al.* | sgSNX5 | GGCCGCGGTTCCCGAGTTGC | 1 | 0 | 1 | 2 | 6 |
| UBR5 | Ubr5 | Schmitz *et al.* | sgUBR5 | GTTTTCCAAGCCCTTATATAC | 1 | 0 | 1 | 2 | 6 |
| ACAD11 | Acad11 | Schmitz *et al.* | sgACAD11 | GGTGACAACAGTGGCGGTCA | 1 | 0 | 0 | 1 | 7 |
| ALKBH1 | Alkbh1 | Schmitz *et al.* | sgALKBH1 | GTGCGTCAGGTACTGGCCAC | 1 | 0 | 0 | 1 | 7 |

*Table S1 - List of Genes with Nonsense or Frameshift Mutations in Burkitt's Lymphoma with the Corresponding Murine Orthologs and Designed sgRNAs*

| *Gene* | *Murine Ortholog* | *Reference* | *sgRNA Name* | *sgRNA Sequence* | *Nonsense* | *Frameshift* | *Missense* | *Total* | *Pool Number* |
|---|---|---|---|---|---|---|---|---|---|
| ATG16L2 | Atg16l2 | Schmitz *et al.* | sgATG16L2 | GGTCATCCCCGTGCAGGGCC | 1 | 0 | 0 | 1 | 7 |
| C18orf54 | 4930503L19Rik | Schmitz *et al.* | sgC18orf54 | GACCTGGTCGATGATACCAG | 1 | 0 | 0 | 1 | 7 |
| C1orf174 | A430005L14Rik | Schmitz *et al.* | sgC1orf174 | GATGACGAGGATGACGCTGA | 1 | 0 | 0 | 1 | 7 |
| DOCK4 | Dock4 | Richter *et al.* | sgDOCK4 | GCCATTTACCCAACACCCG | 1 | 0 | 0 | 1 | 8 |
| CDH26 | Cdh26 | Richter *et al.* | sgCDH26 | GGGAAATTGATCACTATTCA | 1 | 0 | 0 | 1 | 8 |
| CUX1 | Cux1 | Richter *et al.* | sgCUX1 #1 | GAGCAGACCCTGAAGAGTC | 1 | 0 | 0 | 1 | 8 |
| CUZD1 | Cuzd1 | Schmitz *et al.* | sgCUZD1 #2 | GGGATATTCCTTCCTACAAA | 1 | 0 | 0 | 1 | 8 |
| DHX58 | Dhx58 | Schmitz *et al.* | sgDHX58 | GCAGCCTTGCCTACAGACTG | 1 | 0 | 0 | 1 | 8 |
| HNRNPD | Hnrnpd | Richter *et al.* | sgHNRNPD | GATCGACGCCAGTAAGAACG | 1 | 0 | 0 | 1 | 9 |
| IDUA | Idua | Schmitz *et al.* | sgIDUA | GGGCAGAGGTCTCAAAGGCT | 1 | 0 | 0 | 1 | 9 |
| MST1 | Mst1 | Schmitz *et al.* | sgMST1 | GAATGTAACACGAAGTACCG | 1 | 0 | 0 | 1 | 9 |
| MTMR4 | Mtmr4 | Schmitz *et al.* | sgMTMR4 | GCTCAGAGCCAGGAATTTTC | 1 | 0 | 0 | 1 | 9 |
| LCP1 | Lcp1 | Schmitz *et al.* | sgLCP1 | GGCCAGAAAAATCGGAGCAA | 1 | 0 | 0 | 1 | 9 |
| PTPRC | Ptprc | Richte *et al.*;Schmitz *et al.* | sgPTPRC | GGCCTTTGGATTTGCCCTTC | 0 | 1 | 3 | 4 | 10 |
| NHLH1 | Nhlh1 | Richter et al. | sgNHLH1-new | GTCGTGAGGAGCGCAGGCGC | 1 | 0 | 0 | 1 | 10 |
| PLS1 | Pls1 | Schmitz *et al.* | sgPLS1 | GACTGTGTTTGCCTGCTTAA | 1 | 0 | 0 | 1 | 10 |
| POLQ | Polq | Schmitz *et al.* | sgPOLQ | GAGTGAATCTTCCTGCTCGT | 1 | 0 | 0 | 1 | 10 |
| RHBDD3 | Rhbdd3 | Schmitz *et al.* | sgRHBDD3 | GACGAGCAGATGCTACAGGA | 1 | 0 | 0 | 1 | 10 |
| SP3 | Sp3 | Richter *et al.*;Schmitz *et al.* | sgSP3 | GCACACCTGCGTTGGCATTC | 1 | 0 | 0 | 1 | 11 |
| SIN3A | Sin3a | Richter *et al.* | sgSIN3A | GCAGCAGTTTCAGAGGCTCA | 1 | 0 | 1 | 2 | 11 |
| SKA3 | Ska3 | Richter *et al.* | sgSKA3 | GATAATTCTTTTGCCATTCC | 0 | 1 | 0 | 1 | 11 |
| SMARCAD1 | Smarcad1 | Schmitz *et al.* | sgSMARCAD1 | GCTAAGCTTCAGACATTGA | 1 | 0 | 0 | 1 | 11 |
| SPIRE2 | Spire2 | Schmitz *et al.* | sgSPIRE2 | GTGCTCCAGCCGCAAGAGCG | 1 | 0 | 0 | 1 | 11 |
| TMEM30A | Tmem30a | Richter *et al.* | sgTMEM30A | GTTGTATCGTCTCATAGAG | 0 | 1 | 0 | 1 | 12 |
| SRGAP2 | Srgap2 | Schmitz *et al.* | sgSRGAP2 | GCTTCTGATGACTGGTGGGA | 1 | 0 | 0 | 1 | 12 |
| TET2 | Tet2 | Schmitz *et al.* | sgTET2 | GGCAATGTCAACATGCCAGG | 1 | 0 | 0 | 1 | 12 |
| TSC1 | Tsc1 | Schmitz *et al.* | sgTSC1 | GCACATCCTGACCACCTTGC | 1 | 0 | 0 | 1 | 12 |
| KDM6A | Kdm6a | Schmitz *et al.* | sgKDM6A | GCCAATGGACCCTTTTCTGC | 1 | 0 | 2 | 3 | 13 |
| TFAP4 | Tfap4 | Schmitz *et al.*;Richter *et al.* | sgTFAP4 | GCCCTCTTTGCAACATTTC | 1 | 0 | 3 | 4 | 13 |
| ANKMY2 | Ankmy2 | Schmitz *et al.* | sgANKMY2 | GCCACACTCCTACAGCAGC | 1 | 0 | 1 | 2 | 13 |

*Table S1 - List of Genes with Nonsense or Frameshift Mutations in Burkitt's Lymphoma with the Corresponding Murine Orthologs and Designed sgRNAs*

| *Gene* | *Murine Ortholog* | *Reference* | *sgRNA Name* | *sgRNA Sequence* | *Nonsense* | *Frameshift* | *Missense* | *Total* | *Pool Number* |
|---|---|---|---|---|---|---|---|---|---|
| NCOR1 | Ncor1 | Schmitz *et al.*;Richter *et al.* | sgNCOR1 | GTGTGGATGGAGAGCCAGAG | 1 | 1 | 1 | 3 | 13 |
| TSC22D3 | Tsc22d3 | Schmitz *et al.* | sgTSC22D3 | GATGTACGCTGTGAGAGAGG | 1 | 0 | 0 | 1 | 14 |
| TULP3 | Tulp3 | Schmitz *et al.* | sgTULP3-New | GCCTTTGACGATGAGACCCTG | 1 | 0 | 0 | 1 | 15 |
| ARHGAP9 | Arhgap9 | Schmitz *et al.* | sgARHGAP9-New | GAACTGGGGCCCTGCTTGGG | 1 | 0 | 0 | 1 | 15 |
| C3orf52 | BC016579 | Schmitz *et al.* | sgC3orf52-New | GAGGAGTGTGCTAATGAAG | 1 | 0 | 0 | 1 | 15 |
| ZNF239 | Zfp239 | Schmitz *et al.* | sgZNF239-New | GTGCGGGAAGGGTTTCACC | 1 | 0 | 0 | 1 | 15 |
| MYO6 | Myo6 | Richter *et al.* | sgMYO6 | GAAAAAGAAACAGCAAGAGG | 0 | 1 | 0 | 1 | 16 |
| ARHGEF2 | Arfgef2 | Schmitz *et al.* | sgARHGEF2 | GTAACAAGAGCATCACAGCCA | 1 | 0 | 0 | 1 | 16 |
| C10orf26 | Wbp1L | Schmitz *et al.* | sgC10orf26 | GGCAGGCATCGCCGCTTCAC | 1 | 0 | 0 | 1 | 16 |
| GCA | Gca | Schmitz *et al.* | sgGCA | GTGAAGCTGCGCGCCCTGAC | 1 | 0 | 0 | 1 | 16 |
| TMEM179B | Tmem179b | Schmitz *et al.* | sgTMEM179B | GTGTCTGGCTTTGCTGCTCC | 1 | 0 | 0 | 1 | 16 |
| ARID1A | Arid1a | Love *et al.*;Richter *et al.*;Schmitz *et al.* | | | 6 | 1 | 3 | 10 | N/A |
| PCBP1 | Pcbp1 | Love *et al.*;Schmitz *et al.* | | | 3 | 0 | 6 | 9 | N/A |
| CYP4F22 | Cyp4f39 | Love *et al.* | | | 1 | 0 | 4 | 5 | N/A |
| PC | Pcx | Love *et al.*; Schmitz *et al.* | | | 1 | 0 | 5 | 6 | N/A |
| SAPS2 | Ppp6r2 | Love *et al.* | | | 2 | 0 | 3 | 5 | N/A |
| BCL6 | Bcl6 | Love *et al.*;Schmitz *et al.* | | | 4 | 0 | 1 | 5 | N/A |
| RET | Ret | Love *et al.* | | | 1 | 0 | 3 | 4 | N/A |
| CAD | Cad | Love *et al.*;Schmitz *et al.* | | | 1 | 0 | 6 | 7 | N/A |
| CARD4 | Nod1 | Love *et al.* | | | 0 | 1 | 3 | 4 | N/A |
| CCT6B | Cct6b | Love *et al.* | | | 0 | 1 | 4 | 5 | N/A |
| CREBBP | Crebbp | Love *et al.*;Richter *et al.*;Schmitz *et al.* | | | 2 | 1 | 3 | 6 | N/A |
| ID3 | Id3 | Schmitz *et al.*;Richter *et al.*;Love *et al.* | | | 10 | 5 | 27 | 42 | N/A |
| GNA13 | Gna13 | Schmitz *et al.*;Love *et al.* | | | 6 | 1 | 14 | 21 | N/A |
| DDX3X | Ddx3x | Schmitz *et al.*;Richter *et al.* | | | 4 | 1 | 8 | 13 | N/A |
| SRRM2 | Srrm2 | Schmitz *et al.* | | | 1 | 0 | 4 | 5 | N/A |
| PDE4DIP | Pde4dip | Schmitz *et al.* | | | 1 | 0 | 3 | 4 | N/A |
| FANCA | Fanca | Schmitz *et al.* | | | 1 | 0 | 3 | 4 | N/A |
| MRPS34 | Mrps34 | Schmitz *et al.* | | | 1 | 0 | 3 | 4 | N/A |

*Table S1 - List of Genes with Nonsense or Frameshift Mutations in Burkitt's Lymphoma with the Corresponding Murine Orthologs and Designed sgRNAs*



| *Gene* | *Murine Ortholog* | *Reference* | *sgRNA Name* | *sgRNA Sequence* | *Nonsense* | *Frameshift* | *Missense* | *Total* | *Pool Number* |
|---|---|---|---|---|---|---|---|---|---|
| PUSL1 | Pusl1 | Schmitz *et al.* | | | 1 | 0 | 3 | 4 | N/A |
| FBXO11 | Fbxo11 | Schmitz *et al.* | | | 2 | 1 | 2 | 5 | N/A |
| ZNF292 | Zpf292 | Schmitz *et al.* | | | 1 | 0 | 2 | 3 | N/A |

*Table S2 - List of sgRNA and shRNAs used to validate candidate tumor suppressor genes.*

| sgRNA Name | sgRNA Sequence |
|---|---|
| **sgPHIP-2** | GTATCCCATGTATTGCACTG |
| **sgSP3-2** | TTTGTAACTGGATGTTCTG |
| **sgTFAP4-2** | GAGAAAGAAGTGATAGGA |

| shRNA Name | shRNA Oligonucleotide | shRNA Target Site |
|---|---|---|
| **shPHIP-3809** | TGCTGTTGACAGTGAGCGCACGGATCTAAGTACAAT TAAATAGTGAAGCCACAGATGTATTTAATTGTACTT AGATCCGTTTGCCTACTGCCTCGGA | CGGATCTAAGTACAATTAAATA |
| **shPHIP-4131** | TGCTGTTGACAGTGAGCGCACAGAGCTCAGTCTTAC GATATAGTGAAGCCACAGATGTATATCGTAAGACTG AGCTCTGTTTGCCTACTGCCTCGGA | CAGAGCTCAGTCTTACGATATA |
| **shSP3-658** | TGCTGTTGACAGTGAGCGCCCAATCAATAGTGTCGA TCTATAGTGAAGCCACAGATGTATAGATCGACACTA TTGATTGGTTGCCTACTGCCTCGGA | CAATCAATAGTGTCGATCTATA |
| **shSP3-3117** | TGCTGTTGACAGTGAGCGCTCGTTGTAAATTACCAA TAAATAGTGAAGCCACAGATGTATTTATTGGTAATT TACAACGATTGCCTACTGCCTCGGA | CGTTGTAAATTACCAATAAATA |

*Table S3 - PCR Primer sequences used in Chapter 2*

| ID | Sequence |
|---|---|
| sgRNA-ID-F | AGCCCTTTGTACACCCTAAGCCTC |
| sgRNA-ID-R | CTAACTGACACACATTCCACAGGG |
| PHIP-F | CCATCTCATCCCTGCGTGTCTCCGACTCAGTGTAATTTCTTCATCCTAATGTACCA |
| PHIP-R | CCTCTCTATGGGCAGTCGGTGATGTTGGATAGGCCACCACAGT |
| SP3-F | CCATCTCATCCCTGCGTGTCTCCGACTCAGTGGGAAAAAGAAGCAACACA |
| SP3-R | CCTCTCTATGGGCAGTCGGTGATGCCTCTGTAATTCATCACTTCG |
| TSC1-F | CCATCTCATCCCTGCGTGTCTCCGACTCAGTGCTTGTCAACACGTTGGTT |
| TSC2-1 | CCTCTCTATGGGCAGTCGGTGATCTATGGATGAGCTGCTGTGG |
| Sin3a-F | TCAGCTGTGCCACAAAGTTC |
| Sin3a-R | TGTGCCCAGACATGTGTACT |
| Myo6-F | AGTCCACCATGATGACGAGG |
| Myo6-R | CTGGGCTCCACTCTGAAACT |
| Dock4-F | GTTTCTCTTCCCAGCTTCGC |
| Dock4-R | AGGATGAGTCAGATGGTGCT |
| Mst1-F | AGCACTGGTTTTGGCTCAAG |
| Mst1-R | TGGGTATAGCAGGCAAGTGG |
| Polq-F | TGGTTCTGTGGTAATGATTTTGG |
| Polq-R | AGCTCTTACTGGTCAACTTTCA |
| Spire2-F | TCAGAAGTGGCAGGACAAGG |
| Spire2-R | TTGAGAGTCCTGGTGTTGGG |
| Eif2ak3-F | CCTCGTGACGCTTGTTTTCT |
| Eif2ak3-R | TCTGGTAAGTCTGAGTGCCG |
| Rfx7-F | GTGAACCCTGCTCTTGTCAC |
| Rfx7-R | TGGCTGTATGTGTCCTGTGG |
| Ncor1-F | ACCCAGAAATGCAGGTACCA |
| Ncor1-R | ACCAAAGCCACACAATTGCT |

*Table S4 – Blood chemistry analysis of R26-rtTA;TRE-CiG/rtTA mice after 6 months maintenance on 1 mg/mL DOX (n=2).*

| Criterion | Units | Mouse Values | R26-rtTA;TRE-CiG/rtTA (n=2) |
|---|---|---|---|
| Total Protein | g/L | 31-66 | 46 |
| Albumin | g/L | 25-48 | 22 |
| Albumin/Globulin Ratio | | | 0.9 |
| Glucose | mmol/L | 5.0-10.7 | 9.9 |
| BUN Urea | mmol/L | 6.4-10.4 | 7.05 |
| Creatinine | μmol/L | 18-71 | 18 |
| Total Bilirubin | μmol/L | 2-15 | 3 |
| ALT | U/L | 28-132 | 31.5 |
| AST | U/L | 59-247 | 78 |
| Alkaline Phosphatase | U/L | 62-209 | 115 |
| CK | U/L | 68-1070 | 136 |
| Cholesterol | mmol/L | 0.93-2.48 | 2.56 |
| Sodium | mmol/L | 124-174 | 150.5 |
| Potassium | mmol/L | 4.6-8.0 | 4.28 |
| Chloride | mmol/L | 92-120 | 115 |
| Calcium | mmol/L | 1.47-2.35 | 2.105 |
| Phosphorus | mmol/L | 1.97-3.26 | 2.205 |
| Magnesium | mmol/L | 0.33-1.60 | 1.06 |

*Table S5 - Histopathological analysis of wild-type and R26-rtTA;TRE-CiG/rtTA tissues after 6 month doxycycline induction*

| Tissue | Pathology | Genotype | Wild-Type | | R26-rtTA;TRE-CiG/rtTA | |
|---|---|---|---|---|---|---|
| | | **Mouse** | **1** | **2** | **1** | **2** |
| **Heart** | | | N | N | N | N |
| **Lung** | | | A | N | A | A |
| | Peribronchiolar lymphocytic Infiltrate, focal | | 1 | ø | 1 | 2 |
| | Perivascular lymphocytic Infiltrate | | | ø | 2 | 2 |
| | Aleveolar hemorrages, multifocal (probable artifact) | | ø | 2 | ø | ø |
| **Kidney** | | | A | N | A | N |
| | Perivascular lymphocytic Infiltrate, multifocal | | 1 | ø | 1 | ø |
| **Ovaries** | | | N | N | N | N |
| **Oviducts** | | | N | N | | N |
| **Spleen** | | | A | A | A | A |
| | Lymphoid hyperplasia, diffuse, white pulp | | 2 | 1 | 1 | 1 |
| **Pancreas** | | | N | N | N | N |
| **Liver** | | | N | A | A | A |
| | Microgranulomas, multifocal | | ø | 1 | 1 | 1 |
| | lipid vacuoles, multifocal, centrolobular | | ø | 2 | ø | ø |
| | foci of cellular alteration: basophilic, multifocal | | ø | ø | ø | 1 |
| **Skin** | | | | N | | N |
| **Large Intestine** | | | N | N | N | N |
| **Small Intestine** | | | N | N | N | N |

| Key |
|---|
| **A : No significant lesion** |
| **N : Lesion observed** |
| **Ø : none** |
| **1 : modest, rare** |
| **2 : mild, infrequent** |
| **3 : moderate, frequent** |
| **4 : severe, diffuse** |